Kode/Nama Rumpun Ilmu : 421/Teknik Sipil

LAPORAN TAHUN I
PENELITIAN HIBAH KOMPETENSI

STUDI DAMPAK PERUBAHAN IKLIM TERHADAP LONGSORAN LERENG

Tahun ke -1 dari rencana 3 tahun

Dr.Eng. Agus Setyo Muntohar, ST., M.Eng.Sc. NIDN: 0514087501

Jazaul Ikhsan, ST., MT., Ph.D. NIDN: 0524057201

Berdasarkan :
DIPA Kopertis Wilayah V Daerah Istimewa Yogyakarta
Kementerian Pendidikan dan Kebudayaan
Sesuai Surat Perjanjian Pelaksanaan
Nomor: 007/HB-LIT/III/2015 tanggal 25 Maret 2015
Nomor SP-DIPA: 023.04.1.673453/2015 tanggal 14 November 2014

UNIVERSITAS MUHAMMADIYAH YOGYAKARTA
NOVEMBER 2015

HALAMAN PENGESAHAN

Judul	: Studi Dampak Perubahan Iklim Terhadap Longsoran Lereng
Peneliti/Pelaksana	
Nama Lengkap	: AGUS SETYO MUNTOHAR Ph.D
Perguruan Tinggi	: Universitas Muhammadiyah Yogyakarta
NIDN	: 0514087501
Jabatan Fungsional	:
Program Studi	: Teknik Sipil
Nomor HP	: +6282138363248
Alamat surel (e-mail)	: muntohar@umy.ac.id
Anggota (1)	
Nama Lengkap	: JAZAUL IKHSAN S.T., M.T., Ph.D.
NIDN	: 0524057201
Perguruan Tinggi	: Universitas Muhammadiyah Yogyakarta
Institusi Mitra (jika ada)	
Nama Institusi Mitra	: -
Alamat	: -
Penanggung Jawab	: -
Tahun Pelaksanaan	: Tahun ke 1 dari rencana 3 tahun
Biaya Tahun Berjalan	: Rp 145.000.000,00
Biaya Keseluruhan	: Rp 450.000.000,00

Mengetahui,
Dekan

(Jazaul Ikhsan, ST., MT., Ph.D.)
NIP/NIK 19720504199804123037

Yogyakarta, 1 - 12 - 2015
Ketua,

(AGUS SETYO MUNTOHAR Ph.D)
NIP/NIK 19750814199904123040

Menyetujui,
Kepala LP3M

(Hilman Latif, MA., Ph.D.)
NIP/NIK 19750912200004113033

DAFTAR ISI

Ringkasan

Pemanasan global yang melanda dunia menyebabkan perubahan iklim dunia. Potensi perubahan iklim meliputi perubahan regional terhadap temperatur, curah hujan, potensi evaporasi, siklon tropik (*tropical cyclones*) dan badai (IPCC, 2013). Laporan World Meteorological Organization pada tahun 2013 menunjukkan bahwa terjadi peningkatan curah hujan hingga mencapai 90 mm per bulan untuk wilayah Indonesia seperti ditunjukkan oleh WMO (2014). Untuk regional Indonesia, pada rentang 2006-2014, terjadi perubahan intensitas dan sebaran hujan yang menyebabkan longsor sebagai dampak perubahan iklim. Kondisi geohidrologi dan vegetasi pada lereng berkaitan erat dengan iklim. Sehingga dalam unjuk kerja (*performance*) lereng tidak hanya dipicu oleh curah hujan semata tetapi oleh siklus iklim yang dapat dimodelkan dari evapotranspirasi dan infiltrasi hujan pada lereng. Tujuan utama dari penelitian ini adalah untuk mengkaji pengaruh iklim saat ini (*present*) dan yang akan datang (*future*) terhadap unjuk kerja lereng. Penelitian dilaksanakan dalam tiga tahun pelaksanaan. Luaran penelitian pada Tahun Pertama yang telah dicapai adalah publikasi pada (1) International Conference on Landslides and Slope Stability (SLOPE 2015) pada tanggal 27-30 September 2015, (2) 7^{th} Regional Sympsium on Sustainable Infracstructure Develeopment pada tanggal 5-7 November 2015 yang diselenggarakan oleh Kasetsart University (Thailand) – Tokyo Institute of Technology (Japan) – University of Philipne (Philipine) sebagai ***Invited Speaker/Special Guest*** pada, (3) Pertemuan Ilmiah Tahunan ke-19 Himpunan Ahi Teknik Tanah Indonesia pada tanggal 24-25 November 2015, dan (4) sebagai ***Invited Professor/Scienctist*** di Department of Civil & Construction Engineering, Taiwan Tech (Taiwan) pada tanggal 18 – 31 Oktober 2015.

BAB I
PENDAHULUAN

A. Latar Belakang

Pemanasan global yang melanda dunia menyebabkan perubahan iklim dunia. Potensi perubahan iklim meliputi perubahan regional terhadap temperatur, curah hujan, potensi evaporasi, siklon tropik (*tropical cyclones*) dan badai (IPCC, 2013). Laporan World Meteorological Organization pada tahun 2013 menunjukkan bahwa terjadi peningkatan curah hujan hingga mencapai 90 mm per bulan untuk wilayah Indonesia seperti ditunjukkan pada Gambar 1.1 (WMO, 2014). Untuk regional Indonesia, pada rentang 2006-2014, terjadi perubahan intensitas dan sebaran hujan yang menyebabkan longsor sebagai dampak perubahan iklim. Gambar 2.2 menyajikan intensitas hujan rerata bulanan di Indonesia dari tahun 1900 hingga 2009. Indonesia menerima intensitas hujan yang tinggi sepanjang tahun dimana puncak musim penghujan (*wet season*) terjadi pada bulan January dan puncak musim kering (*dry season*) berada pada bulan Agustus (Hendon, 2003; Lee, 2015).

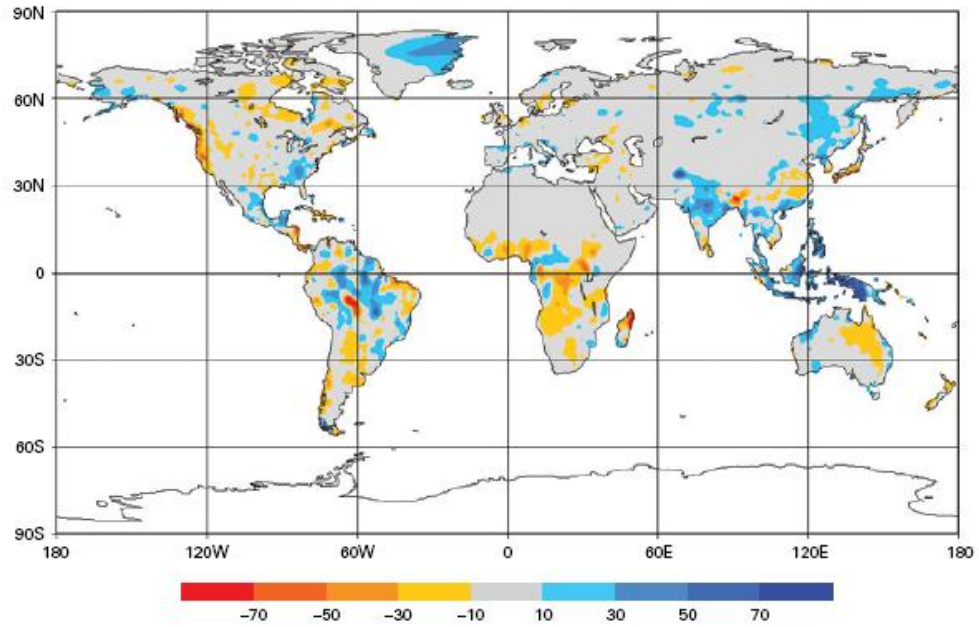

Gambar 1. 1Anomali sebaran hujan global pada tahun 2013 berdasarkan curah hujan bulanan relatif tahun 1951–2000 (World Meteorological Organization, 2014)

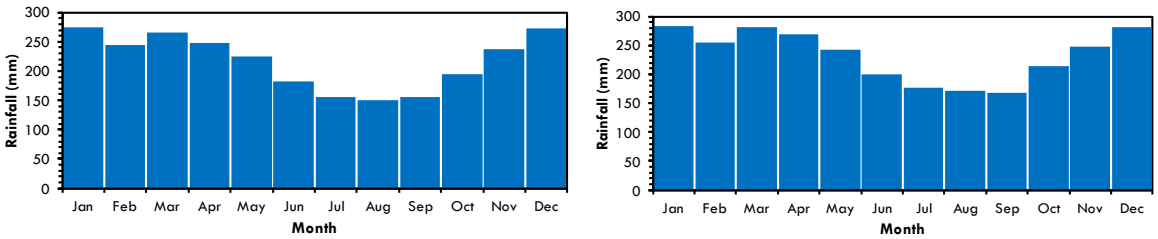

(a) Tahun 1900 – 1930 (b) 1930 – 1960

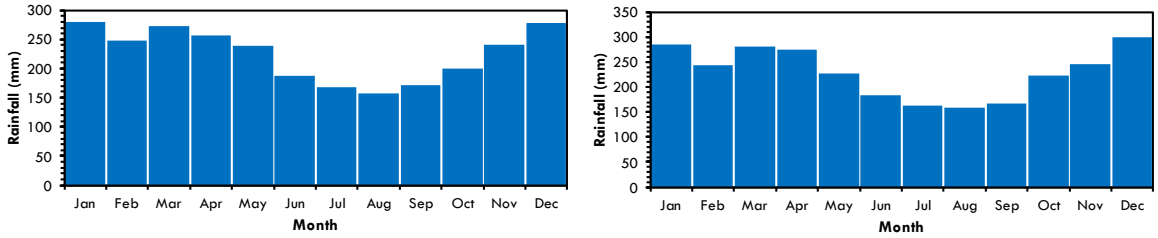

(a) Tahun 1960 – 1990 (b) 1990 – 2009

Gambar 1. 2 Hujan bulanan rata-rata di Indonesia dari tahun 1900 hingga 2009 (World Meteorological Organization, 2014)

Kejadian tanah longsor di Indonesia, khususnya di Pulau Jawa sering terjadi pada area lereng yang ditanami dengan tanaman musim dan produksi seperti kejadian longsor di Banjarmangu (di Banjarnegara, tahun 2006), Mogol (di Karanganyar, tahun 2007), Pasir Jambu Ciwidey (Bandung, tahun 2010), dan Cililin (Bandung, tahun 2013). Hujan secara umum dikenal sebagai faktor pemicu terjadinya tanah longsor (Muntohar and Liao, 2009). Namun demikian, banyak faktor yang menyebabkan terjadinya longsor seperti kondisi geologi, geomorphologi, geohidrologi, vegetasi penutup lahan, dan sebagainya. Kondisi geohidrologi dan vegetasi pada lereng berkaitan erat dengan iklim. Sehingga dalam unjuk kerja (*performance*) lereng tidak hanya dipicu oleh curah hujan semata tetapi oleh siklus iklim yang dapat dimodelkan dari evapotranspirasi dan infiltrasi hujan pada lereng.

B. Peta Jalan Penelitian

Skenario model iklim pada unjuk kerja lereng-lereng pada permukiman dan infrastruktur penting lainnya seperti jalan raya sangat diperlukan guna memprediksi kestabilan lereng tersebut. Selain itu dapat digunakan untuk pekerjaan mitigasi dan metode adaptasi terhadap iklim. Berdasarkan perkembangan penelitian yang telah dilakukan sebelumnya, kajian tentang model infiltrasi air hujan dan vegetasi masih perlu dikembangkan secara bersamaan. Alur pengembangan penelitian tentang infiltrasi dan vegetasi terhadap stabilitas lereng dapat dibuat seperti pada Gambar 1.3. Target akhir penelitian yang dikembangkan adalah penyusunan Sistem Manajemen Pergerakan Lereng Terpadu (*integrated landslides management system*).

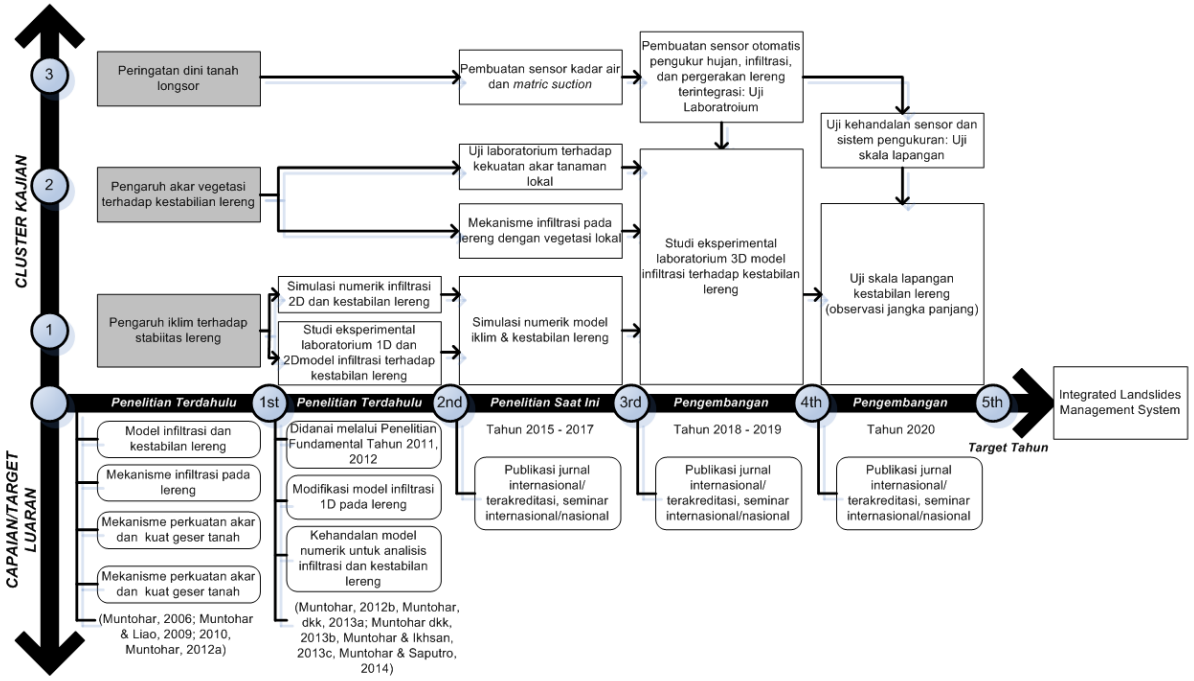

Gambar 1. 3 Diagram posisi dan peran penelitian yang diusulkan serta rencana pengembangannya (*road map*)

BAB II
TINJAUAN PUSTAKA

A. Hasil-Hasil Penelitian Terdahulu

Kajian terhadap stabilitas lereng yang telah dilakukan sebelumnya dapat dikelompokkan ke dalam 3 klaster seperti pada Gambar 2.1 yaitu: (i) **Klaster 1** tentang Pengaruh iklim, (ii) **Klaster 2** Pengaruh akar vegetasi, dan (iii) **Klaster 3** tentang Peringatan dini. Penelusuran pustaka, tidak ada penelitian di Indonesia yang berkaitan model iklim dan hujan terhadap stabilitas lereng. Dalam lingkup global pengaruh hujan karena iklim telah banyak dikaji pengaruhnya terhadap unjuk kerja lereng antara lain oleh Damiano and Mercogliano (2013), Coe and Godt (2012), Rouainia et al. (2009), Schmidt and Dikau (2004). Dalam klaster kajian pertama, penelitian yang banyak dikaji adalah tentang pengaruh hujan terhadap mekanisme pergerakan lereng yang meliputi kajian terhadap infiltrasi dan kondisi muka air tanah antara lain oleh Muntohar and Liao (2009), Muntohar and Liao (2010), Muntohar and Ikhsan (2013), Muntohar et al. (2013), Muntohar and Saputro (2014), Lee et al. (2009b), Rahardjo et al. (2010a), Tsai (2011), Sarah and Soebowo (2011), Tohari (2013), Tohari et al. (2013). Kajian terdahulu tersebut meliputi kajian terhadap lereng yang ada di lapangan maupun model di laboratorium yang terbatas pada kejadian hujan harian dalam rentang waktu tertentu yang mana tidak memperhatikan siklus hujan atau kala ulang. Model perkiraan hujan untuk cakupan Indonesia telah diusulkan oleh Aldrian et al. (2005), dan Vimont et al. (2010) yang menggunakan *downscaling-model* dari data stasiun curah hujan.

Klaster kajian kedua tentang teknik mitigasi dengan vegetasi atau *bioremediation* lebih banyak difokuskan pada pengaruh morfologi, jenis, arsitektur akar tanaman, jenis dan struktur tanah terhadap kekuatan geser tanah dan stabilitas lereng antara lain oleh Fan and Su (2008), Danjon et al. (2008), Ali and Osman (2008), Khalilnejad et al. (2012), Wu (2013). Chirico et al. (2013) dan Leung and Ng (2013) menjelaskan bahwa vegetasi pada lereng memiliki dua pengaruh positif : (i) pengaruh geo-mekanik, yaitu perkuatan tanah oleh akar tanaman, dan (ii) pengaruh hidrologi-tanah, yaitu kemampuan tekanan serap air pada tanah (*soil suction*) yang disebabkan oleh serapan air oleh akar tanaman. Tekanan serap air ini dipengaruhi oleh kondisi evapotraspirasi tanaman yang berkaitan dengan iklim.

Klaster kajian ketiga tentang sistem peringatan dini telah dilakukan untuk menentukan hujan yang memicu terjadinya longsor (*rainfall threshold*) dan monitoring pergerakan lereng (*instrumentation*). Batas hujan yang memicu terjadinya longsor telah dikaji oleh penelitian sebelumnya antara lain oleh Aleotti (2004), Guzzetti et al. (2007), dan Muntohar (2008). Peringatan dini dikeluarkan apabila intensitas hujan yang teramati lebih dari batas hujan. Sistem peringatan dini berdasarkan ambang hujan ini lebih bersifat lokal yang berlaku pada regional tertentu. Monitoring pergerakan lereng dengan instrumentasi yang meliputi sensor tekanan air pori (*tensiometer*), *inclinometer*, dan pengukur curah hujan (*rain gauge*) pada lereng yang berpotensi longsor seperti yang dilakukan oleh Liao et al. (2010) dan Tsaparas et al. (2002). Kombinasi antara ambang hujan dengan data yang berasal dari pengamatan dan pengukuran (*real-time monitoring*) pada jaringan telemetrik hujan dan perkiraan cuaca dapat digunakan untuk mengeluarkan peringatan dini tanah longsor. Prinsip dari sistem ini adalah bila hasil pengukuran curah hujan yang nyata dari waktu ke waktu berimpit atau sama dengan ambang hujan, maka peringatan kejadian longsor dikeluarkan. Namun instrumentasi lereng tersebut memerlukan biaya yang mahal dan peralatan yang rumit. Sehingga instrumentasi pada lereng untuk peringatan dini ini sangat terbatas dan hanya berlaku untuk lereng yang termonitor tersebut.

B. Pemodelan Numerik Infiltrasi-Rembesan Pada Lereng

Muntohar et al. (2013) menyelidiki mekanisme pergerakan tanah akibat rembesan air hujan pada lereng di Dusun Kedungrong, Samigaluh. Model rembesan dianalisis dengan menggunakan perangkat lunak SEEP/W Version 2004, sedangkan analisis stabilitas lereng menggunakan SLOPE/W Version 2004. Model lereng dan kondisi batas seperti pada Gambar 2.1. Pada kasus tersebut, hujan pada permukaan lereng dimodelkan sebagai batas hidraulik *unit flux* (*q*). Untuk menghasilkan infiltrasi ke dalam lereng, batas hidraulik *no flow boundary*(Q = 0) diberikan di tepi kanan dan kiri lereng. Untuk elemen tepi yang berada di bawah muka air tanah, diberikan kondisi batas tinggi tekanan yang sama dengan elevasi muka air tanah (Q = H). Rembesan pada lereng dimodelkan dengan mengaktifkan kondisi batas *seepage face review* di permukaan lereng. Pemodelan ini menghasilkan adanya variasi infiltrasi air hujan ke lereng, rembesan terjadi pada bagian ujung kemiringan. Laju infiltrasi menurun dengan berlalunya waktu curah hujan karena penjenuhan pada permukaan tanah dan menghasilkan tekanan air pori pada bagian atas dan pertengahan lereng. Kesimpulan dari penelitiannya adalah terjadi peningkatan tekanan air pori akibat infiltrasi dan adanya

rembesan ke bagian kaki (*toe*) yang menimbulkan adanya rembesan. Dari penelitian tersebut juga diketahui bahwa kuat geser residu tanah lebih sesuai digunakan untuk analisis stabilitas lereng daripada menggunakan parameter kuat geser puncak tanah.

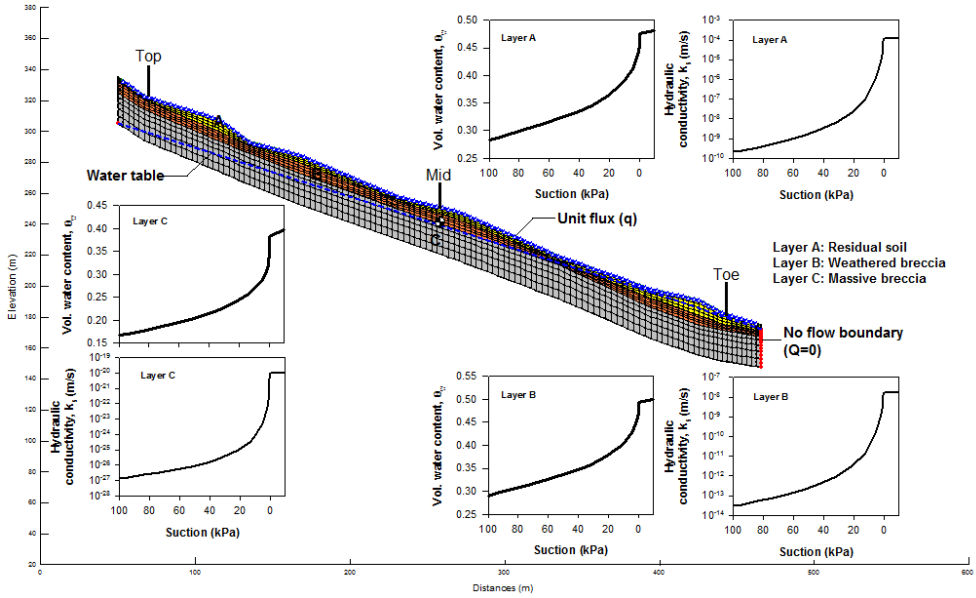

Gambar 2.1 Model analisis infiltrasi pada lereng (Muntohar et al., 2013)

Lee et al. (2009a) membuat suatu model sederhana untuk analisis stabilitas lereng akibat infiltrasi hujan. Penelitian tersebut bertujuan untuk membuktikan model sederhana sebagai evaluasi awal keruntuhan lereng akibat curah hujan. Analisis menggunakan metode numerik dengan aplikasip SEEP/W. Kondisi lereng dan kondisi batasnya seperti disajikan pada Gambar 2.2. Muka air tanah berada pada kedalaman 20 m. Lereng dimodelkan sebagai lereng tak-hingga dengan empat variasi yang tanah yang dievaluasi, yaitu : kerikil-berpasir, kerikil-berlanau, lanau-berpasir, dan lanau. Masing-masing jenis tanah tersebut memiliki koefisien permeabilitas jenuh (k_{sat}) yang berbeda-beda. Dalam penelitian ini, tekanan air pori negative (*initial matric suction*) awal pada lereng dibatasi 10 kPa, 23 kPa, 30 kPa, dan 50 kPa masing-masing untuk kerikil-berpasir, kerikil-berlanau, lanau-berpasir, dan lanau. Pembatasan dilakukan karena apabila menggunakan kondisi tekanan hidrostatis dari muka air air tanah, kondisi awal tekanan air pori negatif akan sangat besar sekali yatu mencapai 196,2 kPa.

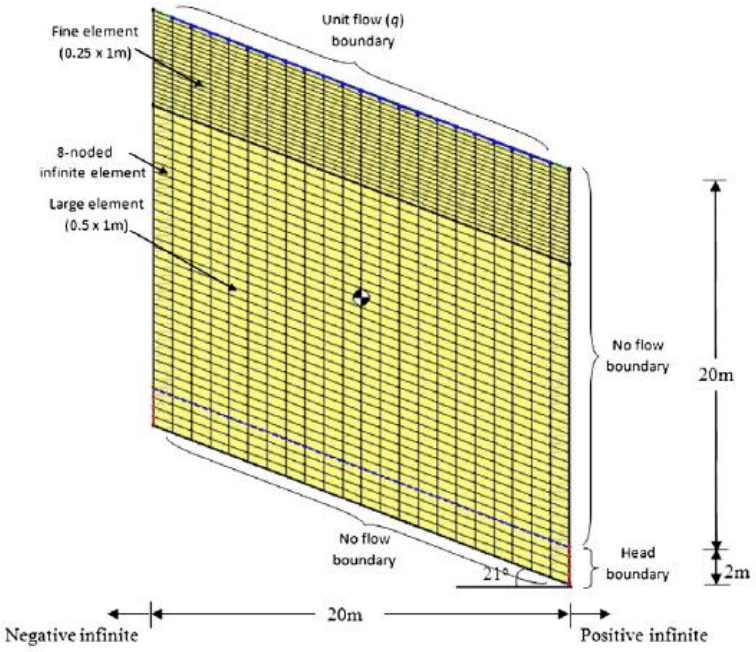

Gambar 2.2 Pemodelan lereng untuk analisis infiltrasi dan rembesan (Lee et al., 2009)

Analisis numerik infiltrasi dan limpasan yang disebabkan oleh curah hujan pada tipe keruntuhan lereng dangkal dalam kondisi tak jenuh dilakukan oleh Cuomo dan Sala (2013). Dalam penelitian ini dilakukan evaluasi terhadap waktu limpasan (*time to runoff*), waktu keruntuhan lereng (time to failure) , dan laju limpasan permukaan (*runoff rates*). Lereng yang dikaji berupa tanah homogen dengan tebal lapisan tanah 2 m dan panjang lereng 150 m dengan sudut kemiringan sebesar 20°, 30°, dan 40° (Gambar 2.3a). Gambar 2.5b-c menyajikan kurva kadar air volumetrik dan kurva koefisien permeabilitas yang digunakan dalam analaisis. Kurva kadar air volumetrik didekati dengan model yang diusulkan oleh Van Genuchten (1980). Hasil yang diperoleh menunjukkan waktu untuk limpasan, waktu keruntuhan lereng dan laju limpasan yang sangat dipengaruhi oleh kurva karakteristik air tanah, kondisi awal tanah, intensitas curah hujan dan sudut kemiringan. Selain itu, analisis stabilitas lereng menunjukkan bahwa waktu keruntuhan lereng dapat terjadi dalam waktu yang cepat atau lama bergantung pada parameter kuat geser tanah.

Penelitian pergerakan lereng di Kalibawang di dekat Saluran Induk Kalibawang KM 15+9 pernah dilakukan oleh Haryanti et al. (2010) dan Subiyanti et al. (2011). Analisis pengaruh karakteristik hujan pada daerah Kalibawang dilakukan oleh Haryanti et al. (2010). Pada penelitian ini model hujan yang digunakan berdasarkan hujan yang terjadi dilapangan, yaitu model hujan yang mewakili hujan deras durasi pendek, hujan normal durasi panjang dan kombinasi hujan deras dan normal. Untuk memodelkan penelitian ini digunakan analisis

numerik dengan SEEP/W dan SIGMA/W yang merupakan perangkat lunak GeoSlope 5. Dari hasil analisis numerik disimpulkan bahwa gerakan atau deformasi lereng oleh hujan deras durasi pendek sangat kecil, sehingga bisa dikatakan hujan deras durasi pendek tidak berpengaruh pada gerakan atau deformasi lereng. Karakteristik hujan yang paling berpengaruh pada lereng adalah hujan normal 20 mm/jam yang terjadi selama 61 hari, yang menyebabkan gerakan atau deformasi lereng terbesar, yaitu sebesar 1,01 m pada hari ke-43.

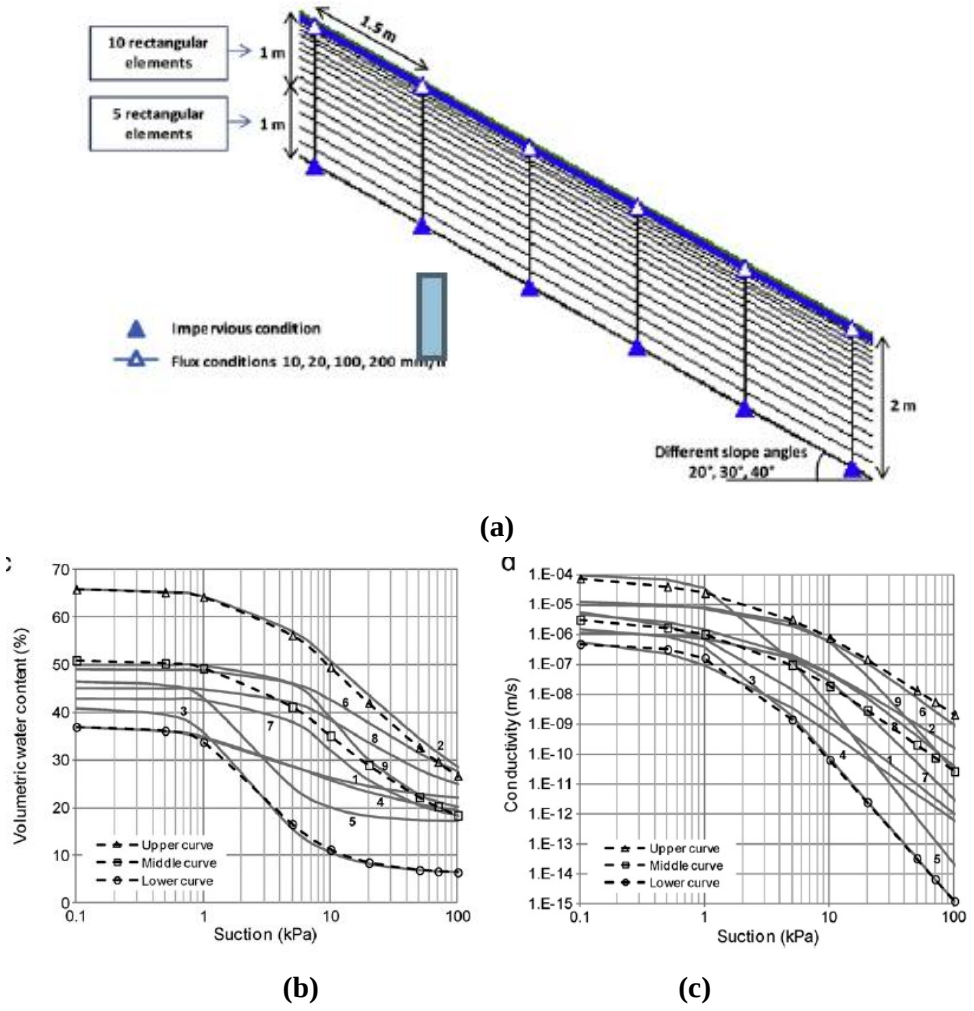

Gambar 2.3 (a) kondisi kemiringan lereng (b) kurva karakteristik kadar air (b) kurva konduktivitas hidraulik (Cuomo and Sala, 2013)

Subiyanti et al. (2011) mengkaji karakteristik hujan yang sering terjadi di lokasi penelitian dan pengaruhnya terhadap perubahan tekanan air pori, serta pengaruh tekanan air pori terhadap kelongsoran lereng Penyelesaian penelitian ini menggunakan analisis numerik dengan perangkat lunak SEEP/W dan SLOPE/W yang merupakan bagian dari perangkat lunak Geoslope Office Versi 5. Kondisi lereng (Gambar 2.4) dimodelkan dengan dua model, yaitu : analisis *steady state* dan kondisi analisis *transient*. Kondisi *steady state* digunakan

sebagai initial condition atau kondisi awal. Sedangkan analisis stabilitas lereng memasukkan output dari SEEP/W ke dalam program SLOPE/W dengan ditambah parameter-parameter tanah hasil laboratorium. Hasil dari analisis tersebut dikatakan bahwa pada posisi yang sama, kondisi sebelum hujan masih terdapat tekanan air pori negatif (*suction*) sebesar -74,8 kPa; akibat hujan deras selama 4 jam *suction* turun menjadi -72,0 kPa; akibat hujan 25 mm dan 40 mm *suction* turun menjadi -14,2 kPa; akibat hujan 20 mm *suction* berubah menjadi tekanann air pori positif sebesar 568,7 kPa; akibat hujan deras diikuti hujan normal *suction* berubah menjadi tekanan air pori positif sebesar 7,9 kPa dan akibat hujan normal diikuti hujan deras *suction* turun menjadi -41,8 kPa. Dari hasil tersebut dapat disimpulkan bahwa hujan normal berdurasi panjang lebih berpengaruh terhadap perubahan tekanan air pori daripada hujan deras berdurasi pendek. Angka aman sebelum hujan sebesar 1,44; angka aman akibat hujan 114 mm selama 4 jam sebesar 1,42; angka aman akibat hujan 25 mm dan 40 mm sebesar 1,208; angka aman akibat hujan 20 mm sebesar 0,98; angka aman akibat hujan deras diikuti hujan normal sebesar 1,39 dan angka aman akibat hujan normal diikuti hujan deras sebesar 1,40. Dari hasil tersebut dapat disimpulkan bahwa kondisi yang paling berpengaruh terhadap stabilitas lereng di lokasi tersebut adalah hujan normal 20 mm berdurasi panjang.

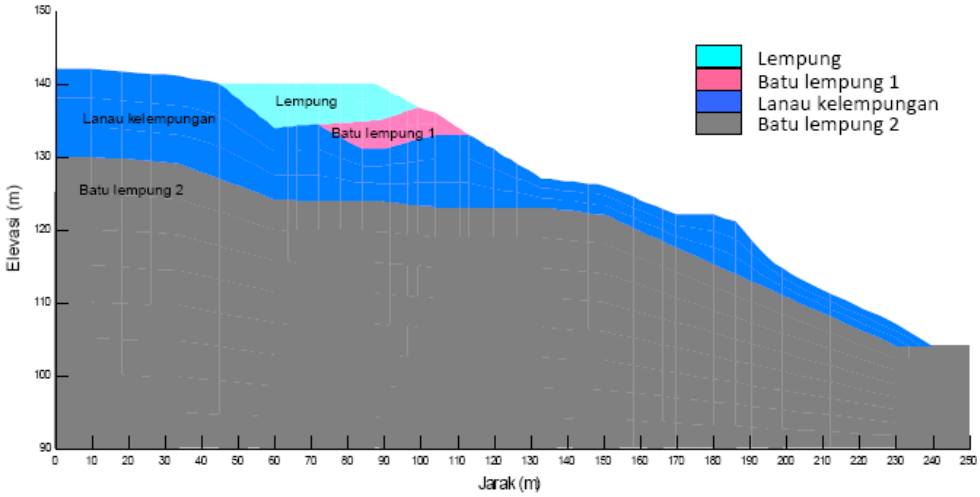

Gambar 2. 4 Profil lereng (Subiyanti et al., 2011)

C. Studi Pengaruh Muka Air Tanah Terhadap Stabilitas Lereng

Rahardjo et al. (2010b) membandingkan pengaruh posisi muka air tanah dengan analisis numerik pada kondisi yang berbeda, yaitu kondisi basah, setengah basah, dan kering dengan intensitas hujan yang berbeda. Model lereng dan kondisi batasnya seperti disajikan pada Gambar 2.5. Variasi faktor aman lereng dengan variasi kedalaman muka air tanah seperti disajikan pada Gambar 2.6. Terjadi perbedaan variasi yang lebih besar antara periode basah

dan kering akibat perubahan elevasi muka air tanah, tetapi perubahan faktor aman saat curah hujan tidak terpengaruh secara signifikan oleh muka air tanah dekat dengan permukaan tanah karena perubahan suction relatif lebih kecil. Suction yang relatif kecil karena tanah telah mencapai kapasitasnya untuk menerima infiltrasi air hujan dengan intensitas yang lebih tinggi dari 22 mm/jam.

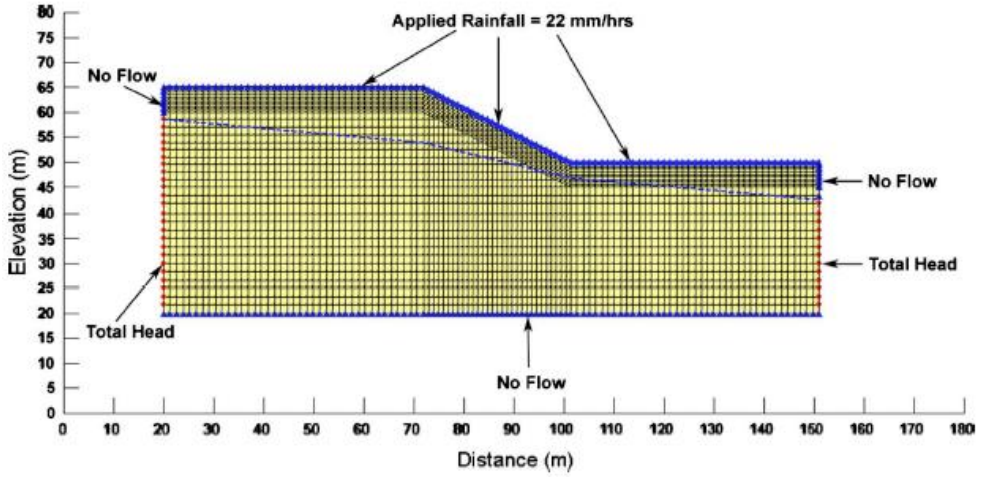

Gambar 2.5 Model lereng untuk studi parametrik (tinggi lereng =15 m dan kemiringan =27°) (Rahardjo et al., 2010b)

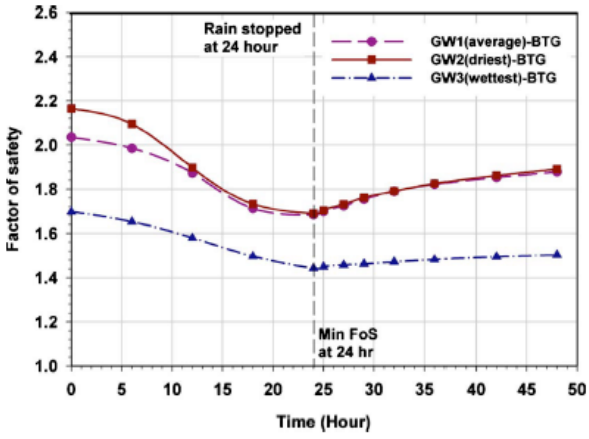

Gambar 2.6 Variasi faktor aman lereng untuk berbagai kedalaman muka air tanah (Rahardjo et al., 2010)

Tsaparas et al., (2002) melakukan kajian terhadap parameter yang mempengaruhi stabilitas lereng tak jenuh air selama hujan. Dalam penelitian ini analisis infiltrasi dilakukan dengan berbagai kondisi hidrologi dengan analisis numerik yang menggunakan perangkat lunak SEEP/W. Sedangkan analisis stabilitas lereng dimodelkan dengan SLOPE/W yang mana tekanan air porinya menggunakan hasil luaran dari SEEP/W. Ada tiga parameter yang digunakan, yaitu hujan komulatif, koefisien permeabilitas tanah, kondisi awal tekanan air pori

negatif. Model lereng yang dikaji adalah lereng tanah residu di Singapura dengan kemiringan 2H:1V dan tinggi 10m. Hasil dari penelitian ini yaitu pada hujan yang sama , hujan dengan intensitas tinggi dengan durasi yang singkat bukan salah satu faktor yang menghasilkan faktor aman yang rendah. Koefisien permeabilitas tanah merupakan parameter yang menentukan infiltrasi. Untuk lereng dengan permeabilitas tinggi (k_{sat} = 10^{-4} m/s) tidak mempengaruhi jumlah hujan kumulatif yang lebih kecil daripada ksat. Sedangkan untuk lereng dengan permeabilitas rendah (k_{sat} = 10^{-6} - 10^{-7} m/s), tekanan air pori tidak terlalu berubah selama hujan, tetapi terjadi kecenderungan untuk meningkat menjadi tekanan air positif setelah hujan kumulatif.

Terjadinya longsor di lereng curam pada tanah residu yang umumnya berada pada daerah tropis dan semi tropik. Terjadinya tanah longsor di lereng dikaitkan dengan banyak faktor. Curah hujan telah dianggap sebagai penyebab utama mayoritas tanah longsor yang terjadi di daerah-daerah mengalami curah hujan yang tinggi. Mekanisme kegagalan lereng bahwa infiltrasi air atau resapan air menyebabkan pengurangan tekanan air pori negative di tanah tak jenuh, sehingga terjadi penurunan kuat geser tanah yag menjadikan lereng tidak stabil. Hossain (2010) menganalisis tekanan air pori negatif akibat curah hujan terhadap stabilitas lereng tanah residual. Sebuah program instrumentasi lapangan dilakukan untuk memantau tekanan air pori negative lapangan (*in situ matrix suction*) di lereng (Gambar 2.7) menunjukkan bagian lereng dengan lokasi dan letak instrumen yang dipasang pada lereng.

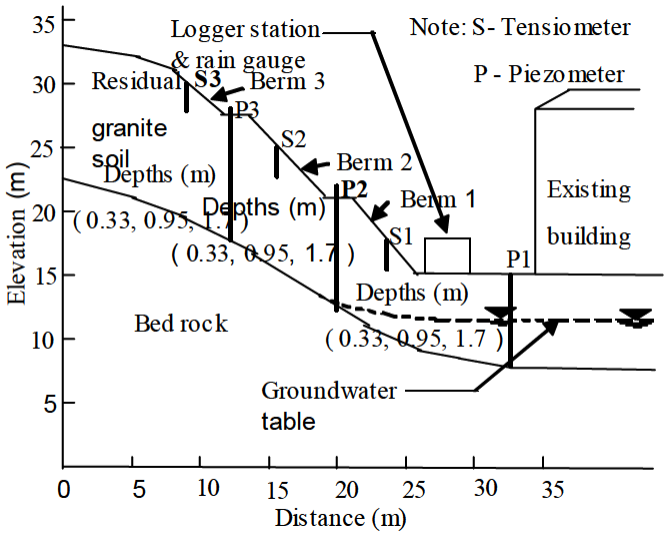

Gambar 2.7 Detail instrumen pada lereng (Hossain, 2010)

Memiliki rata-rata kemiringan dengan sudut 50^{o} terhadap horisontal dan maksimum dengan ketinggian 18 m. Tiga piezometer dengan P1, P2, P3 yang terletak pada permukaan

tanah didekat bagian bawah lereng dengan ujung berpori yang tertahan pada kedalaman 6,5 m di bawah permukaan tanah. Studi stabilitas lereng dilakukan dengan memasukkan parameter tanah yang telah diuji dalam laboratorium yaitu dengan kohesi efektif c'= 40 kPa, sudut gesek internal efektif $\phi' = 26{,}5^{o}$ dan sudut terkait dengan *scution* $\phi^{b} = 17{,}8^{o}$. Hasil dari penelitian ini yaitu saturasi parsial tanah memungkinkan untuk mengembangkan matrik hisap. Kohesi tanah jelas meningkat karena matrik hisap meningkat, tekanan air pori di lereng berubah dengan kondisi curah hujan yang bervariasi. *Matric suction* ada di lereng karena kehilangan kelembaban baik melalui penguapan atau evapotranspirasi. Zona pembasahan yang lebih maju ke permukaan tanah mengakibatkan matric hisap juga mengalami perubahan. Kemudian hasil matrik hisap dianalisis menggunakan SLOPE/W untuk mengetahui berapa faktor aman lereng (Gambar 2.8). faktor aman yang diperoleh yaitu 2,14 dengan rata-rata matrik hisap 30 kPa setelah hujan deras. Untuk kondisi kering, rata-rata matrik hisap sekitar 70 kPa. Hal ini menggamarkan pengaruh *matric suction* terhadap stabilitas lereng.

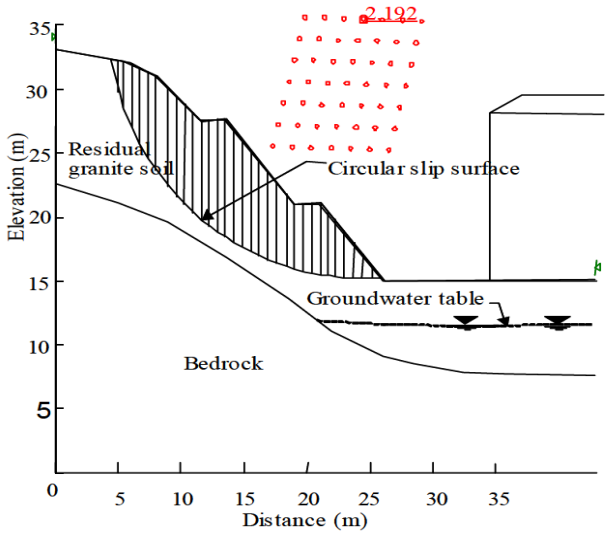

Gambar 2. 8 Analisis menggunakan SLOPE/W (Hossain, 2010)

D. Metode Pemodelan Perubahan Iklim

Model numerik General Circulation Model (GCM), mewakili proses fisik di atmosfer, laut, *cryosphere* dan permukaan tanah, merupakan metode yang paling baik saat ini untuk mensimulasikan respon sistem iklim global untuk mengukur peningkatan konsentrasi gas rumah kaca. Dalam IPCC (2013), dikenal sebagai Kriteria 1 dari skenario iklim (*climate scenarios*) yaitu konsistensi dengan proyeksi global. Model harus konsisten dengan berbagai proyeksi pemanasan global berdasarkan peningkatan konsentrasi gas rumah kaca yang berkisar antara 1,4°C - 5,8°C pada tahun 2100, atau 1,5°C menjadi 4,5°C untuk penambahan

konsentrasi CO_2 di atmosfer (atau dikenal sebagai "sensitivitas iklim ekuilibrium"). Sementara model sederhana juga telah digunakan untuk memberikan perkiraan rata-rata secara global atau regional rata dari respon iklim. Metode GCM yang dihubungkan dengan model wilayah tersarang (*nested region*), memiliki potensi untuk memberikan perkiraan geografis dan fisik yang konsisten perubahan iklim regional yang diperlukan dalam analisis dampak, sehingga memenuhi Kriteria 2 yaitu *physical plausibility*.

Metode GCM yang diperkenalkan dalam IPCC (2013) adalah *Coupled Model Intercomparison Project* fase ke-3 (CMIP5) dan fase ke-3 (CMIP3). Kedua model tersebut didasarkan pada *Atmosphere – Ocean General Circulation Models* (AOGCM) dan *Earth System Model* (ESM). Perbedaan mendasar antara CMIP5 dan CMIP3 adalah penetapan scenario emisi yang digunakan dalam simulasi iklim masa yang akan datang pada abad ke-21. Model CMIP3 mensimulasikan iklim didasarkan ada skenario emisi dari *Special Report On Emissions Scenarios* (SRES) (IPCC, 2000). Sedangkan model CMIP5 mensimulasikan iklim berdasarkan pada *Representative Concentration Pathway*s (RCP). RCP tidak menentukan besaran emisi, tetapi mendefinisikan konsentrasi gas rumah-kaca (*greenhouse*), aerosols, and dan gas-gas kimia aktif. Dalam perkembangannya skenario emisi (Tabel 2.1) digantikan dengan skenario RCP seperti pada Tabel 2.2 (IPCC, 2014).

Tabel 2.1 Ringkasan skenario emisi untuk simulasi iklim abad ke-21 (IPCC, 2000)

	Fokus pada ekonomi	Fokus pada lingkungan
Globalisasi	Skenario A1. Pertumbuhan ekonomi cepat (kelompok: A1T, A1B, A1F1) Perubahan temperature : 1,4 – 6,4^{o}C	Skenario B1. Keberlanjutan lingkungan global Perubahan temperature : 1,1 – 2,9^{o}C
Regionalisasi	Skenario A2. Pertumbuhan ekonomi berorientasi regional Perubahan temperatur : 2,0 – 5,4^{o}C	Skenario B2. Keberlanjutan lingkungan lokal Perubahan temperature : 1,4 – 3,^{8o}C

Tabel 2.2 Ringkasan skenario RCP untuk simulasi iklim abad ke-21 (IPCC, 2014)

Skenario	Perubahan Temperatur (^{o}C)		Perubahan Muka Air Laut (m)	
	2046 – 2065	2081 – 2100	2046 – 2065	2081 – 2100
RCP 2.6	0,4 – 1,6	0,3 – 1,7	0,17 – 0,32	0,26 – 0,55
RCP 4.5	0,9 –2,0	1,1 –2,6	0,19 – 0,33	0,32 – 0,63
RCP 6	0,8 –1,8	1,4 –3,1	0,18 – 0,32	0,33 – 0,63
RCP 8.5	1,4 –2,6	2,6 –4,8	0,22 – 0,38	0,45 – 0,82

Keterangan :
RCP 2.6 mengasumsikan bahwa emisi gas rumah kaca global tahunan (yang diukur dengan CO_2-ekivalen mencapai puncak pada 2010 – 2020, setelah itu emisi cenderung menurun. Emisi maksimum RCP 4.5 terjadi pada sekitar tahun 2040-an, kemudian menurun. Dalam RCP 5, emisi tertinggi dicapai sekitar tahun 2080-an, kemudian berkurang. Sedangkan dalam RCP 8.5, emisi cenderung meningkat hingga abad ke-21.

E. Model Infiltrasi

1. Model Infiltrasi Green – Ampt

Model Green-Ampt diasumsikan untuk memenuhi kondisi-kondisi sebagai berikut :

1. Tekanan air pori negatif (ψ_f) adalah tetap,
2. Perbedaan kadungan air volumetrik ($\Delta\theta$) adalah seragam antara sebelum dan sesudah basah,
3. Koefesien konduktivitas hidraulik (k) adalah tetap dan sama dengan konduktivitas hidrolik jenuh (k_s)

Mein dan Larson (1973) memberikan sebuah metode untuk menentukan infiltrasi pada kondisi tetap atau intensitas air hujan yang konstan. Akan tetapi, penentuan infiltrasi pada kondisi tidak tetap atau intensitas air hujan yang bervariasi juga dapat dilakukan menggunakan metode ini (Bouwer, 1978; Chow et al., 1988). Infiltrasi kumulatif dihitung dari curah hujan sebagai fungsi waktu. Potensi infiltrasi dapat dihitung dari infiltrasi kumulatif menggunakan Persamaan 2.1. Selama hujan berlangsung, tiga kondisi infiltrasi hujan dapat terjadi, seperti yang diperlihatkan pada Gambar 2.9. Kondisi tersebut yaitu :

1. **Kondisi (1)**: Intensitas hujan *I(t)* lebih besar dari potensi laju infiltrasi potensial *f(t)* (Gambar 2.9a). Permukaan tanah menjadi jenuh pada keseluruhan interval waktu (Δt). Sehingga, jumlah air hujan yang terinfiltrasi dapat dihitung dengan menggunakan Persamaan 2.1.

$$F\left(t+\Delta t\right)-F\left(t\right)-\Delta\theta\psi_f \ln\left[\frac{\left(F\left(t+\Delta t\right)+\Delta\theta\psi_f\right)}{\left(F\left(t\right)+\Delta\theta\psi_f\right)}\right]=k_s\cdot\Delta t \tag{2.1}$$

2. **Kondisi (2)**: Intensitas hujan *I(t)* lebih rendah dibandingkan dengan potensi laju infiltrasi *f(t)* pada permulaan interval waktu tertentu, tetapi kemudian, menjadi lebih besar dibandingkan dengan potensi laju infiltrasi (Gambar 2.9b). Akibatnya permukaan tanah berubah menjadi jenuh air pada interval waktu tersebut (Δt). Oleh karena itu, jumlah air hujan yang terinfiltrasi dan waktu yang dibutuhkan untuk mencapai kondisi jenuh dapat dihitung menggunakan masing-masing Persamaan 2.2 dan 2.3 yaitu :

$$F\left(t\right)_{t=t'_p}=\frac{k_s.\left(\Delta\theta\psi_f\right)}{I\left(t\right)-k_s} \tag{2.2}$$

$$t'_p=\frac{F\left|t'_p\right|.-F\left(t\right)}{I\left(t\right)} \tag{2.3}$$

3. **Kondisi (3)**: Intensitas hujan *I(t)* lebih kecil dibandingkan dengan laju infiltrasi potensial *f(t)* selama selang waktu tertentu (Gambar 2.9c). Pada kondisi seperti ini, permukan tanah berada pada kondisi tak jenuh dan semua air hujan terinfiltrasi ke tanah. Sehingga, jumlah infiltrasi adalah sama dengan intensitas hujan dan hujan terakumulasi.

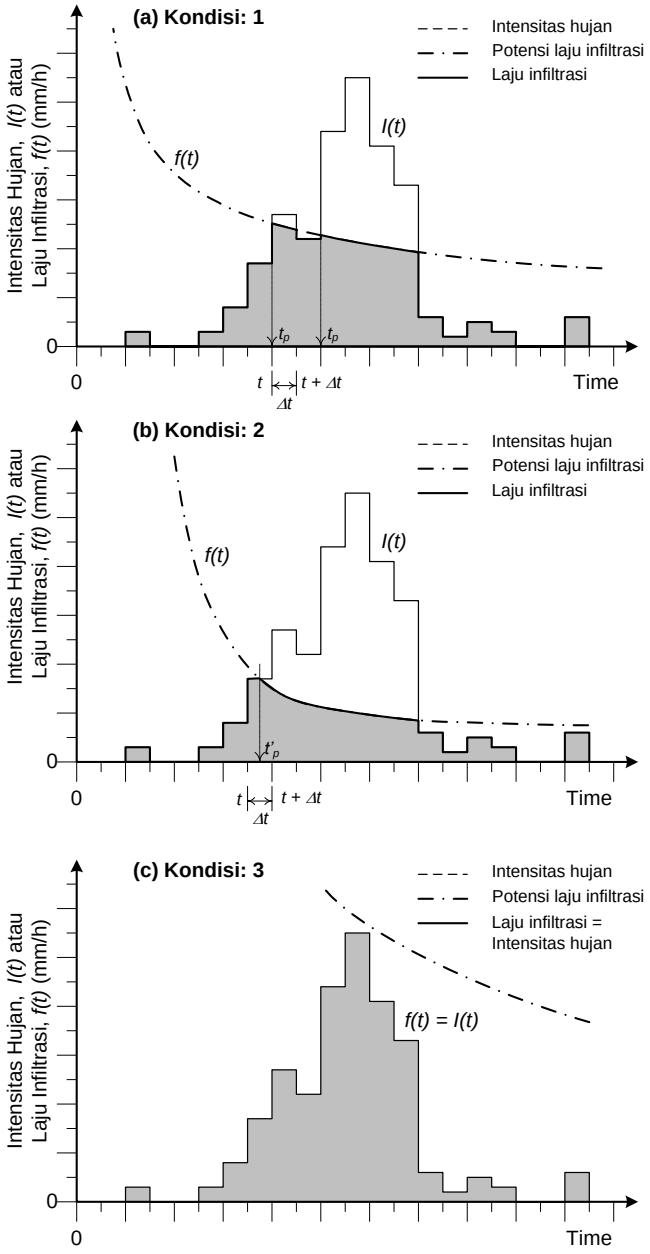

Gambar 2. 9 Mekanisme infiltrasi dari persamaan Green – Ampt (Dimodifikasi dari Chow dkk., 1988)

Notasi persamaan-persamaan di atas adalah :

F(t) = infiltrasi kumulatif pada saat *t*,

I(t) = intensitas hujan pada saat *t*,

f(t) = potensi laju infiiltrasi pada saat *t*,

$\Delta\theta$ = beda kadar air tanah = $\theta_s - \theta_i$,

ψ_f = tinggi tekanan air pori negatif pada bidang pembasahan,

k_s = koefisien permeabilitas tanah pada kondisi jenuh air,

Δt = interval waktu hujan,

t'_p = waktu terjadinya genangan pada interval waktu Δt,

$F(t'_p)$ = infiltrasi kumulatif pada saat t'_p.

Bidang longsor dapat terjadi pada bidang pembasahan. Maka, dalam penelitian ini, kedalaman bidang longsor dianggap sama dengan kedalaman bidang pembasahan. Sehingga, $H = z_w$ yang nilanya ditentukan dari Persamaan 2.4 yang mana akan bervariasi dengan waktu.

$$z_w(t) = \frac{F(t)}{\Delta\theta} \tag{2.4}$$

2. Model Infiltrasi Satu Dimensi Persamaan Richard

Model infiltrasi satu dimensi didasarkan pada persamaan diferensial Richards (Persamaan 2.5) untuk mensimulasikan pergerakan air dalam media yang jenuh air. Persamaan ini diselesaikan dengan menggunakan metode numerik (Šimůnek *et al*., 2005). Persamaan dasar infiltrasi satu dimensi adalah sebagai berikut :

$$\frac{\partial\theta(\psi,t)}{\partial t} = \frac{\partial}{\partial z}\left[K(\psi)\left(\frac{\partial\psi}{\partial z}+1\right)\right] \tag{2.5}$$

dimana ψ adalah tinggi tekaanan air porsi (*soil water pressure head*), $\theta(\psi)$ merupakan kadar air volumetrik tanah (*volumetric water content*), t adalah waktu, z adalah koordinat vertikal dari permukaan tanah (bernilai positif bila ke atas), dan $K(\psi)$ adalah koefiesien permeabilitas tak jenuh air. Sifat-sifat hidraulika tanah tak jenuh ari, $\theta(\psi)$ dan $K(\psi)$), dalam Persamaan (2.4) merupakan fungsi non-linier terhadap tinggi tekanan air pori. Sifat-sifat hidraulika tanah dapat disajikan dalam bentuk model analitik seperti diusulkan oleh Brooks dan Corey (1964), van Genuchten (1980), Vogel and Císlerová (1988), dan Kosugi (1996).

Model Brooks dan Corey (BC)

Fungsi untuk kurva retensi kadar air tanah, $\theta(\psi)$, dan koefisien permeabilitas, $K(\psi)$, menurut Brooks dan Corey [(964) seperti diberikan dalam Persamaan 2.6a dan 2.6b.

$$\theta(\psi) = \theta_r + (\theta_s - \theta_r)\left|\alpha\psi\right|^{-n} \tag{2.6a}$$

$$K(\psi) = K_s \left[\frac{\theta(\psi) - \theta_r}{\theta_s - \theta_r} \right]^{\frac{2}{n}+l+2} \tag{2.6b}$$

Dimana θ_r dan θ_s masing-masing adalah kadar air jenuh air dan residu, K_s adalah koefisien permeabilitas tanah jenuh air, α merupakan inverse dari nilai tekanan udara (*air-entry value* atau *bubbling pressure*), n adalah indeks distribusi ukuran pori tanah, dan l adalah parameter konektifitas pori tanah (*pore-connectivity parameter*) = 2,0 dalam persamaan asal Brooks dan Corey (1964). Parameter-paremeter α, n dan l merupakan koefisien-koefisien empirik yang mempengaruhi bentuk dari fungsi hidraulika tanah tanah jenuh.

Model van Genuchten – Mualem (VGM)

Fungsi hidraulika tanah dari van Genuchten (1980) menggunakan distribusi statistika ukuran pori tanah dari model Mualem (1976). Persamaan van Genuchten [1980] seperti dituliskan pada Persamaan 2.7a dan 2.7b.

$$\theta(\psi) = \theta_r + (\theta_s - \theta_r)\left[1 + |\alpha\psi|^n\right]^{-m} \tag{2.7a}$$

$$K(\psi) = K_s S_e^l \left[1 - \left(1 - S_e^{1/m}\right)^m\right]^2 \tag{2.7b}$$

dengan

$$S_e = \left[\frac{\theta(\psi) - \theta_r}{\theta_s - \theta_r} \right] \tag{2.7c}$$

$$\text{dan, } m = 1 - 1/n \tag{2.7d}$$

Persamaan 2.7 di atas mengandung lima parameter independen yaitu θ_r, θ_s, α, n, dan K_s. Mualem (1976) memberikan estimasi parameter konektifitas pori tanah l = 0,5 dalam fungsi hidraulika tanah untuk tanah secara umum.

Model van Genuchten Termodifikasi (MVG)

Vogel dan Císlerová (1988) memodifikasi persamaan van Genuchten (1980) dengan menambah fleksibilitas dalam deskripsi sifat-sifat hidraulika pada kondisi mendekati jenuh air. Fungsi retensi kadar air, $\theta(\psi)$, dan koefisien permeabilitas, $K(\psi)$, diberikan dalam Persamaan (2.8a) dan (2.8b) respectively.

$$\theta(\psi) = \theta_a + (\theta_m - \theta_a)\left[1 + |\alpha\psi|^n\right]^{-m} \tag{2.8a}$$

$$K(\psi) = K_k + \frac{(\psi - \psi_k)(K_s - K_k)}{(\psi_s - \psi_k)} \tag{2.8b}$$

Karakteristik hidraulika untuk model *MVG* mengandung 9 parameter-parameter yang belum diketahui meliputi θ_r , θ_s, θ_a, θ_m, α, n, K_s, K_k, dan θ_k . Paramter-parameter tersebut seperti diilustrasikan pada Gambar 2.10. Apabila $\theta_a = \theta_r$, $\theta_m = \theta_k = \theta_s$ dan $K_k = K_s$, fungsi koefisien permeabilitas tanah yang diusulkan oleh Vogel dan Císlerová (1988) akan sama dengan model van Genuchten (1980) seperti dalam Persamaan 2.7b.

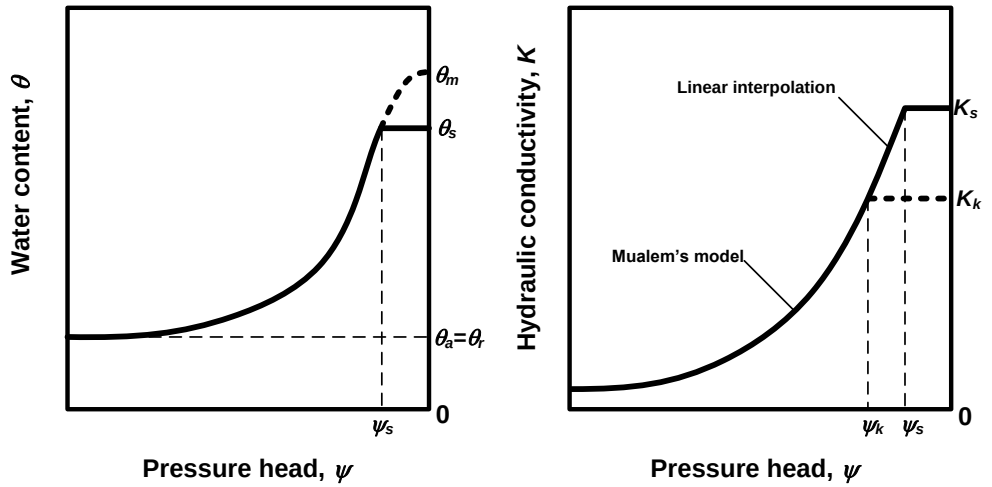

Gambar 2. 10 (a) Schematics of the soil water retention and (b)hydraulic conductivity functions.

Model lognormal Kosugi

Kosugi (1996) merumuskan model distribusi lognormal untuk fungsi hidraulika tanah. Model distribusi lognormal diaplikasikan dalam model distribusi ukuran pori tanah yang dituliskan oleh Mualem (1976). Persamaan 2.9 memberikan fungsi kadar air tanah dan koefisien permeabilitas tanah untuk model lognormal Kosudi (1996).

$$\theta(\psi) = \theta_r + (\theta_s - \theta_r)\frac{1}{2} erfc\left[\frac{\ln(\psi/\alpha)}{\sqrt{2n}}\right] \tag{2.9a}$$

$$K(\psi) = K_s S_e^l \left\{\frac{1}{2} erfc\left[\frac{\ln(\psi/\alpha)}{\sqrt{2n}} + \frac{n}{\sqrt{2}}\right]\right\}^2 \tag{2.9b}$$

F. Model Stabilitas Lereng

Pada kebanyakan kondisi di lapangan, lereng sangat panjang sekali, sehingga dalam analisis stabilitas lereng dapat diidealisasikan sebagai lereng tak-hingga (*infinite slope*). Dalam analisisnya, gaya-gaya yang bekerja ditinjau dalam satu satuan panjang seperti ditunjukkan pada (Gambar 2.11). Gaya geser yang terjadi pada tanah dapat dituliskan:

$$\tau = c' + (\sigma_n - u_w)\tan\phi' \tag{2.10}$$

dengan

τ = tegangan geser,

c’ = kohesi,

σ_n = tegangan normal,

u_w = tekanan air pori,

ϕ’ = sudut gesek internal.

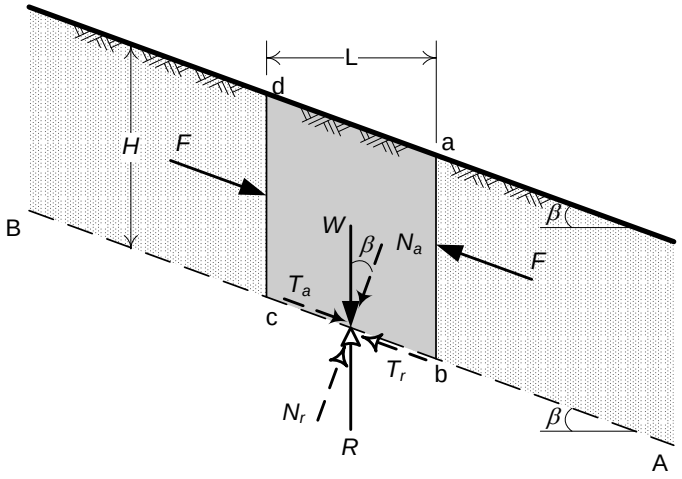

Gambar 2. 11Lereng tak hingga tanpa aliran air rembesan.

Keruntuhan lereng dapat terjadi karena pergerakan tanah di atas bidang **AB** dari kiri ke kanan (Gambar 2.11).. Besarnya faktor aman dari lereng dengan kedalaman bidang longsor *H* pada bidang longsor **AB** dapat ditentukan dengan Persamaan 2.11.

$$FS = \frac{c' + (\gamma_t H \cos^2\beta - u_w)\tan\phi'}{\gamma_t H \cos\beta \sin\beta} \tag{2.11}$$

dengan,

FS = faktor aman,

u_w = tekanan air pori,

γ_t = berat volume total tanah,

c’ = kohesi efektif tanah (kPa),

ϕ’ = sudut gesek internal efektif tanah (derajat),

H = kedalaman bidang longsor (m)

Rahardjo dkk. (1995) mengusulkan beberapa kemungkinan agihan tekanan air pori akibat infiltrasi dapat terjadi pada lereng seperti disajikan pada Gambar 2.11. Lereng

mengalami keruntuhan pada kedalaman z_f, yang berada di atas bidang pembasahan z_w. Maka faktor aman dapat dituliskan kembali seperti pada Persamaan 2.12 hingga 2.14.

a. Permukaan lereng dalam kondisi jenuh. Pada kondisi ini, tekanan air pori negatif berkurang hingga mencapai nol pada permukaan lereng. Pola agihan tekanan air pori seperti ditunjukkan oleh garis **a** pada Gambar 2.12. Faktor aman diberikan oleh Persamaan 2.12.

$$FS = \frac{\tan\phi'}{\tan\beta} + \frac{c'}{\gamma_t z_f \sin\beta\cos\beta} + \frac{\gamma_w y \tan\phi'}{\gamma_t z_w \tan\beta} \tag{2.12}$$

b. Proses penjenuhan hingga bidang pembasahan z_w. Pada kondisi ini tekanan air pori pada bidang longsor mencapai nol. Pola agihan tekanan air pori seperti ditunjukkan oleh garis **b** pada Gambar 2.13. Faktor aman diberikan oleh Persamaan 2.8.

$$FS = \frac{\tan\phi'}{\tan\beta} + \frac{c'}{\gamma_t z_f \sin\beta\cos\beta} \tag{2.13}$$

c. Peningkatan muka air tanah. Pada kondisi ini, tekanan air pori pada bidang pembasahan dipengaruhi oleh kenaikan muka air tanah (garis **c** dalam Gambar 2.11). Faktor aman diberikan oleh Persamaan 2.14.

$$FS = \frac{\tan\phi'}{\tan\beta} + \frac{c'}{\gamma_t z_f \sin\beta\cos\beta} - \frac{\gamma_w \tan\phi'}{\gamma_t \tan\beta} \tag{2.14}$$

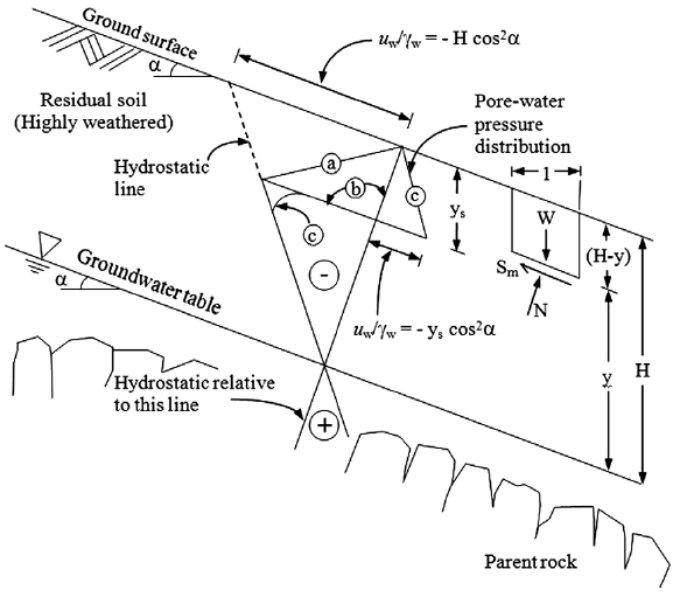

Gambar 2. 12 Beberapa kemungkinan agihan tekanan air pori pada lereng (Rahadjo dkk., 1995)

Metode analisis stabilitas lereng dengan model lereng tak-hingga dan pengaruh infiltrasi dapat memperhitungkan pengaruh perubahan tekanan air pori selama proses infiltrasi. Mengacu pada kriteria keruntuhan Mohr–Coulomb untuk tanah tak jenuh air yang dituliskan dalam Fredlund *et al*. (1978), maka faktor aman lereng dapat dinyatakan dalam Persamaan 2.15.

$$FS = \frac{c' + (\sigma_n - u_a)\tan\phi' + (u_a - u_w)\tan\phi^b}{\gamma_t \cdot z_f \cdot \sin\beta \cdot \cos\beta} \qquad (2.15)$$

dengan,

FS = faktor aman,

γ_t = berat volume total tanah,

c' = kohesi efektif tanah (kPa),

ϕ' = sudut gese internal tanah (derajat),

z_f = kedalaman bidang keruntuhan (m),

β = sudut kemiringan lereng (derajat),

u_w = tekanan air pori (kPa),

u_a = tekanan udara pori (kPa),

(u_a - u_w) = *matric suction* (kPa),

σ_n = tegangan normal total (kPa),

(σ_n - u_a) = tegangan normal pada bidang keruntuhan (kPa), dan

ϕ^b = sudut gesek terkait dengan kuat geser tanah akibat peningkatan *matric suction*

Untuk model kuat geser tanah dalam kondisi tak jenuh air, Vanapalli et al. (1996) mengusulkan hubungan antara kuat geser dan *suction* dengan memperhitungkan fungsi hidraulika tanah. Maka Persamaan 2.15 dapat dituliskan kembali seperti pada Persamaan 2.16a.

$$FS = \frac{c'}{\gamma_t \cdot z_f \cdot \sin\beta \cdot \cos\beta} + \frac{\tan\phi'}{\tan\beta}\left[1 + \frac{\psi \cdot \Theta}{\gamma_t \cdot z_f \cdot \cos^2\beta \cdot}\right] \qquad (2.16a)$$

dengan, $\Theta = \dfrac{\theta(\psi) - \theta_r}{\theta_s - \theta_r}$ (2.16b)

dengan θ_r dan θ_s masing-masing adalah kadar air jenuh air dan residu.

BAB III
TUJUAN DAN MANFAAT PENELITIAN

A. Tujuan Penelitian

Tujuan utama dari penelitian ini adalah untuk mengkaji pengaruh iklim saat ini (*present*) dan yang akan datang (*future*) terhadap unjuk kerja lereng. Secara rinci tujuan penelitian dapat diuraikan sebagai berikut ini.

Tahun ke-1 :

(1) Mempelajari pengaruh rekaman hujan terhadap stabilitas lereng,
(2) Mengkaji pengaruh hujan pada musim basah terhadap stabilitas lereng,
(3) Mempelajari hubungan antara kedalaman muka air tanah terhadap stabilitas lereng,
(4) Menyusun skenario perubahan iklim untuk hujan bulanan rata-rata pada tahun 2020 – 2040 di area D.I. Yogyakarta,
(5) Mengkaji dampak skenario perubahan iklim terhadap stabilitas lereng pada tahun 2020 – 2040.

Tahun ke-2 :

(6) Mengkaji kuat tarik akar rumput dan faktor-faktor yang mempengaruhinya pada lereng,
(7) Mempelajari pengaruh akar vegetasi terhadap stabilitas lereng.

Tahun ke-3 :

(8) Mengembangkan dan menvalidasi prosedur model numerik iklim pada lereng.
(9) Menyusun grafik desain praktis guna mengevaluasi unjuk kerja lereng akibat pengaruh hujan, kondisi vegetasi, dan morfologi lereng.

B. Manfaat Penelitian

Penelitian ini dapat digunakan :

d. untuk memperkirakan (*forecast*) kondisi lereng alam (*natural slope*) dan lereng buatan (*engineered slope*) di masa yang akan datang.
e. untuk menentukan pemilihan metode mitigasi lereng.
f. untuk monitoring dan evaluasi lereng di dekat infrastruktur penting seperti jalan raya, jalan tol, dan permukiman.

BAB IV
METODE PENELITIAN

A. Desain Penelitian

Desain penelitian secara keseluruhan dapat diilustrasikan dalam diagram alir pada Gambar 4.1. Mengacu pada *fishbone diagram* tersebut, penelitian dilaksanakan dalam tiga tahun pelaksanaan dengan uraian kegiatan dan target luaran seperti diringkaskan dalam Tabel 4.1. Sedangkan desain penelitian pada Tahun I secara skematik dijelaskan pada Gambar 4.2.

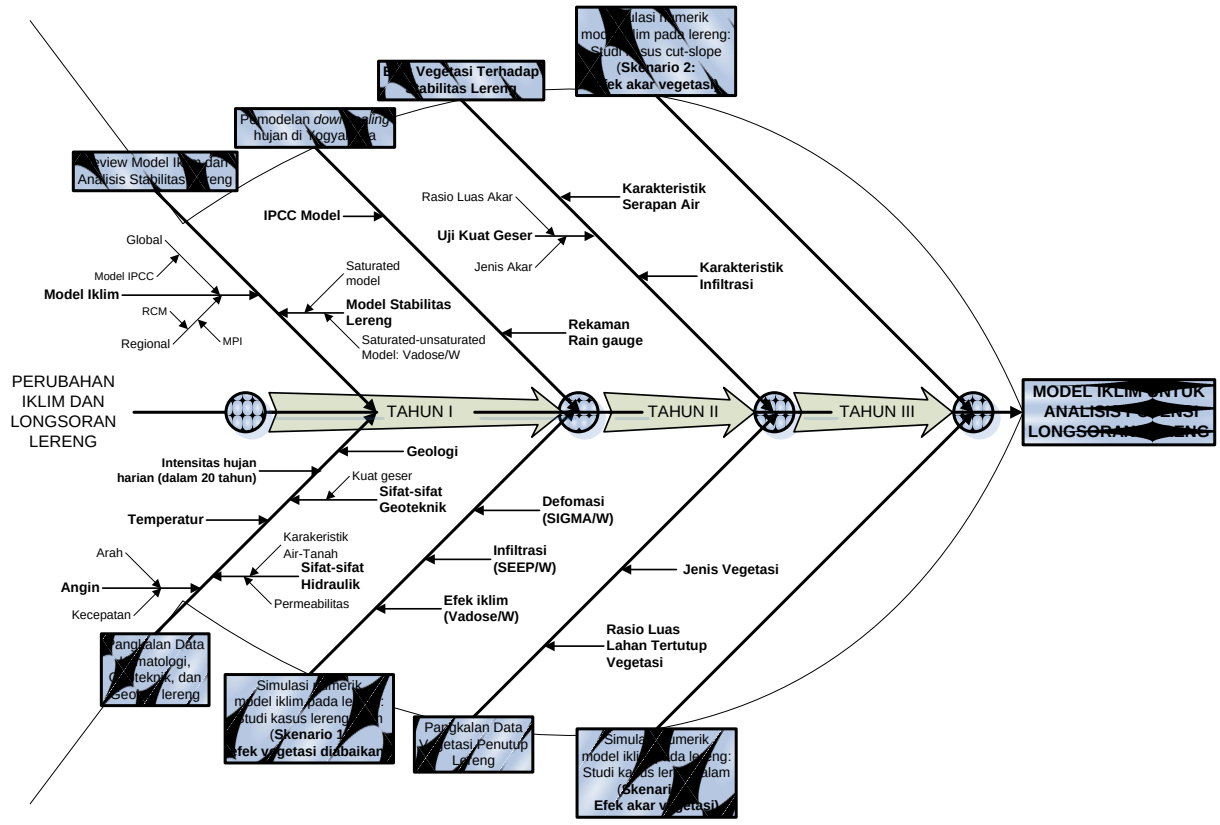

Gambar 4. 1 Diagram alir tahapan pelaksanaan kegiatan.

Kejadian longsor pada lereng di Dusun Kedungrong (Gambar 4.3), Kecamatan Samigaluh, Kulonprogo pada 21 November 2001 merupakan studi kasus yang menarik untuk dikaji. Pada area ini hampir di setiap musim penghujan terjadi pergerakan tanah. Kajian terhadap mekanisme longsoran dan faktor-faktor yang mempengaruhinya telah dikaji dengan pemodelan numerik oleh Muntohar dan Ikhsan (2012). Pada area ini dilakukan kajian terhadap potensi pergerakan tanah dengan menggunakan model probabilitas setelah kejadian

longsor pada tahun 2001. Untuk lokasi studi di Dusun Kalisonggo, Kecamatan Kalibawang, Kulonprogo (Gambar 4.3), kajian yang dilakukan adalah pemodelan numerik untuk menentukan pengaruh kedalaman awal muka air tanah terhadap perubahan stabilitas lereng. Karena pada kajian terdahulu oleh tidak memperhatikan kondisi awal muka air tanah (*initial groundwater level*).

Tabel 4. 1 Uraian kegiatan dan target luaran penelitian tiap tahun

Tahun Pelaksanaan	Uraian Kegiatan	Target Luaran
Tahun I	1. review model iklim dan analisis stabilitas lereng, 2. penyusunan pangkalan data klimatologi (hujan, temperatur, angin), 3. pengumpulan dan pengujian laboratorium sifat-sifat geoteknik dan hidraulik tanah, 4. pengukuran topografi lereng dan potensi bidang pergerakan tanah, 5. analisis *downscaling* pemodelan hujan, dan 6. simulasi numerik model iklim terhadap stabilitas lereng.	Publikasi Jurnal Terakreditasi/ Seminar Nasional
Tahun II	1. penyusunan pangkalan data vegetasi pada lereng, 2. pengujian laboratorium kuat geser tanah dan akar tanaman pada lereng, 3. pengukuran karakteristik kadar air-tanah-akar di lapangan, 4. pengukuran potensi bidang pergerakan tanah,	Draft Naskah Jurnal Internasional
Tahun III	1. pengukuran karakteristik kadar air-tanah-akar di lapangan, 2. pengukuran potensi bidang pergerakan tanah, 3. simulasi numerik model iklim dan akar tanaman terhadap stabilitas lereng.	Draft Buku/Monograf tentang Pemodelan Iklim dan Stabilitas Lereng

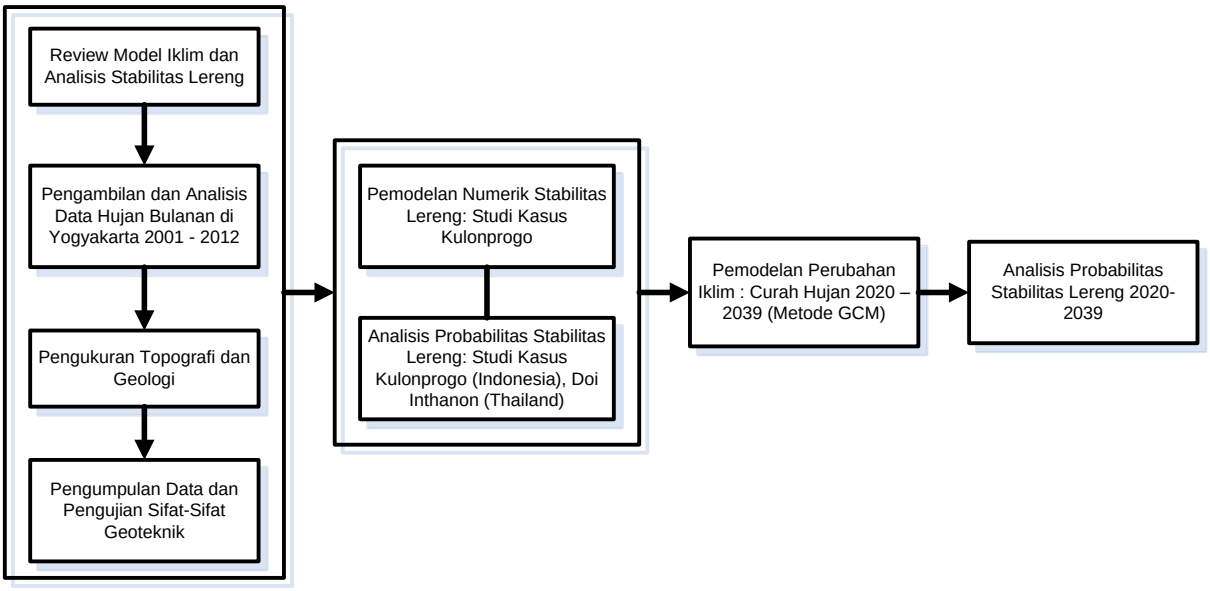

Gambar 4.2 Diagram alir penelitian pada tahun pertama

Lokasi studi untuk area Doi Inthanon, Thailand (Gambar 4.4) berada di bagian utara Thailand. Kejadian longsoran memiliki kemiripan dengan tipe longsoran di Kulonprogo. Kajian longsoran di area Doi Inthanon dilakukan untuk mengkaji pengaruh rekaman hujan

(*hyetograph*) terhadap stabilitas lereng dengan metode probabilitas. Kajian di lokasi ini merupakan kerjasama dengan Geotechnical Engineering Division, di Department of Civil Engineering, Kasetsart Univeristy, Thailand (**Lampiran A**).

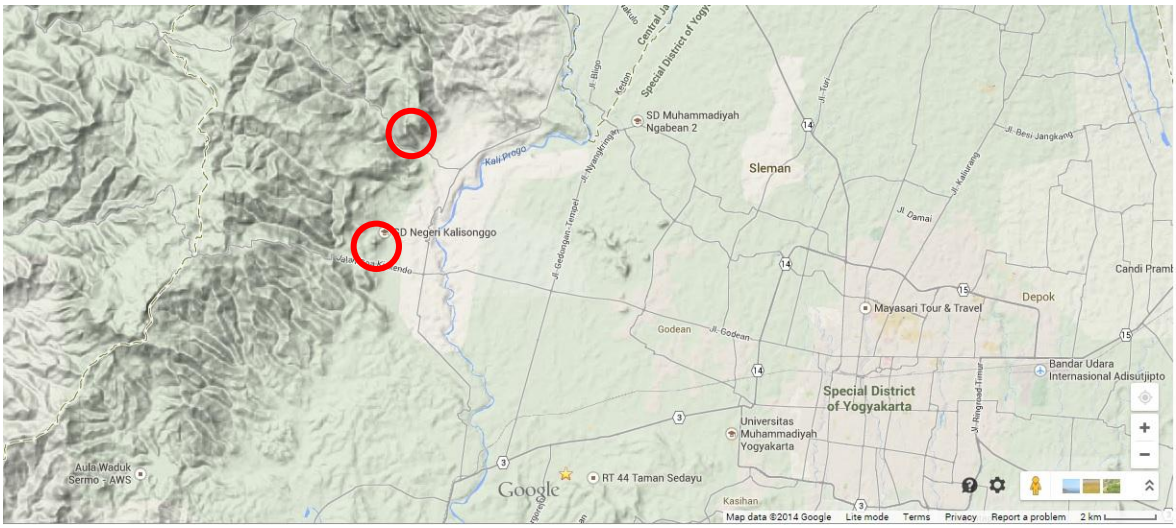

Gambar 4. 3 Lokasi penelitian di Kulonprogo (Indonesia)

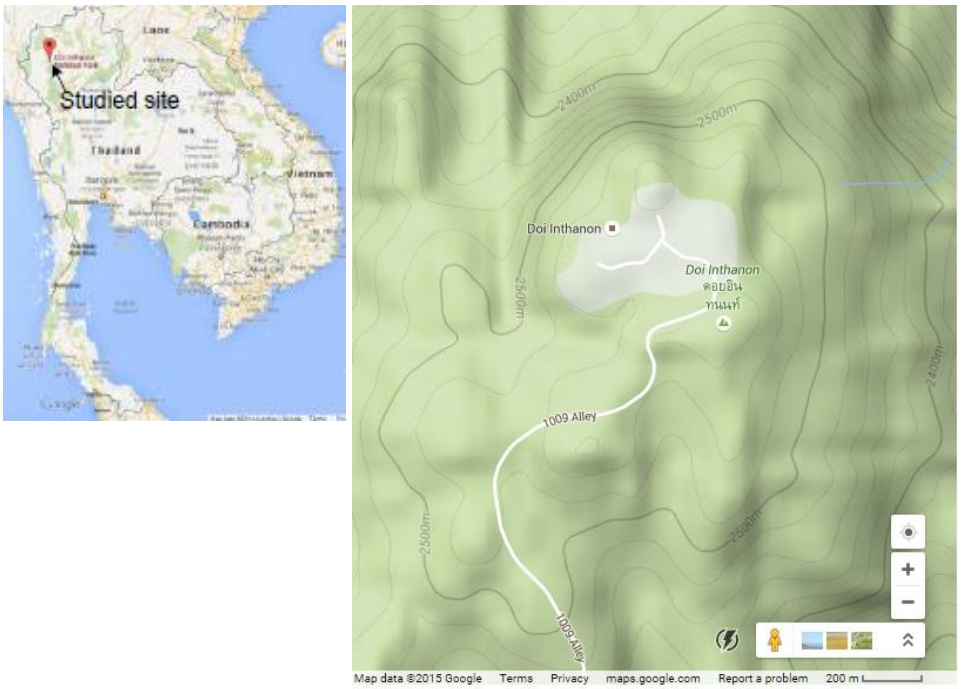

Gambar 4. 4 Lokasi penelitian di Doi Inthanon, Thailand

B. Data Curah Hujan

Data curah hujan seperti disajikan pada Gambar 4.5dan 4.6 masing-masing untuk area Kulonprogo dan Doi Inthanon. Pada Gambar 4.5 disajikan distribusi hujan harian maksimum pada setiap bulan yang diambil dari stasiun pengukur hujan pada koordinat

7.40.33.LS/110.15.49.BT. Sedangkan data curah hujan untuk wilayah Doi Inthanon disediakan oleh Jotisankasa et al. (2015). Curah hujan diukur dari stasiun hujan terdekat pada tanggal 1 - 14 September 2011. Interval waktu pengukuran curah hujan adalah setiap 5 menit (Gambar 4.6a). Rekan hujan dalam interval waktu 1 jam, dan harian seperti pada Gambar 4.6b dan 4.6c. Kumulatif hujan selaam 2 minggu mencapai 520 mm.

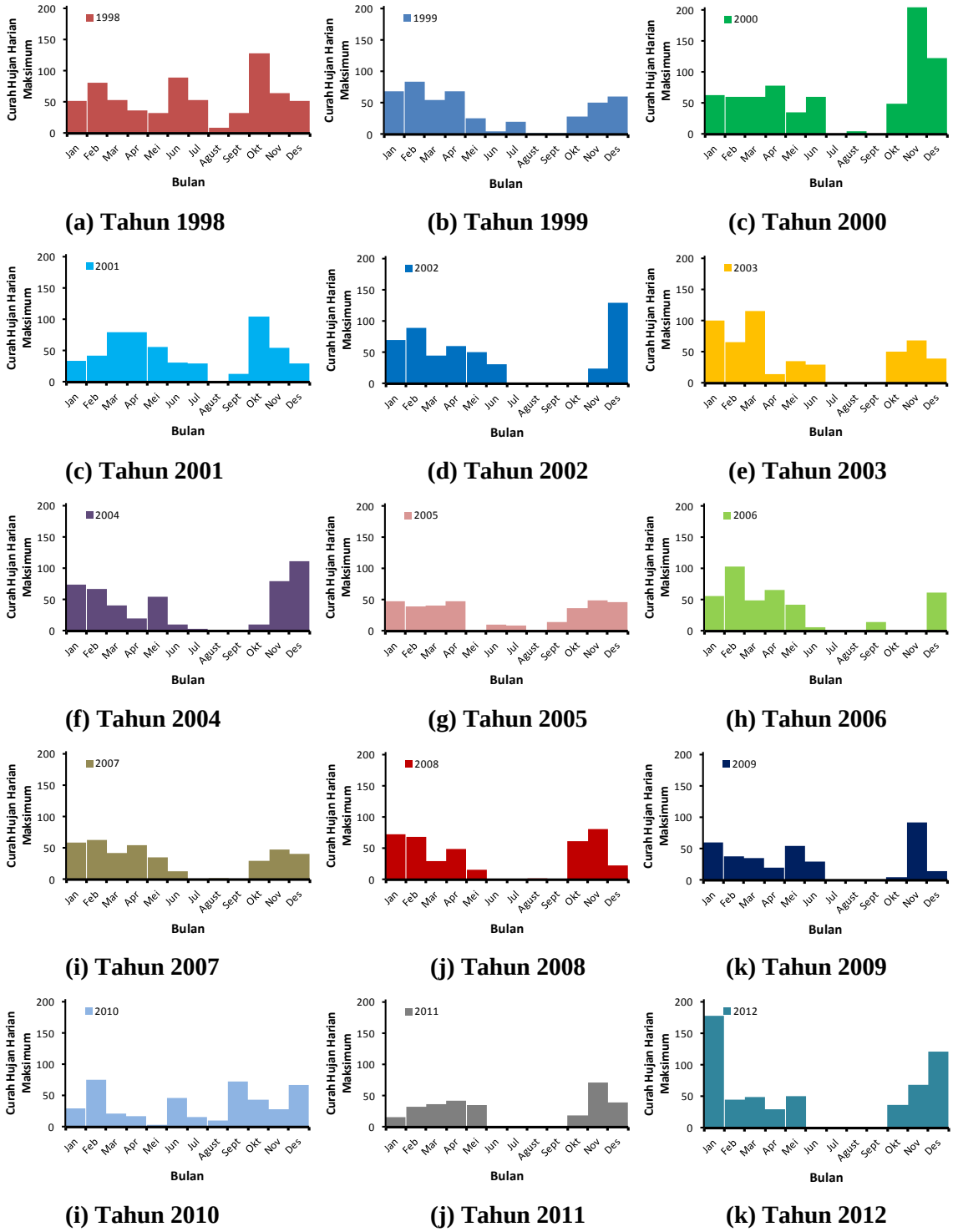

(a) Tahun 1998 **(b) Tahun 1999** **(c) Tahun 2000**

(c) Tahun 2001 **(d) Tahun 2002** **(e) Tahun 2003**

(f) Tahun 2004 **(g) Tahun 2005** **(h) Tahun 2006**

(i) Tahun 2007 **(j) Tahun 2008** **(k) Tahun 2009**

(i) Tahun 2010 **(j) Tahun 2011** **(k) Tahun 2012**

Gambar 4. 5 Distribusi curah hujan harian maksimum Tahun 1998 – 2012 di lokasi Kulonprogo

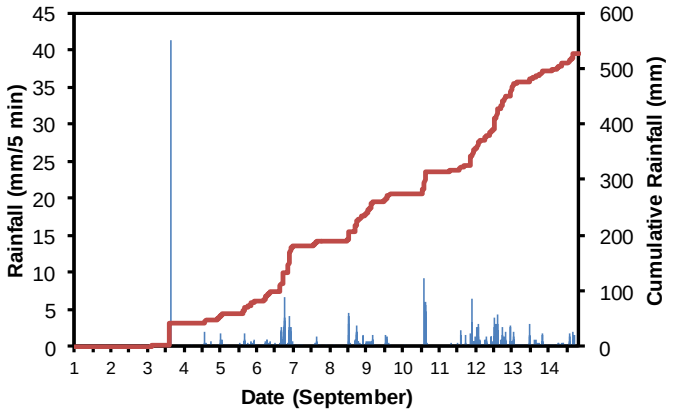

(a)

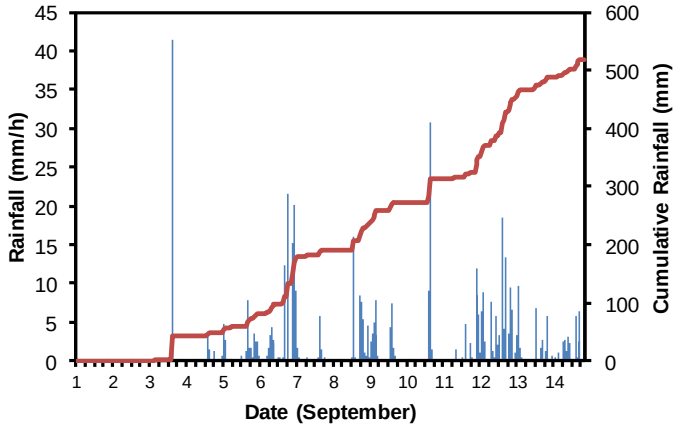

(b)

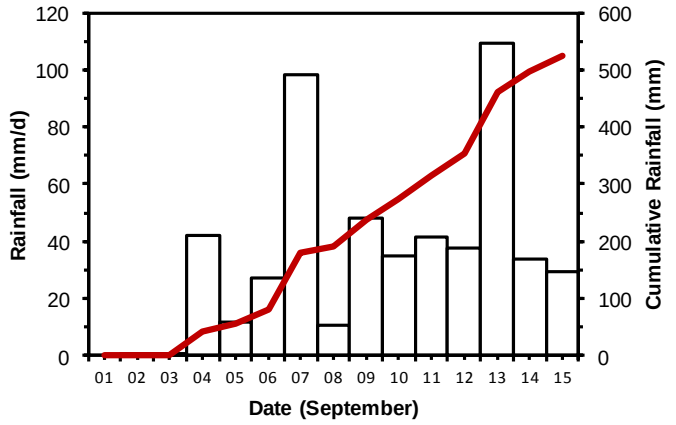

(c)

Gambar 4. 6 Distribusi hujan lokasi Doi Inthanon (a) hujan 5 menitan, (b) hujan jam-jaman, (c) hujan harian

C. Data Geoteknik Lereng

Lereng yang berlokasi di Dusun Kedungrong, Samigaluh, Kulonprogo memiliki kemiringan rata-rata 22^o, dengan kemiringan yang tercuram sebesar 40^o. Lereng memiliki lapoisan tanah berupa tanah residu yang berasal dari pelapukan batuan breksi. Ketebalan lapisan tanah rata-rata (*H*) adalah 8 m, dengan berat volume tanah (γ_t) 22 kN/m^3. Sifat-sifat geoteknik tanah dan lapisan batuan di lokasi Kedungrong seperti disajikan pada Tabel 4.2.

Lereng di lokasi Dusun Kalisonggo, Kulonprogo berkisar anatar 20^o hingga 40^o. Lapisan tanah dengan ketebalan hingga 10 m didominasi oleh lapisan tanah colluvial yang merupakan pelapukan dari batuan breksi-andesit (CH1), lapisan lempung yang berasal dari pelapukan tuffa (CH2), dan lapisan batuan lanau (MH1). Tabel 4.3 menyajikan sifat-sifat geoteknik tanah dan lapisan batuan di lokasi Kalisonggo.

Tabel 4. 2 Parameter tanah untuk lereng di Kedungrong, Kulonprogo

Parameter	Tanah Residu	Breksi	Batuan keras
Kadar air asli, w_N(%)	33,2	39,4	40,2
Berat volume tanah, γ_b (kN/m^3)	17,7	15,1	14,8
Berat volume kering, γ_d (kN/m^3)	13,4	12,1	11,7
Derajat jenu air, S_r (%)	90,1	64,8	41,9
Kadar air volumerik jenuh, θ_s	0,48	0,53	0,50
Koefisien permeabilitas jenuh, k_{sat} (m/s)	$1{,}19\text{x}10^{-4}$	$1{,}74\text{x}10^{-8}$	-
Kohesi (puncak), c' (kPa)	1.7	48	-
Sudut gesek internal (puncak), ϕ' (_^{o})	19,6	10	-
Sudut peningkatan kuat geser tak jenuh, ϕ^b (_^{o})	15	8	-

Tabel 4.3 Parameter kuat geser dan hidraulika tanah di lokasi Kalisonggso, Kulonprogo

Parameter	Tanah MH-1	Tanah CH-1	Tanah CH-2	Batuan keras
Berat volume, γ_b (kN/m^3)	15,95	15,96	15,85	
Kohesi, c' (kPa)	4,875	4,1125	5,45	*Bedrock*
Sudut gesek internal, ϕ'	$25{,}5^o$	$7{,}87^o$	$18{,}74^o$	
Koefisien permeabilitas jenuh air, k_{sat} (m/d)	$5{,}63 \times 10^{-5}$	$9{,}62 \times 10^{-5}$	$2{,}8\times 10^{-4}$	$1{,}00 \times 10^{-8}$
Kadar air volumetrik jenuh air, θ_{sat} (m^3/m^3)	0,592	0,575	0,576	0,299

Karakteristik hidraulik tanah residu di area Kedungrong diuji dengan alat *miniature KU tensiometer* (untuk *suction* ψ < 100 kPa) dan filter paper (untuk *suction* ψ > 100 kPa) guna memperoleh kurva karakteristik kadar air (*Soil-Water Characteristics Curve, SWCC*). *Filter paper* yang digunakan adalah Whatman No. 42 yang dikalibrasi ASTM D5298. Gambar 4.7 dan 4.8 menggambarkan skema dari peralatan tensiometer dan filter paper yang digunakan dalam penelitian. Ukuran benda uji yang digunakan untuk uji *SWCC* adalah berdiameter 63 mm dan ketebalan 20 mm sesuai dengan prosedur yang dijelaskan dalam Jotisankasa et al. (2010b). Benda uji mengalami pembasahan secara bertahap, dan setiap tahapan pembasahan nilai suction diamati hingga mencapai nilai konstan. Durasi setiap tahapan pembahasan berkisar antara 2-3 hari. Gambar 4.9 hingga 4.11 menyajikan *SWCC* dari lokasi di Kedungrong, Kalisonggo, dan Doi Inthanon. Untuk lokasi di Kalisonggo, *SWCC* dihasilkan dari pengujian menggunakan metode *filter paper* saja, sedangkan untuk lokasi di Kedungrong menggunakan gabungan metode *miniature KU tensiometer* dan *filter paper*.

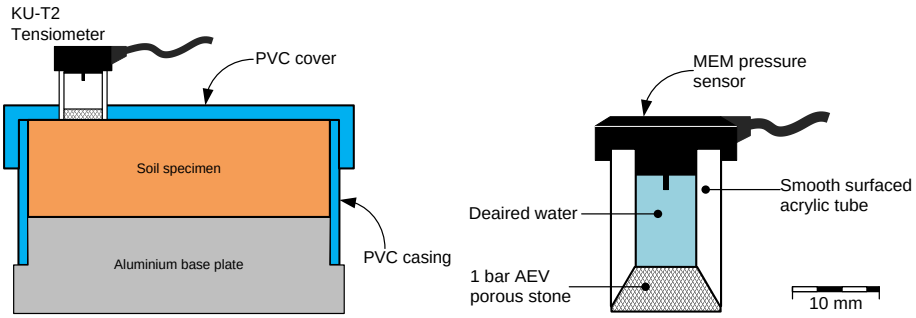

(b) (b)

Gambar 4.7 (a) Skema penampang pengujian SWCC menggunakan *KU tensiometer*, (b) Skema penampang *KU tensiometer*.

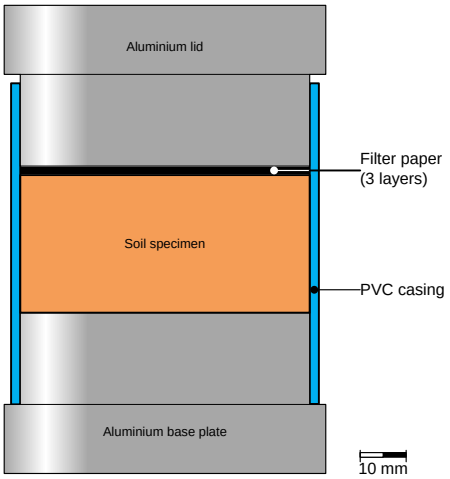

Gambar 4.8 Skema penampang pengujian SWCC menggunakan *filter paper*.

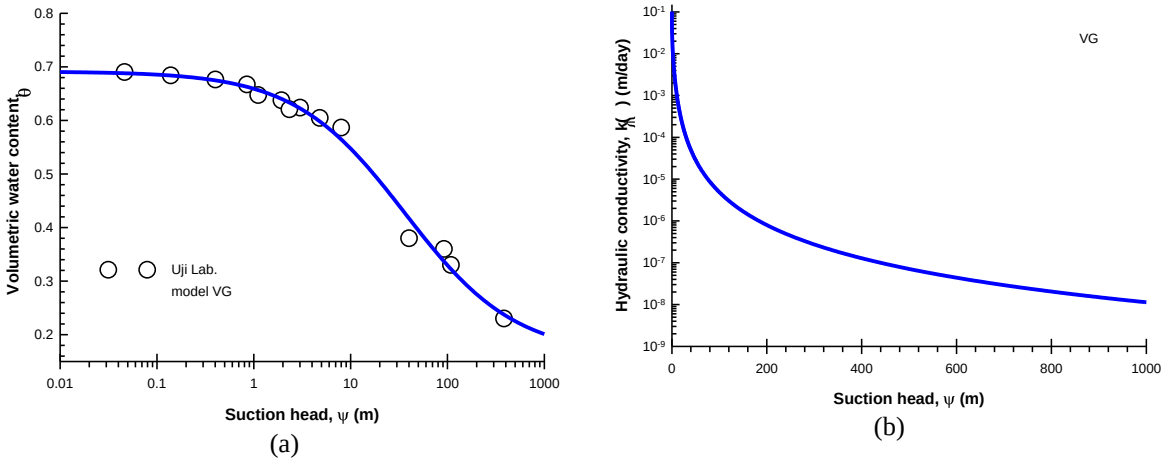

(a) (b)

Gambar 4. 9 (a) Kurva kadar air volumetrik, (b) Kurva koefisien permeabilitas tanah residu di Kedungrong.

Variabel yang digunakan untuk analisis probabilitas di lokasi Doi Inthanon, berupa topografi dan data geoteknik, diperoleh dari Jotisankasa et al. (2015). Lereng tersusun dari pelapukan atau dekomposisi batuan granite berupa lapisan tanah pasir berlempung (*SC*) berwarna kemerahan, dan pasir berlanau (*SM*) berwarna keputih-putihan. Bongkahan batuan

granite bercampur dengan lapisan tanah. Lapisan tanah kedap air atau batuan diperoleh hingga kedalaman 2 m. Sifat-sifat geoteknik dari lapisan tanah seperti disajikan pada Tabel 4.4. Kurva karakteristik kadar air tanah seperti disajikan pada Gambar 4.11.

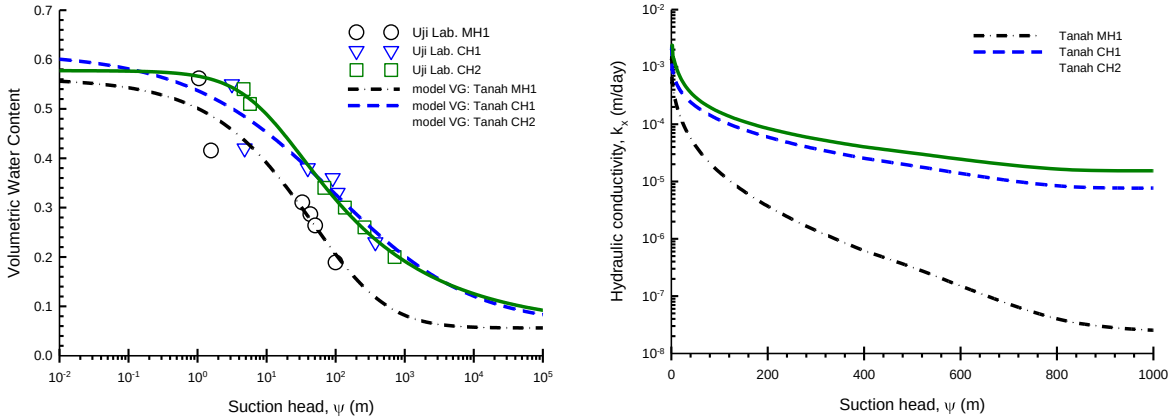

(a) (b)

Gambar 4. 10 (a) Kurva kadar air volumetrik, (b) Kurva koefisien permeabilitas tanah coluvial di Kalisonggo

Tabel 4. 4 Soil properties of the slope

Jenis tanah	Kemiringan lereng α	Koefisien permeabilitas k_s (mm/h)	Beda kadar air $\Delta\theta = \theta_s - \theta_i$	Suction zona basah ψ_f (mm)	Kohsi c' (kPa)	Sudur gesek ϕ'	Berat volume tanah γ_t (kN/m^3)
SM	33^o	91.8	0.32	300	10.1	26.7^o	21.8
SC	33^o	0.4248	0.29	400	15.3	22.7^o	20

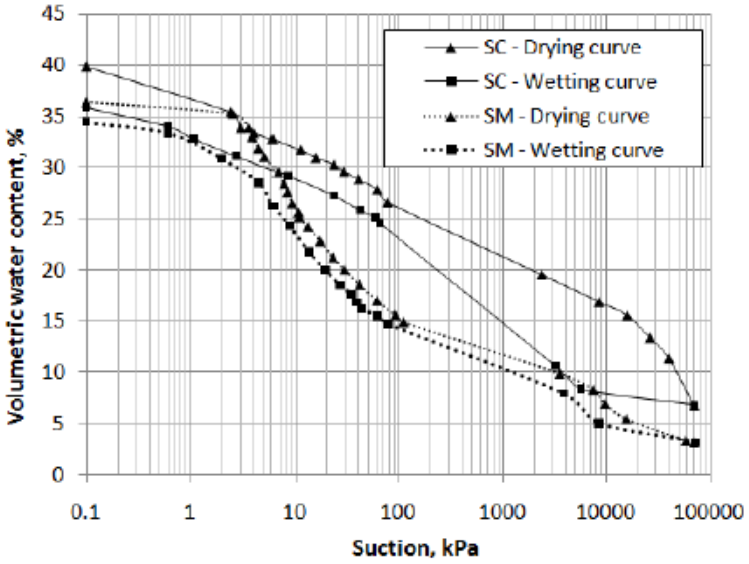

Gambar 4.11 Kurva kadar air volumetrik tanah untuk lokasi di Doi Inthanton (Jotisanka et al., 2015)

D. Analisis Probabilitas

1. Model Infiltrasi – Stabilitas Lereng

Analisis infiltrasi 1D dan stabilitas lereng dilakukan berdasarkan model infiltrasi Green – Ampt sebagaimana telah diuraikan dalam Bab II Tinjauan Pustaka. Penyelesaian model infiltrasi dijelaskan pada diagram alir Gambar 4.12. Sedangkan penyelesaian tekanan air pori dan stabilitas lereng seperti disajikan pada Gambar 4.13. Diagram alir ini merupakan perbaikan dari alur yang diselesaikan oleh Muntohar dan Liao (2010). Perangat lunak MATLAB version 7.6.0.324 R2008a digunakan untuk penghitungan.

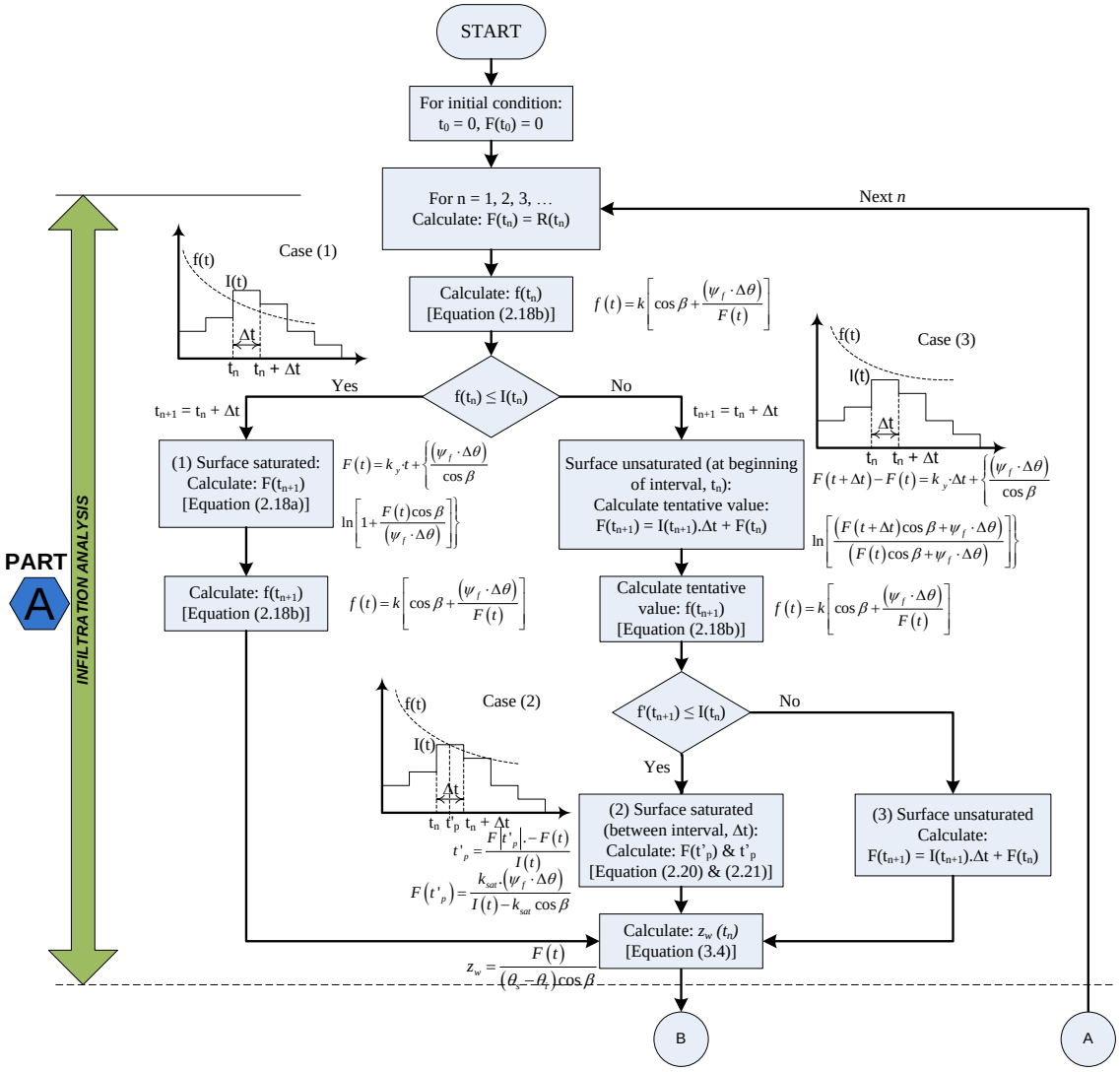

Gambar 4. 12 Diagram alir untuk analisis infiltrasi air hujan pada lereng (Muntohar & Ikhsan, 2013)

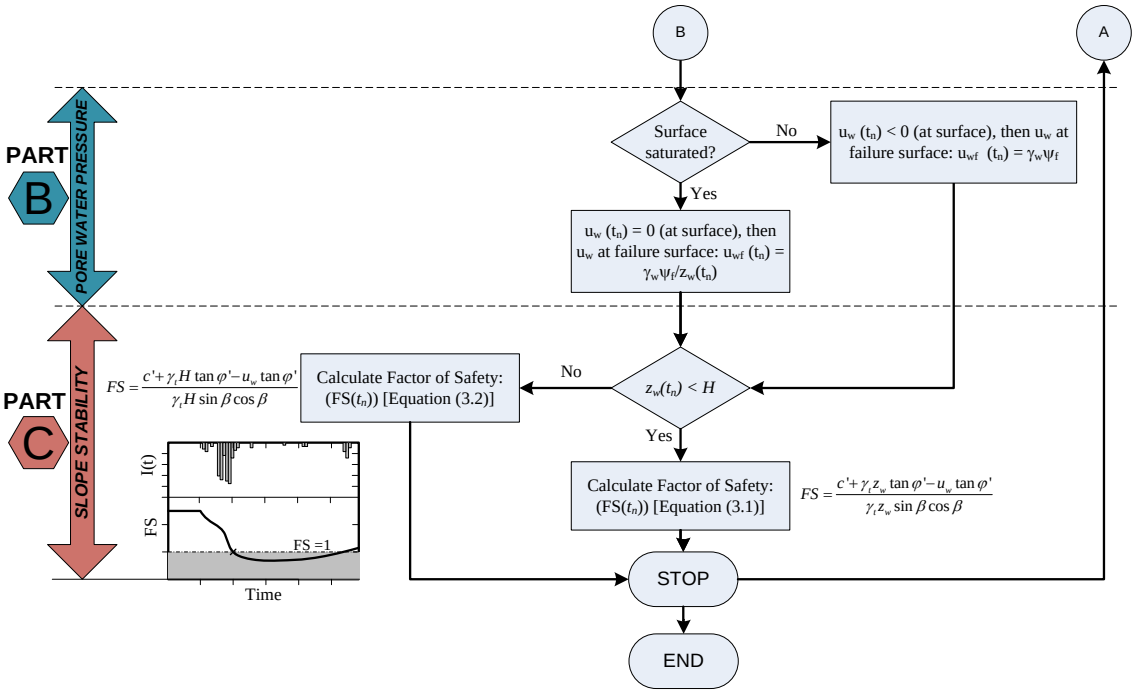

Gambar 4. 13 Diagram alir untuk analisis infiltrasi air hujan pada lereng (Muntohar & Ikhsan, 2013)

2. Analisis Realiabilitas Stabilitas Lereng

Keandalan atau reliabilitas (*reliability*) adalah probabilitas (*probability*) suatu obyek atau sistem yang unjuk kerjanya memenuhi fungsi yang sesuai untuk suatu kondisi dan periode waktu tertentu (Harr, 1989). Dengan demikin dalam hal ini, reliabilitas suatu lereng merupakan probabilitas yang menyatakan kondisi lereng tetap stabil dibawah kondisi tertentu. Dalam analisis reliabilitas, fungsi unjuk kerja $G(X)$ lereng dapat dinyatakan dengan persamaan faktor aman seperti pada persamaan 4.1.

$$G(X) = \frac{c' + \left(\gamma_t z_w \cos^2\alpha - u_w\right)\tan\phi'}{\gamma_t z_w \sin\alpha \cos\alpha} \quad \text{..... (4.1)}$$

Variabel $X = \{x_{1\ldots n}\}$ terdiri atas n variabel acak sebagai parameter masukan dalam analisis stabilitas lereng. Variabel-variable tersebut adalah $X_i = \{\alpha_i, c_i', \phi'_i, \gamma_{t,i}, H_{b,i}, k_{s,i}, \psi_{f,i}, \Delta\theta_i\}$. Fungsi $G(X,t)$ menyatakan unjuk kerja atau kondisi dari lereng yang merupakan fungsi dari waktu t. Suatu lereng dinyatakan stabil apabila $G(X,t) > 0$, sebaliknya dinyatakan tidak stabil atau mengalami keruntuhan apabila $G(X,t) < 1$, dan berada dalam kondisi batas jika $G(X,t) = 1$, yang mana disebut kondisi batas lereng.

Pada penelitian ini, metode *Direct Monte Carlo Simulation* (*MCS*) digunakan untuk menentukan probabilitas keruntuhan. Nilai dari setiap variabel diambil secara acak sebagai

data *identically-independent distribution* (i.i.d) dari fungsi distribusi probabilitasnya atau probability distribution function (*PDF*) untuk setiap *N* –kali simuasi. Jumlah simulasi yang dilakukan adalah N = 10.000. Distribusi setiap parameter didekati dengan fungsi distribusi probabilitas *lognormal* PDF (Muntohar & Ikhsan, 2012).

Indek reliabilitas β terhadap stabilitas lereng dapat dinyatakan dalam persamaan 4.2. apabila distribusi probabilitas dari faktor aman berupa fungsi distribusi normal. Sedangkan apabila distribusi probabilitas dari faktor aman berupa fungsi distribusi lognormal, nilai β diberikan oleh persamaan 4.3.

$$\beta = \frac{\mu_{FS(X,t)} - 1}{\sigma_{FS(X,t)}} \tag{4.2}$$

$$\beta = \frac{\ln\left[\mu_{FS(X,t)} \Big/ \sqrt{1+\left(\sigma_{FS(X,t)} \Big/ \mu_{FS(X,t)}\right)^2}\right]}{\sqrt{\ln\left[1+\left(\sigma_{FS(X,t)} \Big/ \mu_{FS(X,t)}\right)^2\right]}} \tag{4.3}$$

dengan $\mu_{FS(X,t)}$ dan $\sigma_{FS(X,t)}$ adalah nilai rerata dan deviasi standar dari faktor aman hasil simulasi Monte Carlo. Kemudian, probabilitas keruntuhan dapat dihitung dari nilai index realibilitas yang telah diperoleh dari persamaan 4.2 atau 4.3 dengan menggunakan persamaan 4.4. Probabilitas keruntuhan didefinisikan sebagai probabilitas untuk faktor aman minimum kurang dari satu yaitu $P_f = P(FS < 1)$.

$$P_f = 1 - \Phi(\beta) \tag{4.4}$$

dengan, $\Phi(\beta)$ adalah fungsi distribusi kumulatif untuk masing-masing jenis distribusi probabilitas (*normal* atau *lognormal PDF*) dari nilai β.

Untuk area Kulonprogo, analisis probabilitas keruntuhan lereng dilakukan dalam periode waktu musim penghujan basah pada bulan Desember – Maret mulai dari tahun 2000 – 2012. Rekaman curah hujan harian dalam interval waktu tersebut seperti disajikan pada Gambar 4.14. Dalam rentang musim penghujan basah tersebut, kumulatif hujan berkisar dari 480 mm hingga 2000 mm. Hujan terendah terjadi pada periode waktu Desember 2009 – Maret 2010 (Gambar 4.14j), dan hujan tertinggi pada Desember 2002 – Maret 2003 (Gambar 4.14c).

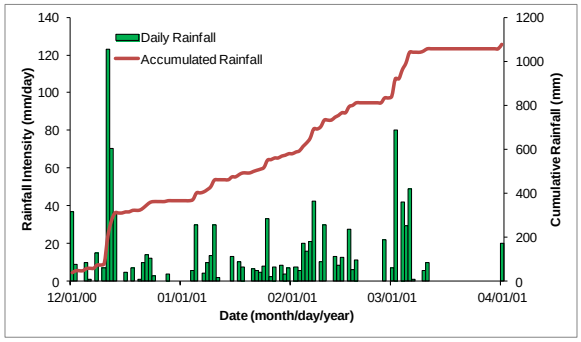

(a) Desember 2000 – Maret 2001

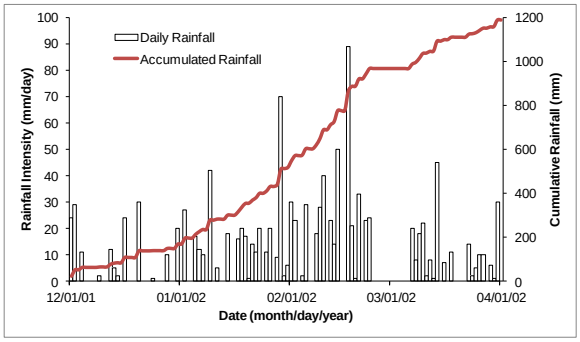

(b) Desember 2001 – Maret 2002

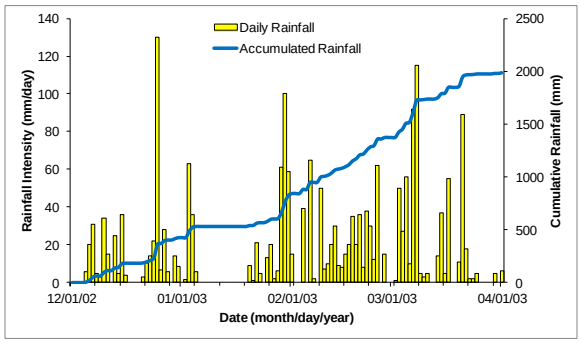

(c) Desember 2002 – Maret 2003

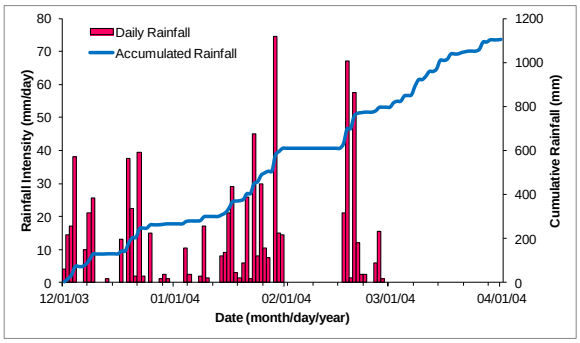

(d) Desember 2003 – Maret 2004

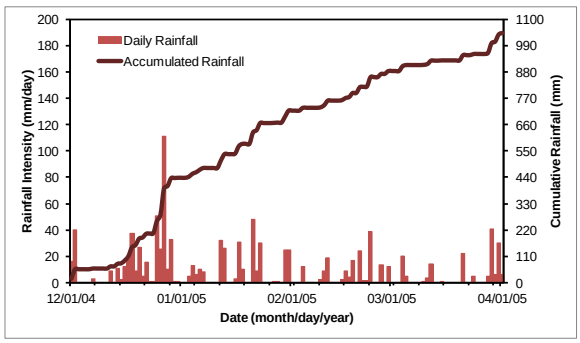

(e) Desember 2004 – Maret 2005

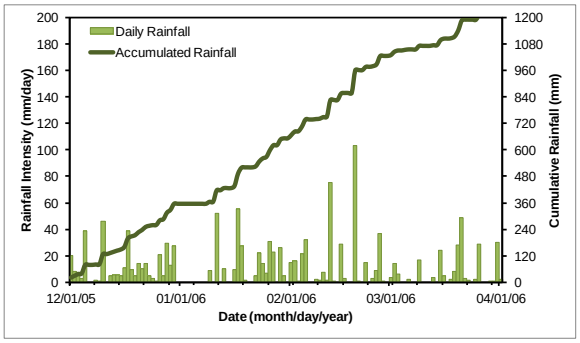

(f) Desember 2005 – Maret 2006

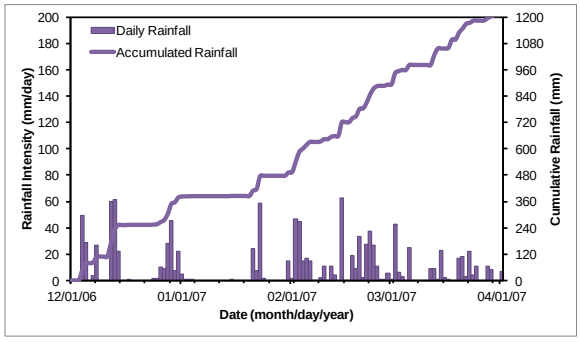

(g) Desember 2006 – Maret 2007

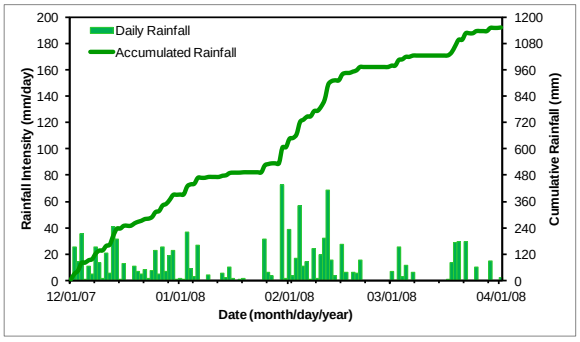

(h) Desember 2007 – Maret 2008

Gambar 4.14 Rekaman curah hujan harian pada musim penghujan basah Desember - Maret

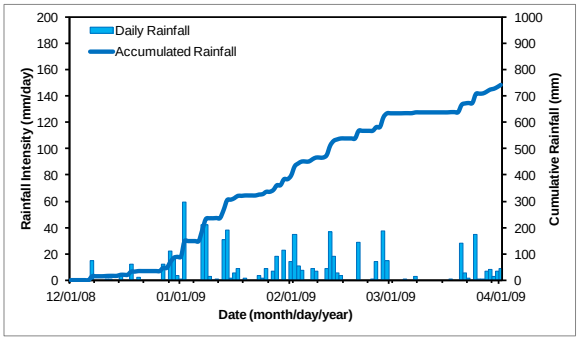

(i) Desember 2008 – Maret 2009

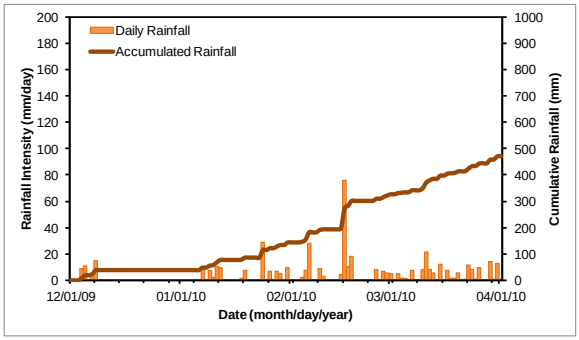

(j) Desember 2009 – Maret 2010

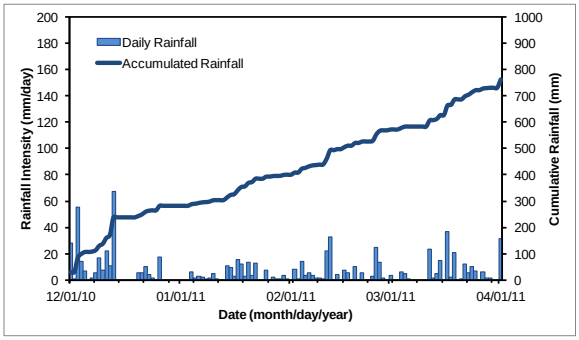

(k) Desember 2010 – Maret 2011

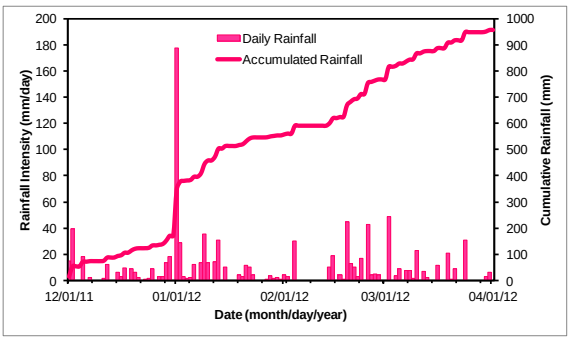

(l) Desember 2011 – Maret 2012

Gambar 4.14 (Lanjutan)

E. Pemodelan Numerik

1. Geometri Lereng di Kalisonggo, Kulonprogo

Penampang lereng yang dianalisis seperti disajikan pada Gambar 4.15a. Litologi lereng didominasi oleh lapisan lanau (MH-1) dan lempung (CH-1 dan CH-2). Lapisan tidak lolos air berupa batulempung (*claystones*) berada di bawah lapisan MH-1 sebagai batuan dasar (*bedrock*). Bidang keruntuhan terdapat pada bidang antara lapisan CH-1 dan MH-1. Parameter kuat geser dan hidraulika masing-masing contoh tanah seperti disajikan pada Tabel 4.3 dan Gambar 4.10. Profil kuat geser lapisan tanah dan batuan dari hasil uji SPT seperti disajikan pada Gambar 4.15b.

2. Pemodelan Infiltrasi – Rembesan dan Stabilitas Lereng

Pada penelitian ini analisis infiltrasi-rembesan dimodelkan secara numerik dengan menggunakan perangkat lunak SEEP/W (Geoslope International, 2007a). Geometri lereng dan kondisi batas seperti digambarkan pada Gambar 4.15c. Elemen-elemen *triangular* sebanyak 8485 elemen berukuran lebar 2 m. Curah hujan didefinisikan sebagai *unit flux* (q) dalam fungsi waktu dengan intensitas seperti pada Gambar 4.16. *Unit flux* diberikan pada permukaan lereng dengan kondisi batas *seepage face review*. Sedangkan di bawah lapisan batulempung diberikan kondisi batas *no flow* sebagai *unit flux* $q = 0$ agar terjadi infiltrasi satu arah.

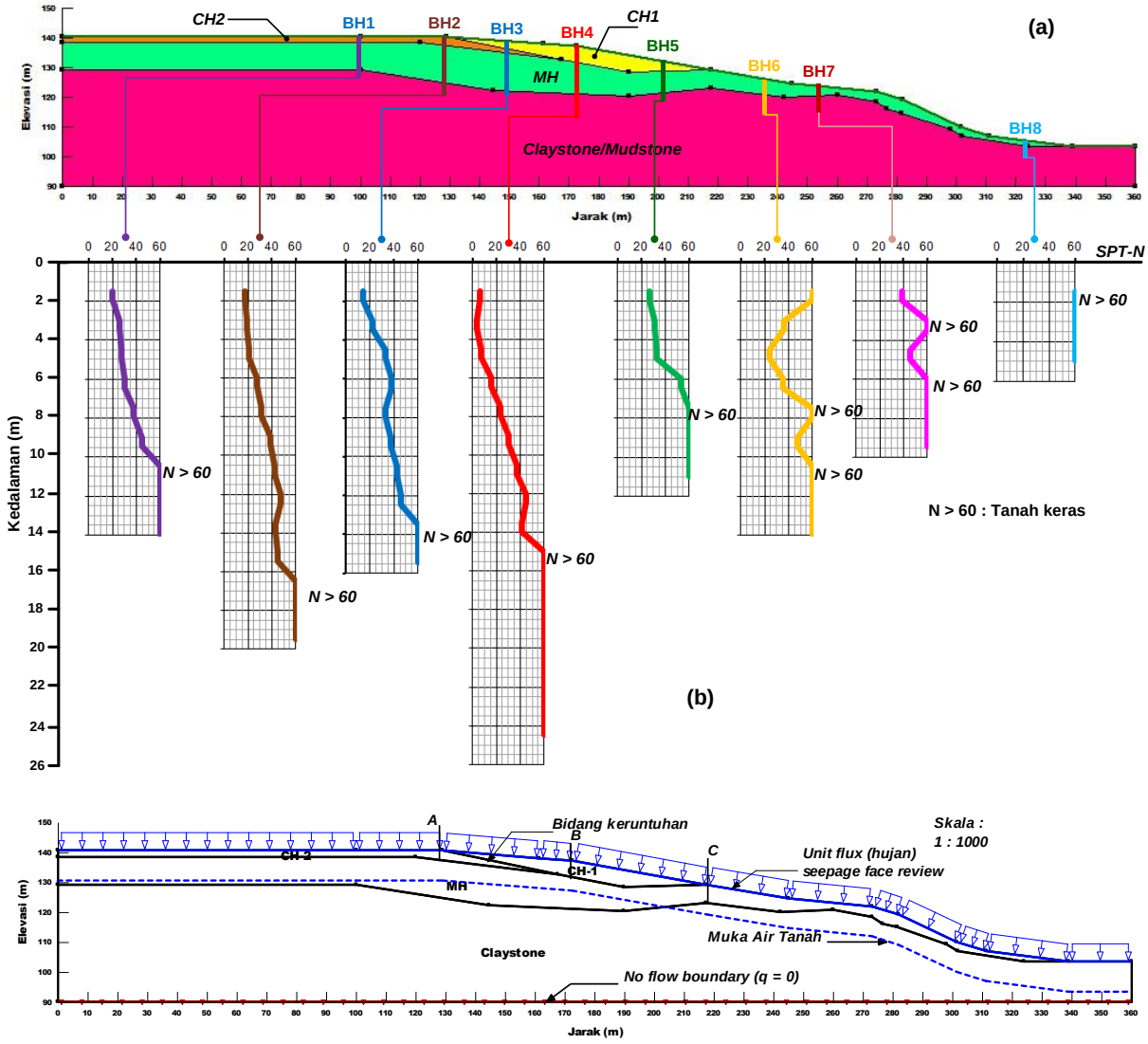

(c)

Gambar 4. 15 (a) Litologi lereng di Kalisonggo,(b) Profil nilai N-SPT, (c) Model lereng dan kondisi batas dalam analisis numerik.

Model analisis *transient* dimana tekanan air pori awal dibangkitkan dari muka air tanah dilakukan dalam interval waktu 1 hari selama 30 hari. Pada penelitian ini, kondisi muka air tanah awal divariasikan 1 m, 2 m, 3 m, 4 m, 5 m, dan 10 m. Untuk mengetahui pengaruh muka air tanah terhadap perubahan tekanan air pori dan stabilitas lereng, ditinjau dari 3 titik di masing-masing potongan yaitu di bagian atas bidang keruntuhan (**A**), di tengah bidang keruntuhan (**B**), dan di kaki bidang keruntuhan (**C**).

Analisis stabilitas lereng dimodelkan dengan SLOPE/W (Geoslope International, 2007b) yang didasarkan pada konsep keseimbangan batas (*limit equilibrium*). Stabilitas lereng dihitung dengan menggunakan metode Morgenstern – Price (MP) dimana bidang keruntuhan lereng telah ditentukan (*fully-specified slip surface*). Bidang keruntuhan seperti ditunjukkan pada Gambar 4.14b. Tekanan air pori dari SEEP/W diperhitungkan dalam tegangan geser

yang dianalisis oleh SLOPE/W seperti dalam persamaan 4.5. Dalam keadaan terjadi tekanan air pori negatif, nilai sudut gesek tanah tak jenuh air (ϕ^b) diperkirakan dari fungsi kurva kadar air volumetrik (Gambar 4.10a) sebagaimana dirumuskan oleh Vanapalli dkk. (1996) dalam persamaan 4.5. Kondisi ini memudahkan penghitungan faktor aman lereng untuk setiap interval waktu yang diberikan.

$$s = c' + (\sigma_n - u_a)\tan\phi' + (u_a - u_w)\left[\left(\frac{\theta_w - \theta_r}{\theta_s - \theta_r}\right)\tan\phi'\right] \quad (4.5)$$

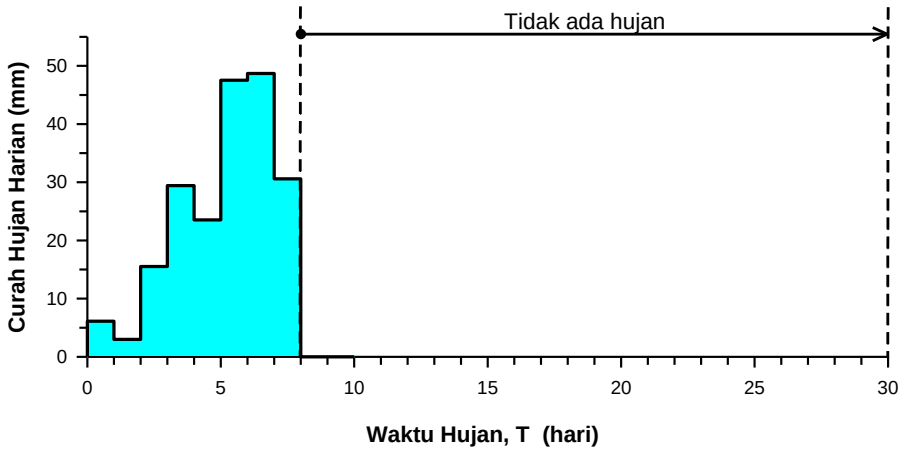

Gambar 4.16 Intensitas dan lama hujan.

3. Proyeksi Hujan Bulanan Rata-Rata pada Tahun 2020 – 2040

Perkiraan curah hujan bulanan rata-rata di area Kulonprogo untuk tahun 2020 – 2040 dilakukan dengan perangkat yang telah disediakan oleh *Climate Change Knowledge Portal* (Gambar 4.17). Pemodelan didasarkan pada model perubahan iklim GCM CMIP5 and CMIP3. Dalam penelitian ini, empat model perubahan iklim digunakan sebagai pembanding besarnya curah hujan bulanan rata-rata yaitu seperti disajikan pada Tabel 4.5. Sebagai pembanding hasil proyeksi digunakan data hujan bulanan rata-rata tahun 1998 – 2012 yang diambil dari stasium hujan Kalibawang (Gambar 4.18).

Tabel 4.5 Nama model perubahan iklim

Kelompok Model	Nama Model	Negara	Skenario Iklim
CMIP5	BCC-CSM1.1	China	*RCP*2.6
	CESM1 (CAM5)	Amerika Serikat	*RCP*4.5
	CSIRO-MK3.6.0	Australia	*RCP*6
	IPSL-CMSA-LR	Perancis	*RCP*8.5
CMIP3	CGCM3.1(T47)	Kanada	
	ECHAM5-MPI	Jerman	*A*2
	CSIRO-MK3.5	Australia	*B*1
	GFDL2.0	Amerika Serikat	

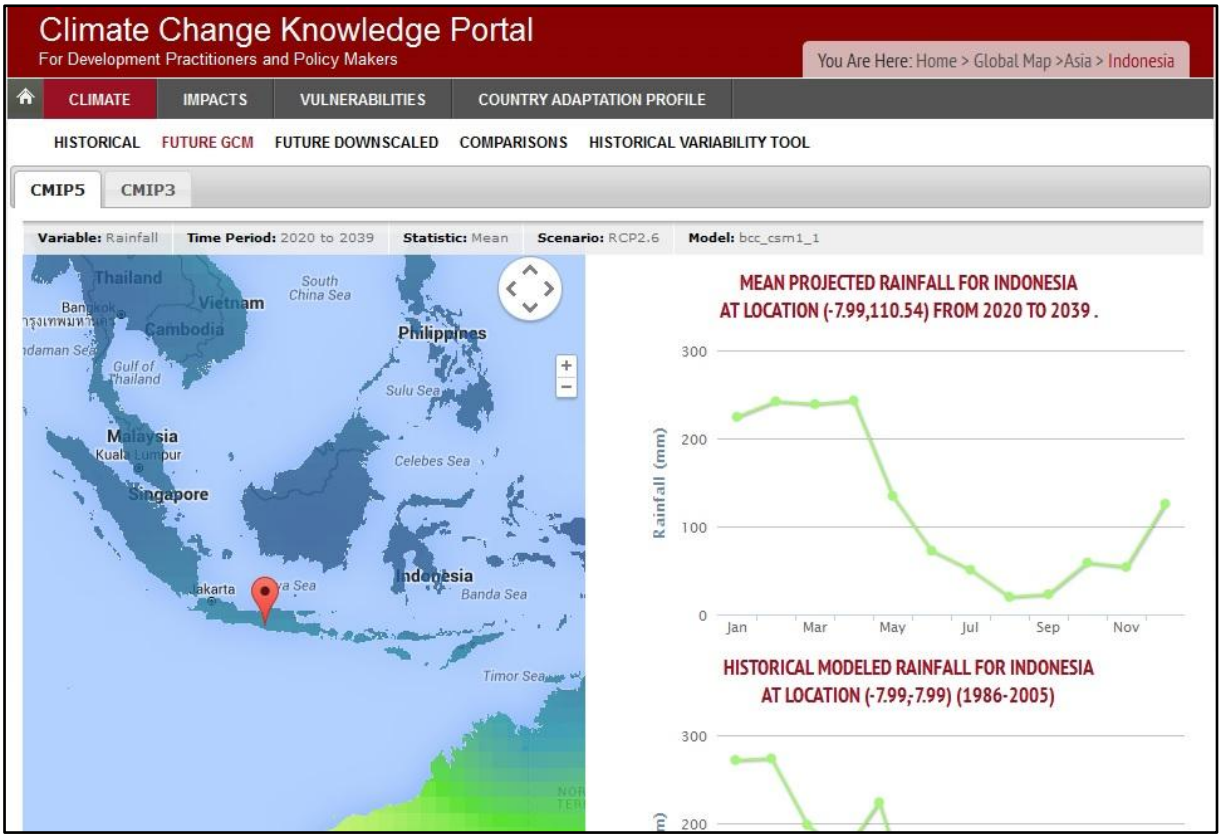

Gambar 4.17 Tampilan perangkat simulasi perubahan iklim *Climate Change Knowledge Portal*.

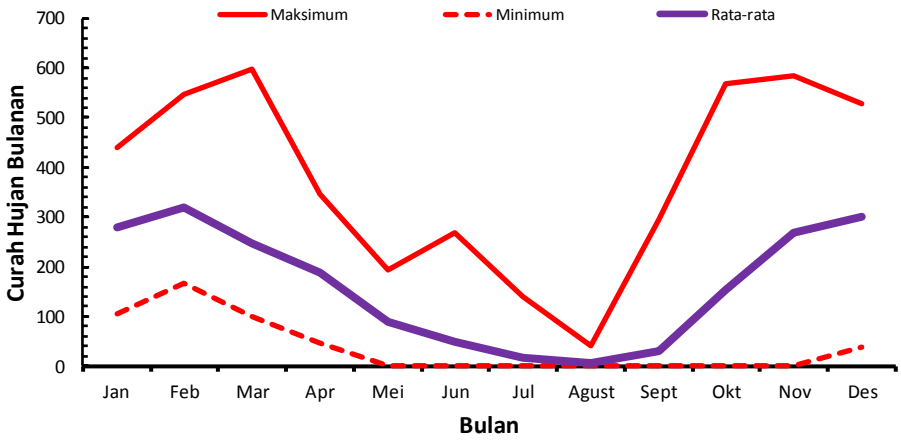

Gambar 4.18 Curah hujan bulanan di Kulonprogo tahun 1998-2012.

BAB V
HASIL YANG DICAPAI

A. Luaran Penelitian

Luaran penelitian pada Tahun ke-1 berupa naskah untuk seminar Internasional, seminar Nasional, dan jurnal Internasional sebagaimana ditampilkan pada Tabel 5.1. Masing-masing naskah disertakan pada Lampiran B.

Tabel 5. 1 Luaran penelitian pada Tahun ke-1

No.	Nama Jurnal/Seminar	Tingkat	Judul Naskah	Status
1	International Conferece on Landslide and Slope Stability (SLOPE 2015), 27 - 30 September 2015, Bali, Indonesia	International	Stability Analysis of A Shallow Slope Failure During Rainy Season in Kulonprogo, Indonesia	*Published*
2	7th Regional Symposium on Infrastructure Development (RSID 7), 4-7 November 2015, Bangkok, Thailand	International	Predicting of Shallow Slope Failure Using Probabilistic Model: a Case Study of Granitic Fill Slope in Northern Thailand	*Published*
3	Pertemuan Ilmiah Tahunan ke-19/Konferensi Geoteknik Indonesia X, 24-25 November 2015, Jakarta	Nasional	Influence of the Soil-Water Retention Curve Models on the Stability of Residuals Soils Slope	*Published*
4	Jurnal Teknologi (*Sciences and Engineering)*	International (SCOPUS: h-index = 7, SJR = 0.15)	Factors Affecting Rain Infiltration on A Slope Using Green-Ampt Model	*Submitted*

B. Hasil Penelitian

1. Estimasi Kedalaman Zona Pembasahan Lereng di Kedungrong

Zona pembasahan lereng akibat infiltrasi air hujan pada lereng di Kedungrong dikaji dari perubahan tekanan air pori dengan kedalaman. Pengaruh model fungsi retensi kadara air tanah telah dikaji dalam penelitian ini meliputi model BC, VG, MCG, dan KLN. Keempat model tersebut diperbandingkan untuk menentukan perubahan tekanan air pori dan faktor aman lereng selama periode hujan. Gambar 5.1 menyajikan perubahan tekanan air pori terhadap kedalaman dan waktu hujan. Tekanan air pori awal di permukaan lereng dan lapisan tanah terbawah sebesar -490 kPa dan -410 kPa. Tekanan air pori ini meningkat seiring dengan waktu hujan. Perbandingan profil tekanan air pori pada Gambar 5.1a dan 5.1c dengan Gambar 5.1b dan 5.1d, maka model BC dan MVG menghasilkan distribusi tekanan air pori yang mirip, sedangka model VG dan KLN memberikan pola distribusi tekanan air pori yang

serupa. Hasil ini mengindikasikan bahwa model SWRC yang berbeda akan mempengaruhi pola distribusi tekanan air pori pada lereng. Model VG dan KLN menghasilkan perubahan tekanan air pori yang lebih jelas (*sharp*) dalam menentukan kedalaman zona pembasahan. Pada Gambar 5.1b dan 5.1d diperlihatkan bahwa kedalaman zona pembasahan mencapai 5 m dan 3 m masing-masing untuk model VG dan KLN. Sementara, kedalaman zona pembasahan tidak secara jelas ditunjukkan oleh model BC dan MVG.

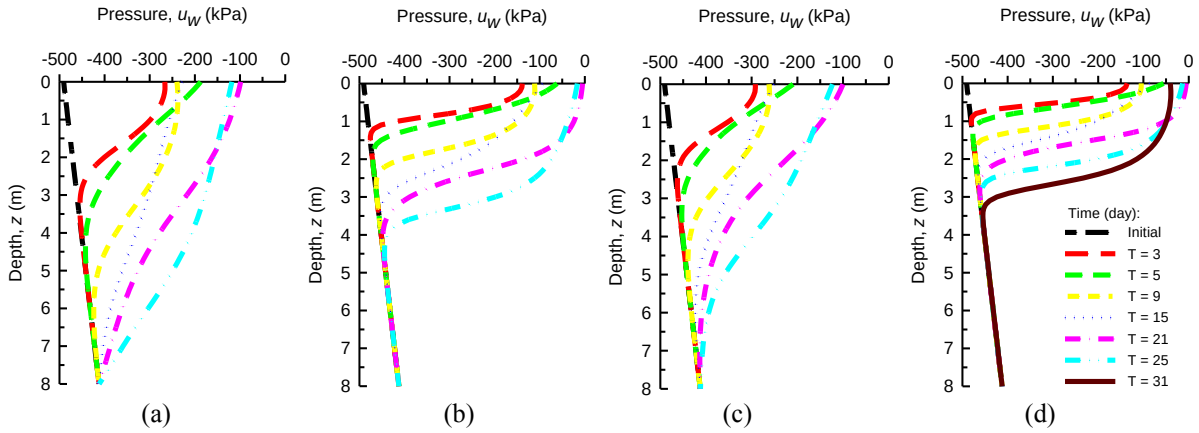

Gambar 5. 1 Profil perubahan tekananair pori terhadap kedalaman untuk model (a) BC, (b) VG, (c) MVG, (d) KLN.

Pada prinsipnya, kurva SWRC merupakan is hubugan secara grafik antara jumlah air dalam tanah yang sering dinyatakan sebagai kadar air gravimetrik (*w)*, kadar air volumetrik (θ_w) atau derajat jenuh air *S* (Fredlund dan Rahardjo, 1993), dengan tekanan air pori negatif (ψ). Seperti dijelaskan oleh Fredlund (2006), bagian kurva SWRC dapat dibedakan menjadi tiga zona yaitu zona batas pengaruh (*boundary effect zone*), zona transisi (*transition zone*), dan zona residu (*residual zone*) yang dipisahkan oleh nilai tekanan udara (*air-entry value*) dan tekanan air pori negative residu. Zhai dan Rahadjo (2013) menyebutkan bahwa tekanan air pori negatif lebih bervariasi pada zona transisi. Pada zona ini disarankan untuk melakukan pengukuran yang lebih banyak guna memperoleh kurva SWRC yang lebih akurat. Model BC secara matematika merupakan fungsi pangkat (*power function*) dari tekanan air pori negative yang mana tidak secara jelas menunjukkan titik infleksi. Kondisi ini yang memungkinkan bahwa zona pembasahan tidak secara jelas untuk model BC. Berkaitan dengan keakuratan dalam memperkirakan kadar air tanah pada kondisi dekat jenuh air, van Genuchten dan Nielsen (1985) menyimpulkan bahwa model VG memiliki unjuk kerja yang lebih baik daripada model BC karena kurva θ-ψ memiliki titik infleksi (ψ_o). Kosugi (1996b) menjelaskan bahwa model VG serupa dengan model KLN pada kondisi batas nilaitekanan udara $\psi_c = 0$, sedangkan model BC akan sama dengan model KLN apabila ψ_c dekat dengan

nilai tekanan air pori pada titik infleksi ($\psi_c \rightarrow \psi_o$). Perbandingan keempat model SWRC di atas, Kosugi (1996a) menyebutkan bahwa model-model SWRC yang tidak didasarkan dari distribusi pori-pori tanah, atau hanya didasarkan pada model fisika – parameter empiric, maka model-model tersebut kurang tepat digunakan untuk mengevaluasi pengaruhnya terhadapaliran air di dalam tanah.

Menggunakan persamaan 2.16, Gambar 5.2 menyajikan variasi faktor aman (FS) terhadap kedalaman dan waktu hujan. Pada awal hujan, lereng cenderung berada dalam keadaan yang stabil yang ditunjukkan dengan nilai faktor aman yang hingga mencapai 100 (Gambar 5.2) pada bidang longsor dekat dengan permukaan tanah. Kondisi ini dicapai karena tekanan air pori negative yang besar pada kondisi awal. Secara umum dapat diketahui bahwa faktor aman cenderung berkurang dengan kedalaman. Faktor aman terendah (FS_{min}) untuk masing-masing model adalah 2,05 untuk model BC, 1, 59 untuk model VG, 2,10 untuk model MVG, dan 1,89 untuk model KLN. Pada akhir waktu hujan, potensi bidang keruntuhan Z_f dapat diperkirakan pada kedalaman 5 m, 2.5 m, 7 m, dan 1.7 m masing-masing untuk model BC, VG, MVG, dan KLN.

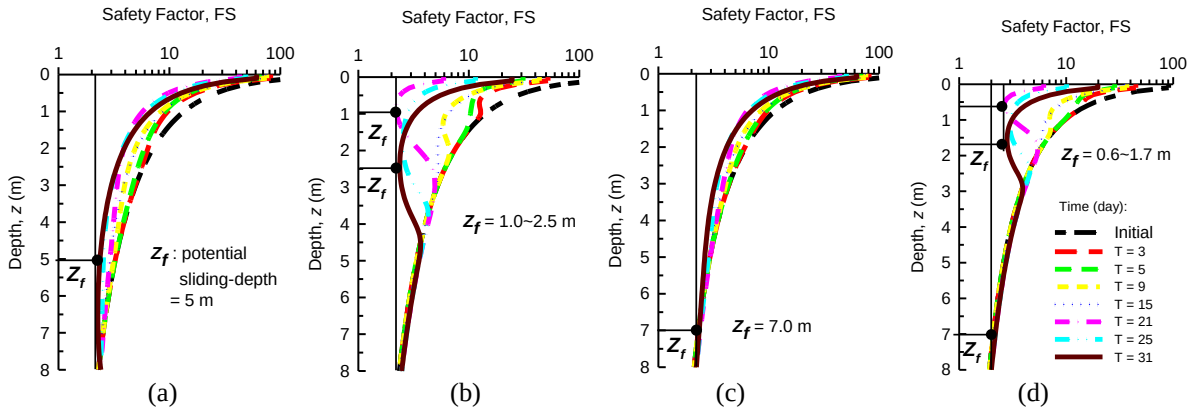

Gambar 5. 2 Saftey factor variation with depth for various elapsed time of rainfall, (a) BC, (b) VG, (c) MVG, (d) KLN models.

Tekanan air terendah pada akhir waktu hujan dapat ditetapkan sebagai batas terbawah (*lower bound*) untuk menghitung faktor aman lereng. Batas terendah tekanan air pori ini oleh Lee *et al*. (2009) disebut dengan selubung tekanan air pori negative (*suction envelope*). Selubung tekanan air pori negative ini mengindikasikan tekanan air pori negative minimum yang terdapat pada tanah akibat lamanya hujan. Dengan menggunakan selubung ini, Gambar 5.3a menyajikan redistribusi tekanan air pori pada lereng. Fourie *et al*. (1999) mengidentifikasi bahwa tekanan air pori merupakan faktor kunci yang berperan dalam kesatabilan lereng yang curam. Pada Gambar 5.3b disajikan profil faktor aman minimum

yang dihitung dengan mendasarkan pada profil tekanan air pori pada Gambar 5.3a. Gambar 5.3b ini menegaskan kembali bahwa stabilitas lereng dipengaruhi oleh model SWRC yang digunakan dalam analisis.

Tekanan air pori awal pada permukaan lereng sebesar - 490 kPa meningkat menjadi - 4 kPa selama hujan (Gambar 5.4). Tekanan air pori negative dapat bertambah hanya jika permukaan lereng mencapai kondisi jenuh air dimana intenstitas hujan di permukaan lereng sama atau lebih besar daripada koefisien permeabilitas tanah. Sehingga profile tekanan air pori akan dikontrol pula oleh fungsi koefisien permeabilitas tanah. Dengan demikian, faktor aman lereng dikontrol pula oleh fungsi koefisien permeabilitas tanah (Rahimi *et al*., 2010; Rahardjo *et al*., 2007). Seperti diketahui bahwa fungsi fungsi koefisien permeabilitas tanah diperkirakan dari kurva SWRC, sehingga pengukuran dan pemilihan model SWRC akan sangat menentukan stabilitas lereng. Rahimi *et al*. (2015) menjelaskan bahwa rentang dan kualitas pengukuran SWRC merupakan hal yang sangat penting daripada pemilihan model SWRC. Hasil ini menyimpulkan bahwa model SWRC model harus diterapkan secara seksama, karena model yang digunakan akan memberikan kesimpulan stabilitas lereng yang berbeda-beda.

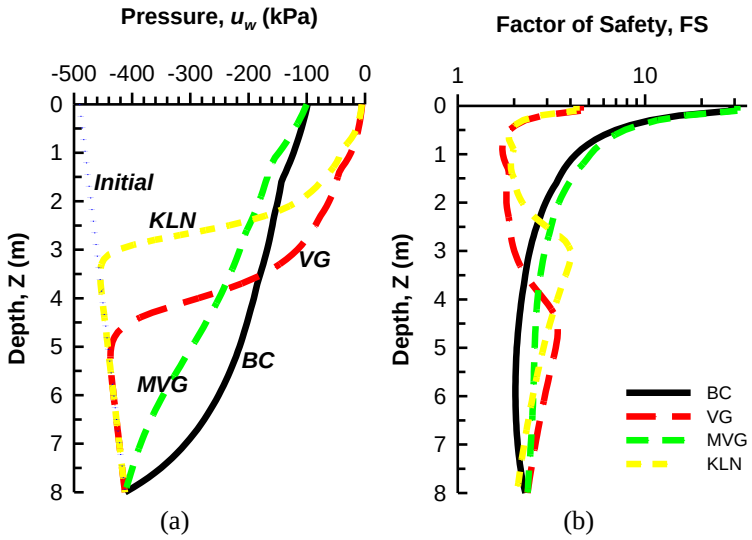

Gambar 5. 3 (a) Selubung tekanan air pori, (b) Faktor aman terendah untuk berbagai model SWRC

Gambar 5.5 menyajikan hubungan antara variasi faktor aman lereng terhadap waktu hujan untuk kedalaman bidang runtuh 1 m hingga 3 m. Secara umum untuk semua model SWRC, faktor aman lereng cenderung berkurang seiring dengan waktu hujan. Besarnya faktor aman terlihat berubah-ubah terhadap waktu bergantung pada besarnya intensitas hujan yang terjadai pada waktu itu. Pada kedalaman z_f = 1 m, model VG dan KLN menghasilkan faktor

aman yang lebih rendah hingga 60% daripada model lainnya. Perubahan FS yang relatif besar terjadi pada kedalaman yang relatif dangkal (Gambar 5.5a), sedangkan perubahan FS relatif kecil pada kedalaman bidang runtuh yang lebih dalam (Gambar 5.5c). Kondisi ini disebabkan oleh tekanan air pori yang relatif sama pada kedalaman yang lebih dalam. Perubahan faktro aman yang besar ini terjadai pada waktu hujan hari ke-6 dan ke-21. Faktor aman terendah terjadi hujan pada hari ke-21 setelah terjadi hujan selama enam hari (Gambar 5.5). Hasil ini juga mengindikasikan bahwa hujan kumulatif sebelum terjadi longsor (*antecedent rainfall*) menentukan kestabilan lereng. Karakteristik ini seperti dijelaskan pula oleh Rahardjo dan Rahimi (2015).

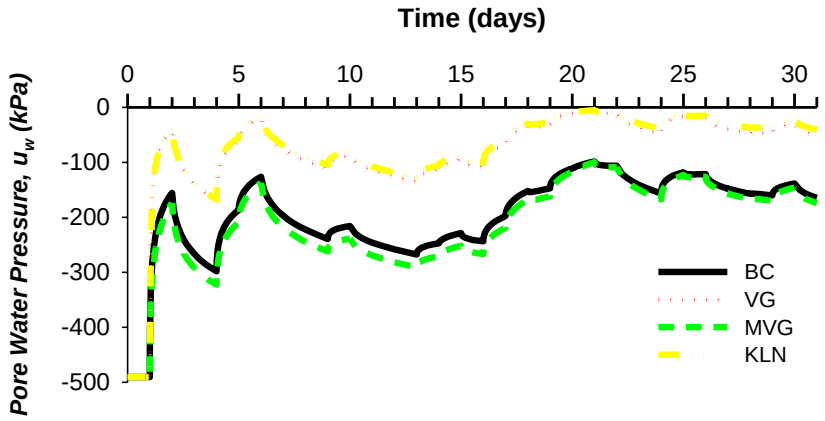

Gambar 5. 4 Variasi tekanan air pori terhadap waktu hujan untuk berbagai model SWRC

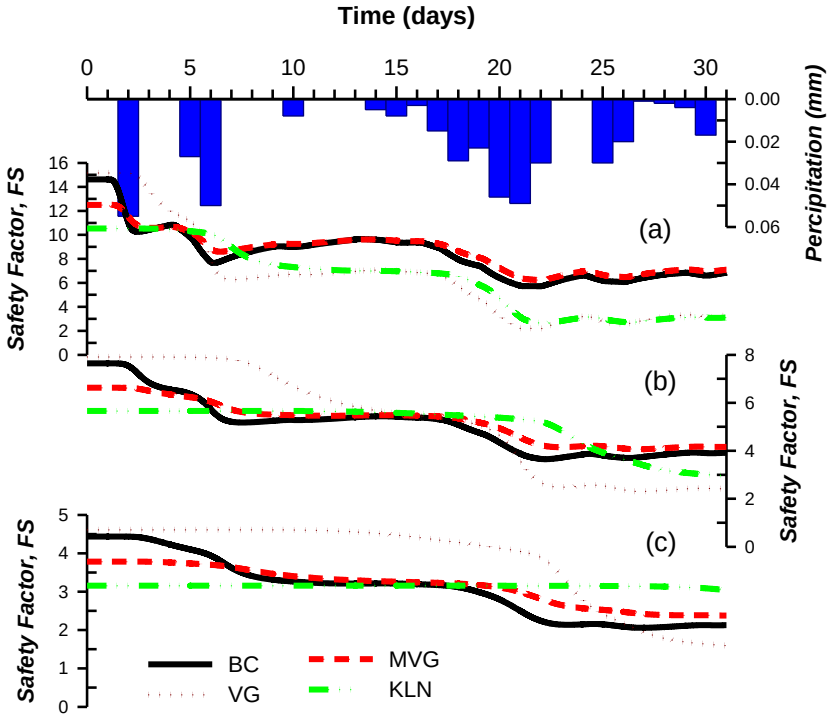

Gambar 5. 5 Variasi faktor aman terhadap waktu hujan untuk kedalaman bidang longsor (a) z_f = 1 m, (b) z_f = 2m, (c) z_f = 3 m.

2. Stabilitas Lereng Pada Musim Basah Tahun 2000 – 2012 di Kulonprogo

Gambar 5.6 menyajikan nilai maksimum dari probabilitas keruntuhan lereng di Kulonprogo dalam periode musim penghujan basah (*rainy season*) Desember – Maret selama rentang waktu 2000 – 2012. Hasil simulasi menunjukkan bahwa probabilitas keruntuha lereng berkisar dari 0,126 hingga 0,302. Nilai probabilitas keruntuhan terendah dan tertinggi dicapai masing-masing pada musim hujan periode Desember 2009 – Maret 2010 dan Desember 2005 – Maret 2006. U.S. Army Corps of Engineers (1997) memberikan suatu panduan umum untuk mengukur tingkat unjuk kerja dari komponen dan sistem geoteknik berdasarkan nilai indek reliabilitas β dan probabilitas keruntuhan P_f seperti disajikan pada Tabel 5.2. Mengacu pada kriteria tersebut, maka tingkat unjuk kerja lereng di Kulonprogo dikategorikan dalam tingkat "*hazardous*". Dalam praktek, perencanaan pekerjaan geoteknik mensyaratkan nilai indek reliabilitas suatu sistem $\beta \geq 2$ atau $P_f < 0{,}023$). Pada nilai ini, sistem geoteknik harus memiliki tingkat unjuk kerja lebih baik dari ''*poor*''. Secara umum, nilai probabilitas keruntuhan yang tinggi mengindikasikan bahwa kejadian lereng untuk mengalami keruntuhan adalah tinggi pula, dan sebaliknya nilai probabilitas yang rendah menyatakan kondisi lereng lebih dekat dalam keadaan stabil. Dengan demikian dapat disimpulkan bahwa kondisi lereng di area studi Kedungrong berada dalam kondisi rentan terhadap bahaya longsor.

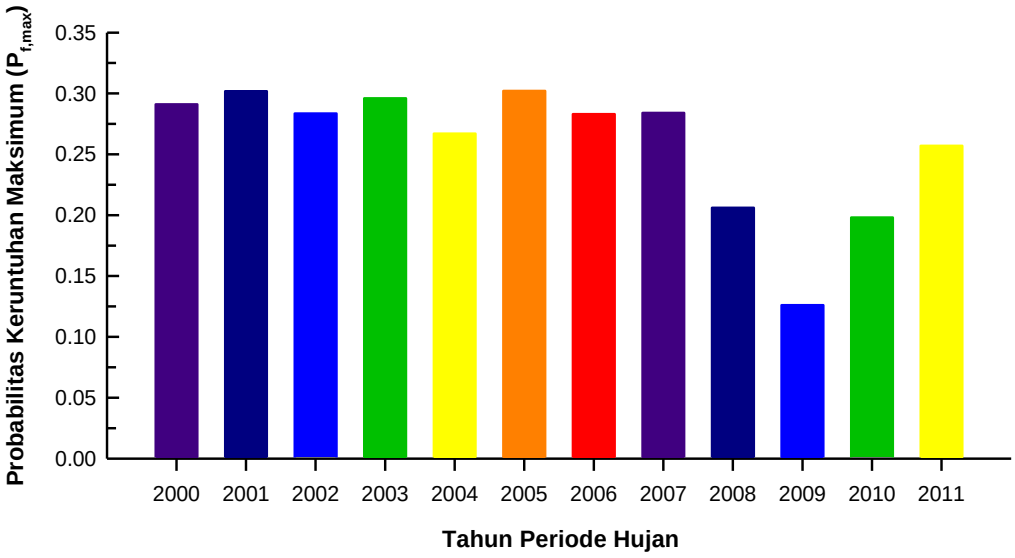

Gambar 5.6 Variasi probabilitas keruntuhan lereng pada periode 2000 - 2012

Analisis probabilitas yang dilakukan dalam penelitian ini difokuskan untuk mengukur stabilitas lereng akibat ketidaktentuan (*uncertainty*) parameter sifat-sifat geoteknik tanah dan fluktuasi curah hujan. Untuk analisis stabilitas lereng, peneliti-peneliti seperti Lumb (1969), Lind (1983), dan Malkawi et al. (2000) menyebutkan bahwa ditribusi probabilitas yag dihasilkan untuk setiap variabel acak merupakan suatu proses pencocokan (*fitting process*)

terhadap keterbatasan data dari pengukuran atau eksperimen. Ketidaktentuan hasil distribusi probabilitas dalam analisis probabilitas disebabkan oleh tiga sumber utama yaitu ketidaktentuan karakterisasi lapangan, ketidaktentuan model, dan ketidaktentuan parameter. Pada penghitungan indek reliabilitas (Persamaan 4.4), sebaran faktor aman yang memiliki variansi (*variance*) yang besar akan menghasilkan perkiraan probabilitas keruntuhan yang lebih besar (*overestimated*) karena nilai untuk FS < 1 berada pada bagian tepi fungsi distribusi probabiltas (*tail*). El-Ramly et al. (2012) memberikan catatan penting bahwa bagaimanapun masih terdapat ketidaktepatan (*errorneous*) dan kesalahan pemahaman (*misleading*) dalam analisis probabilitas. Lebih lanjut dijelaskan bahwa perkiraan unjuk kerja lereng yang berlebihan dapat dikarenakan oleh tidak diperhitungkannya variabilitias spasial sifat-sifat tanah dalam analisis (Santoso et al., 2011), dan asumsi korelasi antar parameter yang sangat mendekati distribusi probabilitas yang sempurna serta penyederhanaan analisis.

Tabel 5.2 Hubungan antara indek reliabilitas dan the probabilitas keruntuhan (U.S. Army Corps of Engineers, 1997).

Indek Reliabilitas, β	Probabilitas keruntuhan, $P_f = \Phi(-\beta)$	Tingkat Unjuk kerja Sistem
1,0	0,16	Bahaya (*Hazardous*)
1,5	0,07	Tidak Memuaskan (*Unsatisfactory*)
2,0	0,023	Buruk (*Poor*)
2,5	0,006	Dibawah rata-rata (*Below average*)
3,0	0,001	Diatas rata-rata (*Above average*)
4,0	0,00003	Baik (*Good*)
5,0	0,0000003	Tinggi (*High*)

3. Probabilitas Keruntuhan Lereng Doi Inthanon, Thailand

Simulasi Monte Carlo menghasilkan perubahan faktor aman lereng terhadapwaktu hujan seperti ditampilkan pada Gambar 5.7. Berdasarkan hasil simulasi, faktor aman yang dihitung tidak terdistribusi normal, tetapi lognormal. Dengan demikian, indek reliabilitas dihitung menggunakan persamaan 4.3, dan probabilitas keruntuhan dihitung dari fungsi distribusi probabilitas lognormal. Gambar 5.8 hingga 5.10 menampilkan variasi densitas probabilitas dan probabilitas keruntuhan terhadap waktu hujan untuk masing-masing pola hujan 5 menitan, hujan jam-jaman, dan hujan harian dengan tiga nilai koefisien variansi (cov = 0,005; cov = 0,01; cov = 0,02). Probabilitas keruntuhan lereng pada pola hujan 5 menitan berkisar dari 0,05 hingga 0,37 (Gambar 5.8). Sementara pada pola hujan jam-jaman dan harian, probabilitas keruntuhan lereng masing-masing adalah 0,04 – 0,36 (Gambar 5.9) dan 0,05 –

0,38 (Gambar 5.10). Hasil ini menunjukkan bahwa probabilitas keruntuhan maksimum untuk masing-masing parameter masukan dalam simulasi adalah berkisar 0,36 – 0,38.

Densitas probabilitas terhadap waktu dapat dipergunakan untuk menentukan probabilitas kejadian keruntuhan lereng. Dalam kajian ini, densitas probabilitas pada Gambar 5.8 hingga 5.10 diperkirakan dengan menggunakan fungsi distribusi probabilitas normal (*normal probability density function)*. Muntohar (2010) mengusulkan metode untuk menentukan waktu terjadinya keruntuhan lereng sebagai *mean time to failure* (MTTF) dengan menggunakan sifat-sifat statistika dari fungsi densitas probabilitas (PDF), yaitu rata-rata (*mean*), μ, dan variansi (*variance*), σ^2, atau deviasi standar (*standard deviation*), σ. Nilai μ menentukan titik tengah atau pusat dari *PDF*, dan nilai σ^2 menunjukkan lebar dari PDF. Nilai variansi yang kecil mengindikasikan bahwa waktu terjadinya keruntuhan lebih dekat ke nilai titik tengah atau derajat ketidaktentuannya kecil.

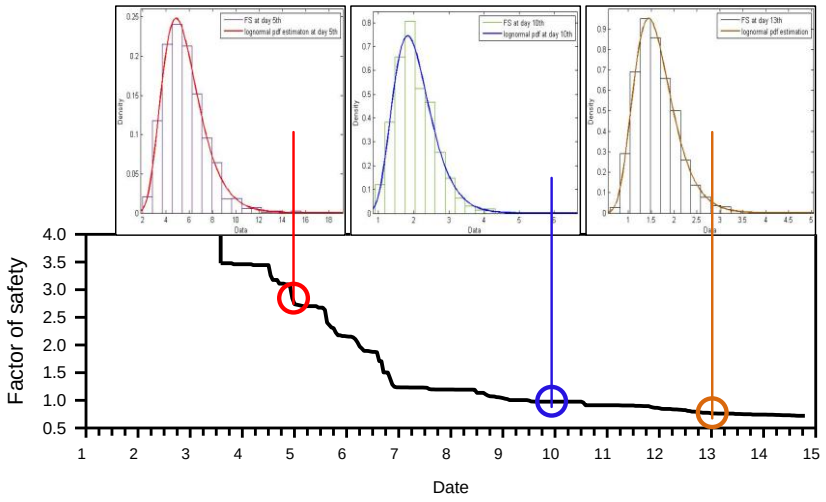

Gambar 5.7 Tipikal perubahan faktor aman dan fungsi distribusi probabilitas terhadap waktu hujan.

Tabel 5.3 menyajikan MTTF untuk ketiga pola hujan dan nilai *cov* dari parameter masukan. Muntohar (2010) menyebutkan bahwa probabilitas keruntuhan lereng selama hujan dapat pula dinyatakan sebagai “degree of belief” untuk memperkirakan potensi keruntuhan lereng. Secara umum dapat dinyatakan bawha semakin besar nilai probabilitas keruntuhan, maka potensi keruntuhan lereng pada suatu rentang waktu tertentu juga semakin besar. Berdasarkan dari hasil analisis pada Tabel 5.3, maka dapat dibuat estimasi terjadinya keruntuhan lereng antara tanggal 9 - 13 September 2011 yang mana bergantung pada pola hujan dan variansi dari parameter masukan untuk analisis. Probabilitas keruntuhan pada rentang waktu tersebut adalah sebesar 0,38. Zhang et al. (2010) menjelaskan bahwa apabila

pengukuran atau variabel tekanan air pori relatif tidak menentu, akan derajat ketidaktentuan tekanan air pori lebih mendominasi hasil analisis probabilitas keruntuhan lereng.

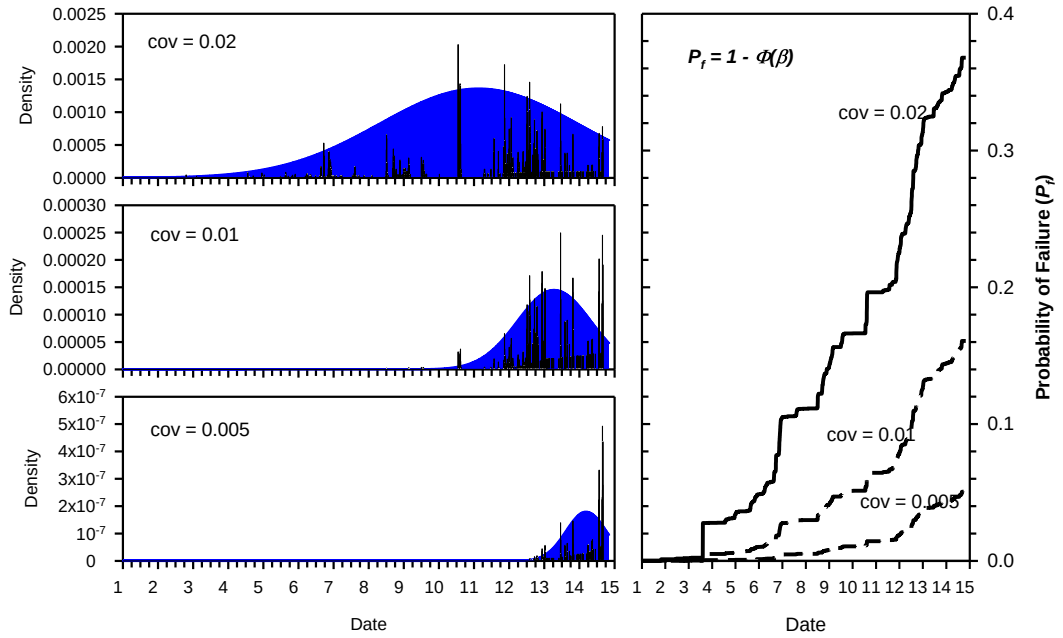

Gambar 5.8 Distribusi kejadian dan probabilitas keruntuhan terhadap waktu akibat hujan 5 menitan.

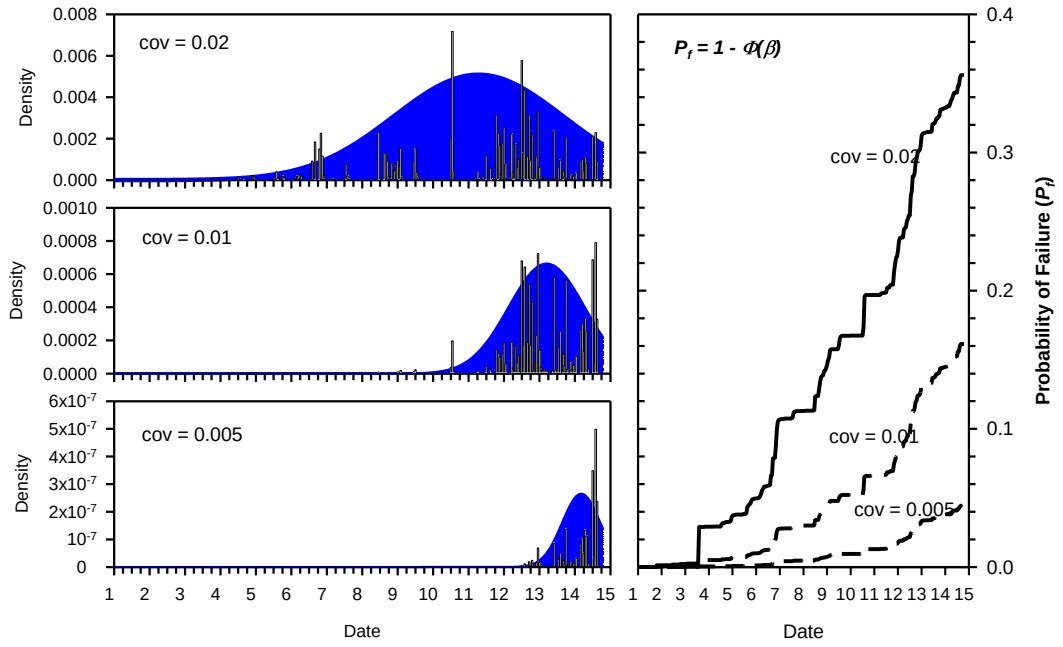

Gambar 5. 9 Distribusi kejadian dan probabilitas keruntuhan terhadap waktu akibat hujan 1 jam-an.

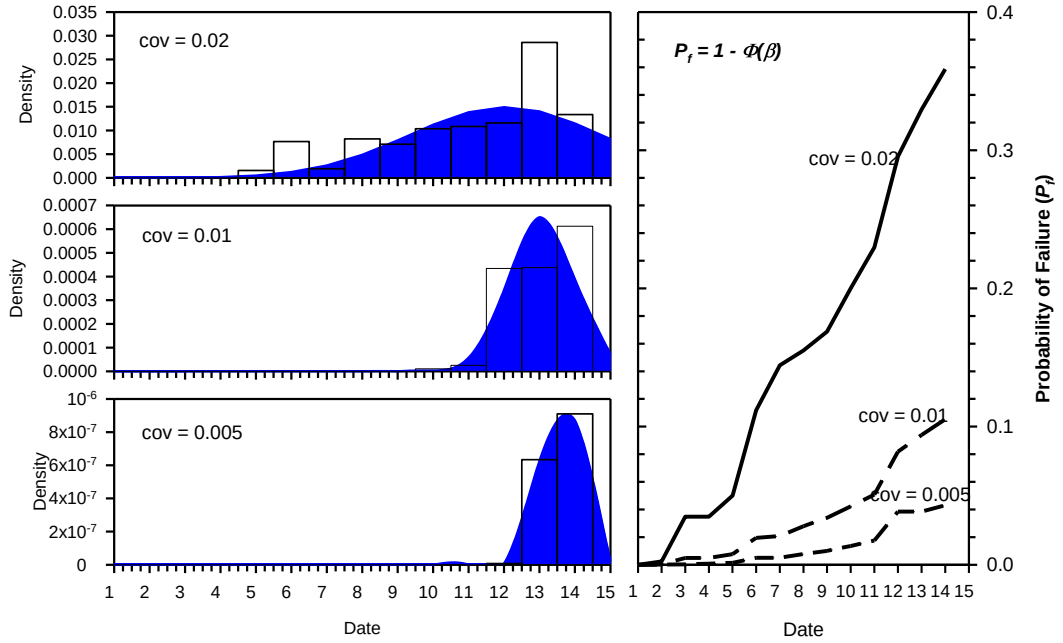

Gambar 5. 10 Distribusi kejadian dan probabilitas keruntuhan terhadap waktu akibat hujan 1 hari-an

Tabel 5. 3 Sifat-sifat statistika dari PDF untuk menentukan waktu keruntuhan lereng.

Pola rekaman hujan	*cov* parameter	Estimasi waktu keruntuhan (hari)		Probabilitas Keruntuhan Maksimum (P_f)
		Mean, μ	Variance, σ^2	
5 minutes	0.02	9.725	7.305	0.37
	0.01	11.785	1.007	0.16
	0.005	12.659	0.300	0.05
Hourly	0.02	10.321	5.680	0.37
	0.01	12.241	1.148	0.16
	0.005	13.217	0.289	0.04
Daily	0.02	12.043	7.294	0.38
	0.01	13.051	0.871	0.11
	0.005	13.582	0.253	0.05

Simulasi yang dilakukan pada kajian ini menggunakan konsep sampel variabel acak (*random sampling*). Pengaruh derajat ketidaktentuan parameter telah dikaji dengan memvariasikan tiga niai koefisien variansi yaitu 0,02; 0,01, dan 0,005. Nilai cov yang besar mengindikasikan derajat ketidaktentuan variabel yang tinggi, sehingga menghasilkan lebar distribusi faktor aman yang besar pula. Hubungan pada Gambar 5.3 hingga 5.5 menunjukkan bahwa densitas probabilitas terhadap waktu terdistribusi lebih lebar untuk ilai *cov* yang besar (*cov* = 0,02), dan sebaliknya untuk nilai *cov* yang kecil (*cov* = 0,005), maka densitas distribusi probabilitas lebih rapat. Pada studi ini nilai *cov* menunjukkan ketidaktentuan parameter masukan yang digunakan dalam analisis probabilitas. Gambar 5.6 memberikan hubungan antara probabilitas keruntuhan dan nilai *cov* dari parameter.

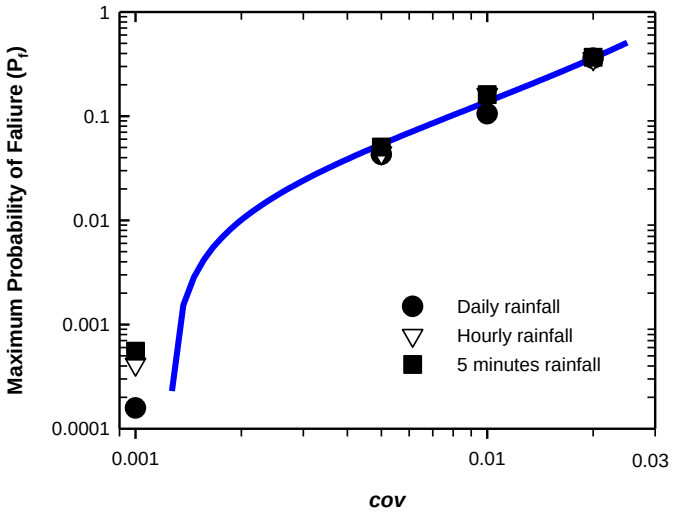

Gambar 5. 11 Relationship between failure probability and *cov*.

Hubungan pada Gambar 5.11 tersebut menunjukkan dengan jelas bahwa probabilitas keruntuhan lereng cenderung meningkat dengan bertambahnya nilai *cov* dari parameer. El-Ramly et al. (2005) menjelaskan bahwa sebaran parameter masukan dalam analisis dikarenakan oleh sebaran spasial tanah yang beragam, yang dalam analisis statistika bentuk sebaran data tanah tersebut disederhanakan dalam suatu hubungan empirik. Sementara Zhang et al. (2010) menyatakan bahwa faktor aman lereng berubah sangat besar disebabkan oleh besarnya derajat ketidaktentuan dalam distribusi probabilitas masing-masing parameter masukan dalam analisis. Namun, alasan ini lebih abah jika parameter tersebut tidak memiliki hubungan statistika satu dengan lainnya (*independent- distribution*).

4. Pengaruh Infiltrasi Hujan dan Kedalaman Muka Air Tanah

Variasi faktor aman (*FS*) lereng terhadap waktu hujan untuk berbagai kedalaman muka air tanah awal ditunjukkan pada Gambar 5.12. Hasil ini menunjukkan bahwa kedalaman muka air tanah mempengaruhi faktor aman awal ($FS_{(t\,=\,0)}$) dan faktor aman minimum yang terjadi selama hujan. Semakin dekat kedalaman muka air tanah ke permukaan lereng, faktor aman awal yang diperoleh semakin rendah. Kondisi disebabkan oleh infiltrasi air hujan yang menyebabkan permukaan tanah menjadi jenuh air. Sebagai akibatnya akan meningkatkan kedalaman zona pembasahan (*wetting zone*) dan pengurangan *suction* atau peningkatan tekanan air pori. Kondisi ini terjadi untuk $H_{w(init)}$ = 1 m, 2 m, dan 3 m yang ditunjukkkan pada Gambar 5.12a hingga 5.12c, dimana faktor aman (*FS*) berkurang secara drastis pada aktu mendekati berakhirnya hujan, dan setelahnya tidak terjadi perubahan faktor aman yang sangat kecil. Faktor aman minimum yang terendah dicapai pada kondisi $H_{w(init)}$ = 1 m. Hal ini dapat

disebabkan oleh peningkatan muka air tanah secara cepat yang memperbesar tekanan air pori pada lereng. Sedangkan untuk $H_{w(init)}$ = 4 m, 5 m, dan 10 m (Gambar 5.12d hingga 5.12f), faktor aman masih cenderung berkurang walaupun hujan telah berhenti hingga waktu 30 hari.

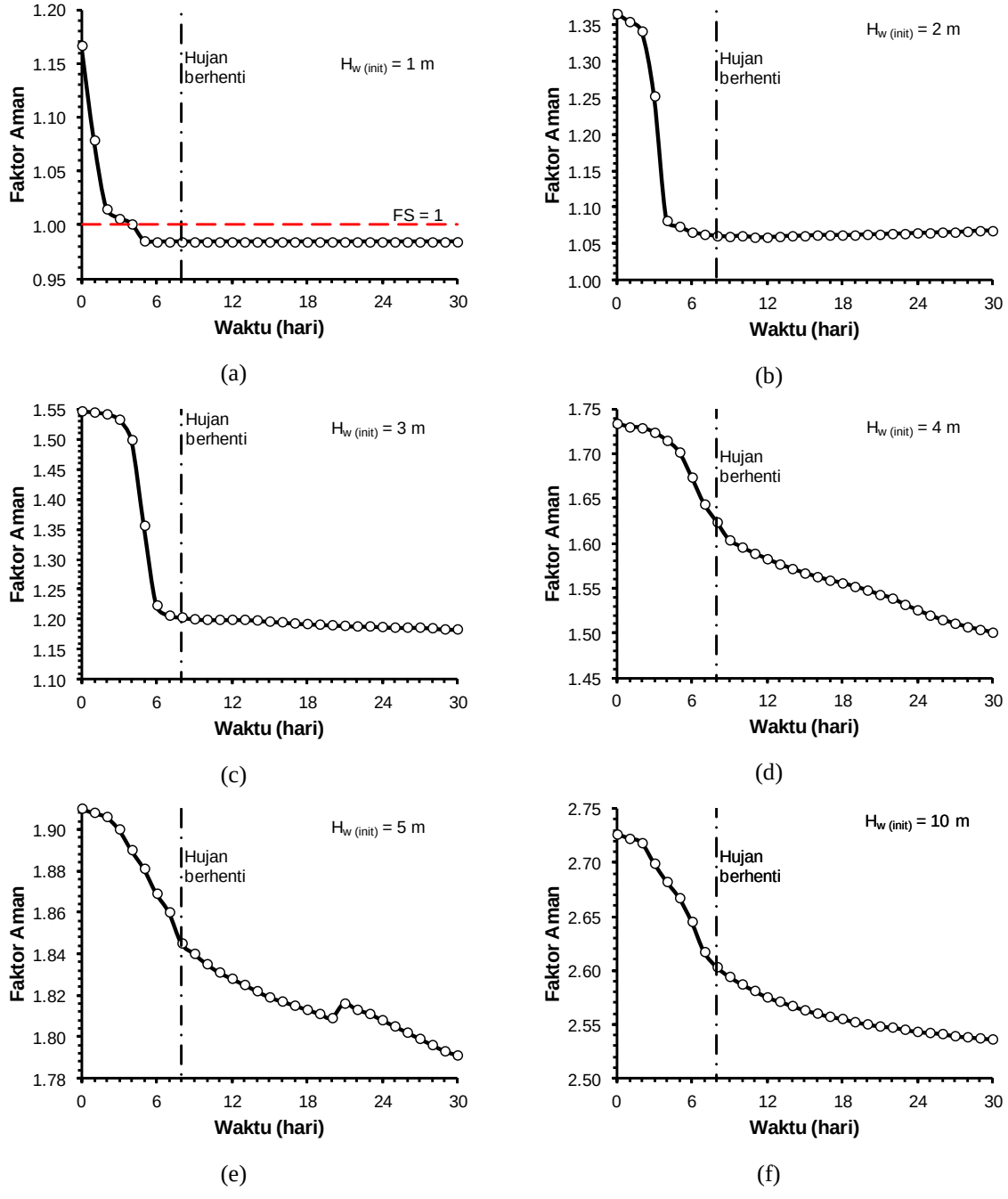

Gambar 5.12 Perubahan faktor aman lereng terhadap waktu untuk berbagai kondisi muka air tanah awal ($H_{w(init)}$) (a) $H_{w(init)}$ = 1 m, (b) $H_{w(init)}$ = 2 m, (c) $H_{w(init)}$ = 3 m, (d) $H_{w(init)}$ = 4 m, (e) $H_{w(init)}$ = 5 m, (f) $H_{w(init)}$ = 10 m.

Untuk menjelaskan perubahan faktor aman akibat perubahan tekanan air pori disajikan Gambar 5.13 yang memberikan ilustrasi perbandingan distribusi tekanan air pori untuk $H_{w(init)}$

= 3 m dan $H_{w(init)}$ = 10 m. Hujan yang terjadi selama 8 hari menyebabkan permukaan lereng lebih cepat mengalami penjenuhan dimana zona pembasahan hingga mencapai 3 m (Gambar 5.13a). Kondisi jenuh air memicu kenaikan muka air tanah yang menyebabkan peningkatan tekanan air pori (Gambar 5.13c dan 5.13e). Peningkatan muka air tanah dan tekanan air pori ini menyebabkan kuat geser tanah berkurang, sehingga faktor aman lereng berkurang secara drastis. Kondisi berbeda ditunjukkan pada Gambar 5.13b-f untuk kedalaman muka air tanah awal $H_{w(init)}$ = 10 m. Untuk muka air tanah awal yang lebih dalam, terjadi penundaan zona pembasahan dan tidak terjadi perubahan muka air tanah. Hujan yang terjadi belum cukup untuk menurunkan *suction* pada zona pembasahan, sehingga faktor aman lereng masih lebih dari 1,5 selama durasi hujan. Hal ini dimungkinkan karena *suction* awal yang digunakan dalam analisis sangat tinggi sehingga terjadi penundaan terhadap perubahan tekanan air pori. Melihat distibusi tekanan air pori pada Gambar 5.13, dapat diketahui bahwa tekanan air pori mulai berubah pada kedalaman 3-4 m. Pada kondisi ini tekanan air pori yang dicapai sebesar – 68 kPa. Dengan demikian dalam studi ini, kedalaman muka air tanah yang diberikan sebagai kondisi awal adalah 3 m atau *suction* maksimum dibatasi 68 kPa. Gofar dan Lee (2008), Lee et al., (2009), dan Rahardjo et al. (2007) menyebutkan bahwa *suction* awal sebesar 50-70 kPa akan menghasilkan analisis yang realistis untuk kondisi tanah residual di area tropis (seperti Singapura dan Malaysia).

Pada Gambar 5.14 disajikan gabungan perubahan tekanan air pori terhadap kedalaman untuk berbagai kondisi awal muka air tanah. Apabila masing-masing kedalaman zona pembasahan pada saat akhir waktu hujan t_8 dihubungkan, maka akan diperoleh batas atau selubung redistribusi tekanan air untuk masing-masing lokasi yaitu di puncak (A), lereng (B), dan kaki (C).

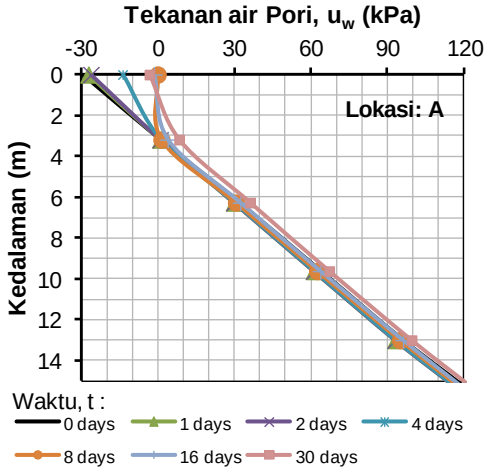

(a) $H_{w(init)}$ = 3 m

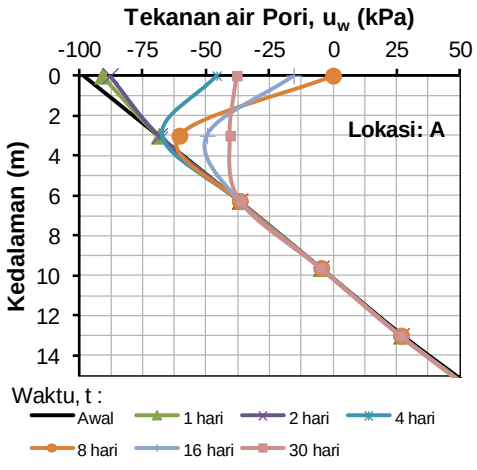

(b) $H_{w(init)}$ = 10 m

Gambar 5.13 Distribusi tekanan air pori terhadap waktu untuk di lokasi A, B, dan C.

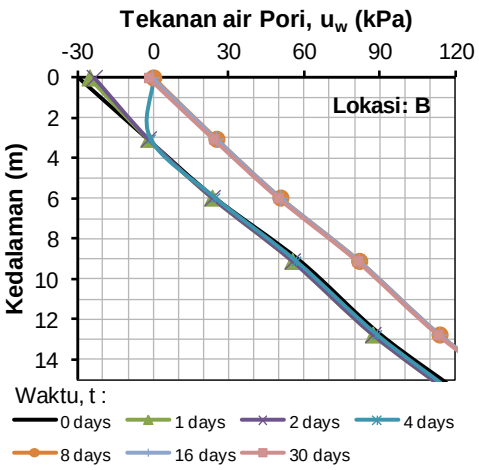

(c) $H_{w(init)}$ = 3 m

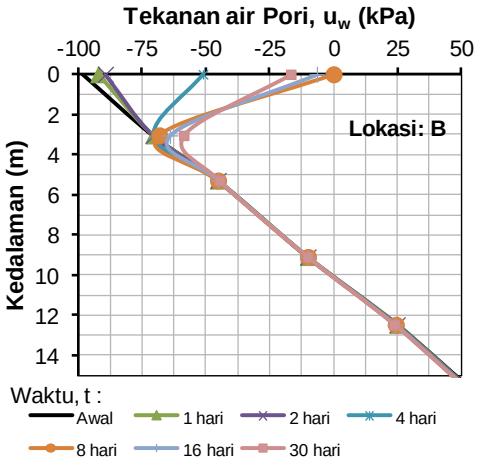

(d) $H_{w(init)}$ = 10 m

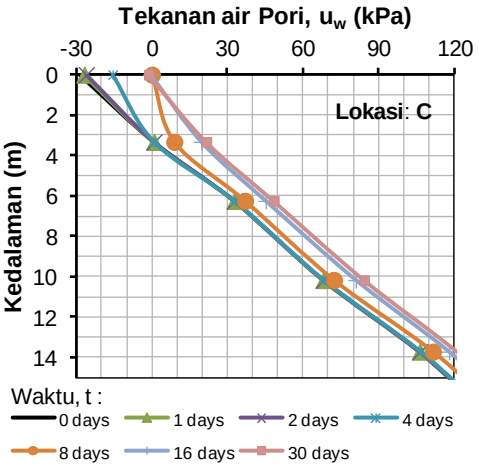

(e) $H_{w(init)}$ = 3 m

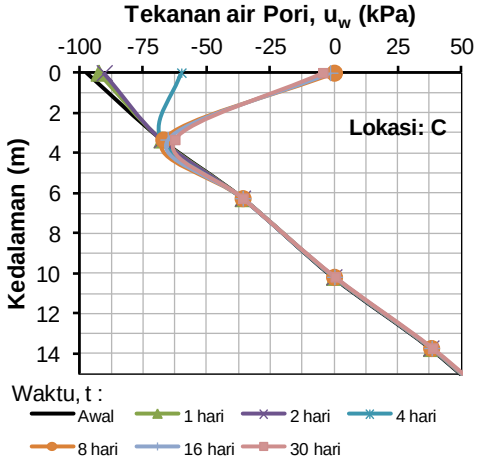

(f) $H_{w(init)}$ = 10 m

Gambar 5.13 Lanjutan

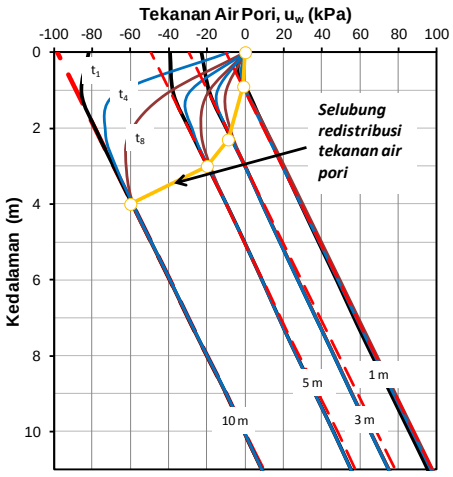

(a)

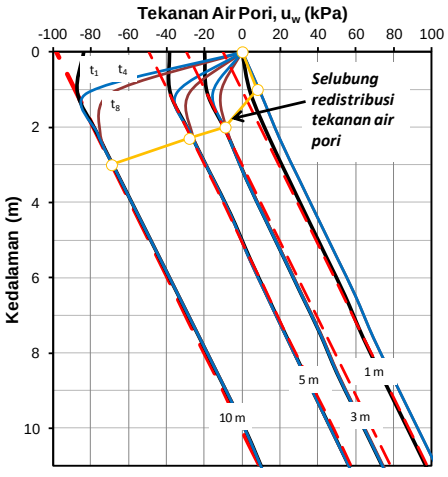

(b)

Gambar 5.14 Redistribusi tekanan air pori (a) lokasi A, (b) lokasi B

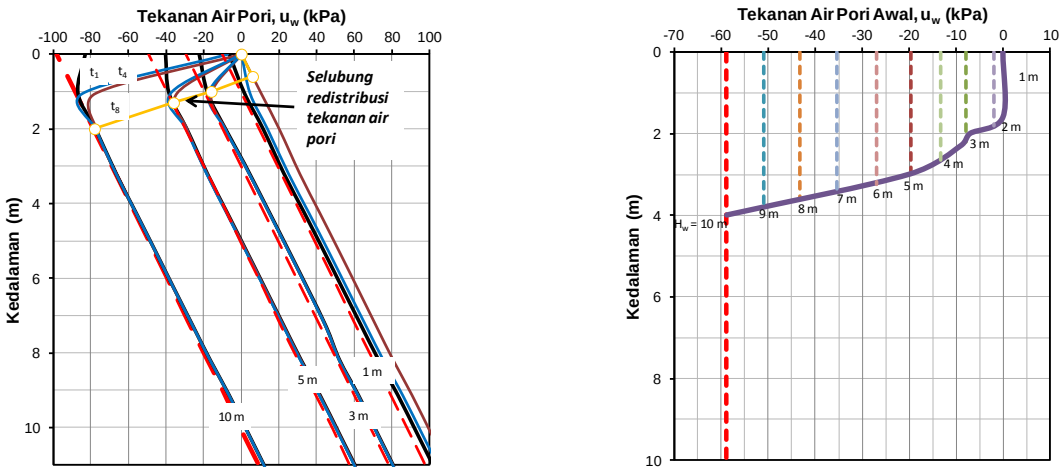

Gambar 5.14 Lanjutan: (c) lokasi C, dan (d) selubung redistribusi tekanan air pori awal.

5. Proyeksi Hujan Bulanan Rata-Rata pada Tahun 2020 – 2040

Prediksi rekaman curah hujan bulanan rata-rata (*historical rainfall*) pada tahun 1980 – 2000 yang dihasilkan dari pemodelan iklim CMIP3 dan CMIP5 seperti disajikan pada Gambar 5.15. Sebagai pembanding hasil prediksi rekaman hujan tersebut ditampilkan pula dalam curah hujan bulanan rata-rata tahun 1998 – 2012 yang diambil dari stasiun hujan Kalibawang. Berdasarkan Gambar 5.15 diketahui bahwa model iklim CESM1-CAM5 memberikan pola distribusi rekaman hujan 1980 -2000 lebih dekat daengan pola rekaman hujan 1998 – 2012. Proyeksi curah hujan bulanan rata-rata di area Kulonprogo untuk tahun 2020 – 2040 yang dihasilkan dari perangkat *Climate Change Knowledge Portal* untuk model ikim CMIP5 dan CMIP3 masing-masing seperti disajikan pada Gambar 5.16 dan 5.17. Perbedaan curah hujan dari skenario perubahan iklim pada model CMIP3 (scenario A2 dan B1) dan CMIP5 (skenario RCP2.6, RCP4.5, RCP6, dan RCP8.5) tidak berbeda banyak. Curah hujan bulanan rata-rata tertinggi dicapai pada scenario RCP4.5 yaitu sebesar 330,35 mm yang terjadi pada bulan Januari. Sedangkan curah hujan bulanan rata-rata terendah terjadi pada bulan Juli pada skenario RCP6 yaitu sebesar 38,5 mm.

Klasifikasi tipe iklim Oldeman (1975) merupan tipe iklim yang dikembangkan berdasarkan kriteria bulan-bulan basah dan bulan-bulan kering yang terjadi secara berturut-turut. Kriteria bulan basah dan bulan kering dalam pengklasifikasian tipe iklim Oldeman adalah apabila jumlah curah hujan dalam satu bulan > 200 mm maka dinyatakan sebagai bulan bulan basah dan apabila curah hujan dalam satu bulan < 100 mm maka dinyatakan sebagai bulan kering. Tabel 5.4 dan Tabel 5.5 masing-masing menyajikan bulan-bulan basah dan kering hasil dari proyeksi perubahan iklim model CMIP5 dan CMIP3.

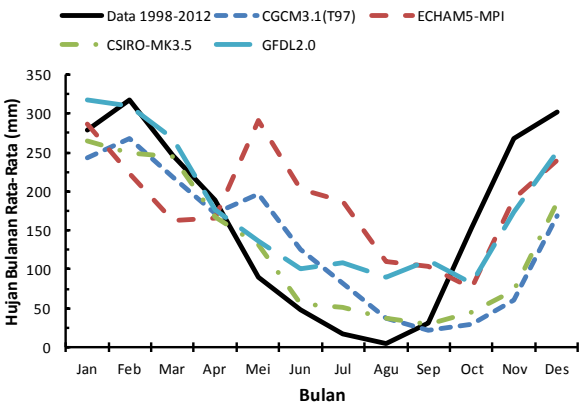

(a) Model iklim CMIP3

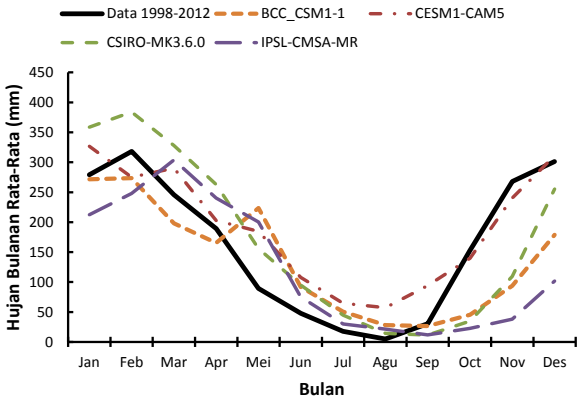

(b) Model iklim CMIP5

Gambar 5. 15 Estimasi rekaman curah hujan bulanan rata-rata tahun 1980 – 2000 untuk berbagai model iklim CMIP3 dan CMIP5 di Kulonprogo

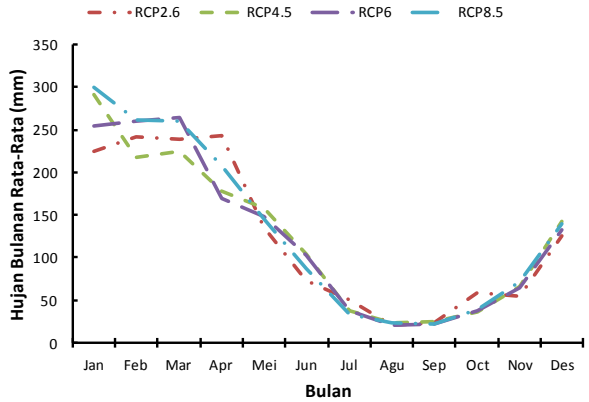

(a) BCC-CSM1.1

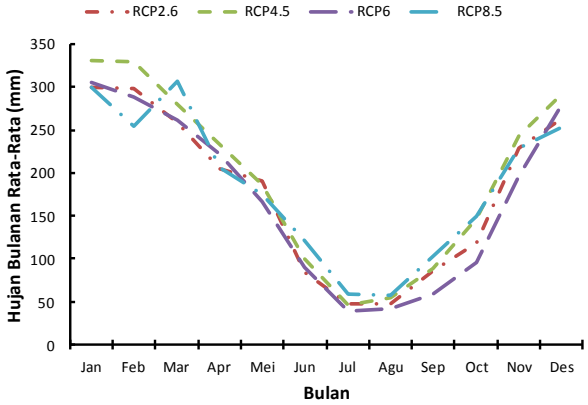

(b) CESM1 (CAM5)

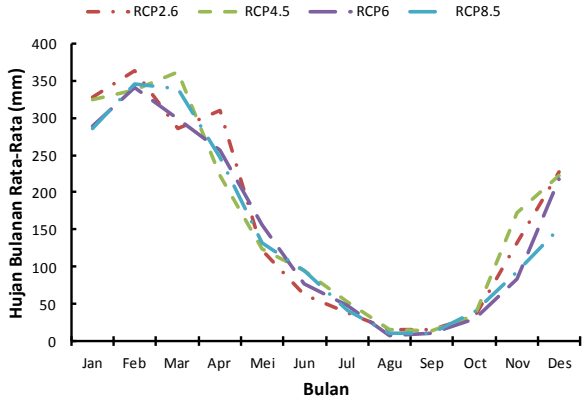

(c) CSIRO-MK3.6.0

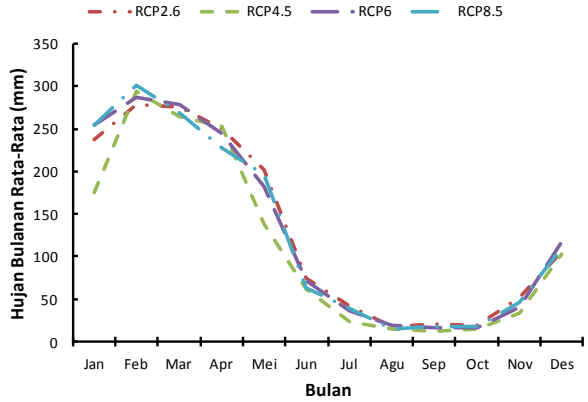

(d) IPSL-CMSA-MR

Gambar 5.16 Proyeksi curah hujan bulanan rata-rata model perubahan iklim GCM CMIP5

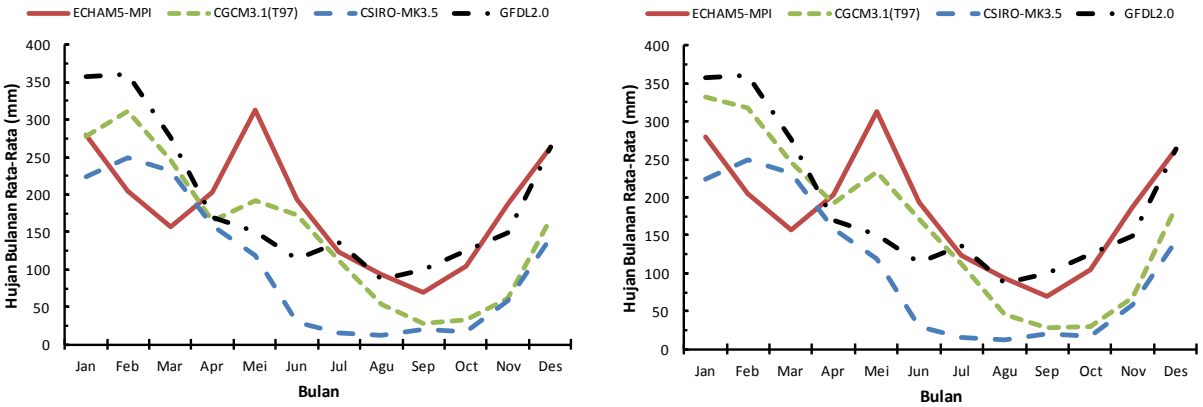

(a) Skenario A2 (b) Skenario B1

Gambar 5. 17 Proyeksi curah hujan bulanan rata-rata model perubahan iklim GCM CMIP3

Tabel 5. 4 Bulan-bulan basah dan kering menurut kriteria Oldeman untuk proyeksi perubahan iklim model CMIP5 tahun 2020 – 2040 di Kulonprogo

Skenario	Model	Bulan											
		Jan	Feb	Mar	Apr	Mei	Jun	Jul	Agu	Sep	Okt	Nov	Des
RCP2.6	BCC-CSM1.1	■	■	■	■	▨	▨	▨	▨	▨	▨	▨	▨
	CESM1 (CAM5)	■	■	■	■	▨	▨	▨	▨	▨	▨	■	■
	CSIRO-MK3.6.0	■	■	■	■	▨	▨	▨	▨	▨	▨	▨	■
	IPSL-CMSA-MR	■	■	■	■	■	▨	▨	▨	▨	▨	▨	▨
RCP4.5	BCC-CSM1.1	■	■	■	▨	▨	▨	▨	▨	▨	▨	▨	▨
	CESM1 (CAM5)	■	■	■	■	▨	▨	▨	▨	▨	▨	■	■
	CSIRO-MK3.6.0	■	■	■	■	▨	▨	▨	▨	▨	▨	▨	■
	IPSL-CMSA-MR	■	■	■	■	▨	▨	▨	▨	▨	▨	▨	▨
RCP6	BCC-CSM1.1	■	■	■	▨	▨	▨	▨	▨	▨	▨	▨	▨
	CESM1 (CAM5)	■	■	■	■	▨	▨	▨	▨	▨	▨	▨	■
	CSIRO-MK3.6.0	■	■	■	■	▨	▨	▨	▨	▨	▨	▨	■
	IPSL-CMSA-MR	■	■	■	■	▨	▨	▨	▨	▨	▨	▨	▨
RCP8.5	BCC-CSM1.1	■	■	■	■	▨	▨	▨	▨	▨	▨	▨	▨
	CESM1 (CAM5)	■	■	■	■	▨	▨	▨	▨	▨	▨	■	■
	CSIRO-MK3.6.0	■	■	■	■	▨	▨	▨	▨	▨	▨	▨	▨
	IPSL-CMSA-MR	■	■	■	■	▨	▨	▨	▨	▨	▨	▨	▨
Keterangan		■ : bulan basah				▨ : bulan kering							

Tabel 5. 5 Bulan-bulan basah dan kering menurut kriteria Oldeman untuk proyeksi perubahan iklim model CMIP3 tahun 2020 – 2040 di Kulonprogo

Skenario	Model	Bulan											
		Jan	Feb	Mar	Apr	Mei	Jun	Jul	Agu	Sep	Okt	Nov	Des
A2	CGCM3.1(T97)	■	■	■	▨	▨	▨	▨	▨	▨	▨	▨	▨
	ECHAM5-MPI	■	■	■	■	■	▨	▨	▨	▨	▨	▨	■
	CSIRO-MK3.5	■	■	■	▨	▨	▨	▨	▨	▨	▨	▨	▨
	GFDL2.0	■	■	■	▨	▨	▨	▨	▨	▨	▨	▨	■
B1	CGCM3.1(T97)	■	■	■	▨	▨	▨	▨	▨	▨	▨	▨	▨
	ECHAM5-MPI	■	■	■	■	■	▨	▨	▨	▨	▨	▨	■
	CSIRO-MK3.5	■	■	■	▨	▨	▨	▨	▨	▨	▨	▨	▨
	GFDL2.0	■	■	■	▨	▨	▨	▨	▨	▨	▨	▨	■
Keterangan		■ : bulan basah				▨ : bulan kering							

6. Estimasi Stabilitas Lereng Pada Tahun 2020 – 2040 di Kulonprogo

Estimasi stabilitas lereng akibat perubahan iklim pada tahun 2020 – 2040 untuk berbagai skenario perubahan iklim CMIP5 model CESM1 (CAM5) seperti disajikan pada Gambar 5.18. Pada tersebut disajikan perubahan faktor aman minimum lereng dan probabilitas keruntuhan terhadap waktu (bulan). Secara umum, faktor aman minimum menyatakan batas faktor aman terendah terhadap hujan harian yang terjadi pada satu bulan. Faktor aman minimum FS ≤ 1 atau FS ≤ 1,5 terjadi bulan-bulan Januari, Februari, November, dan Desember. Faktor aman minimum pada bulan-bulan tersebut berkisar 0,84 – 1,33 untuk semua skenario perubahan iklim. Pada kondisi ini, secara deterministik, lereng dapat dikategorikan berada dalam kondisi tidak stabil atau berpotensi mengalami keruntuhan. Probabilitas keruntuhan pada bulan-bulan tersebut berkisar 0,29 – 0,40. Sedangkan pada bulan-bulan kering Mei – Oktober, faktor aman minimum lereng FS > 1,5, dengan probabilitas keruntuhan mendekati nol. Dengan demikian pada bulan-bulan kering ini, lereng cenderung berada dalam kondisi stabil. Mengacu kriteria yang diberikan dalam Tabel 5.2, maka tingkat unjuk kerja lereng di Kulonprogo dikategorikan dalam tingkat "*hazardous*" pada bulan-bulan basah, sedangkan pada bulan-bulan kering berada dalam tingkat "*good*" hingga "*high*".

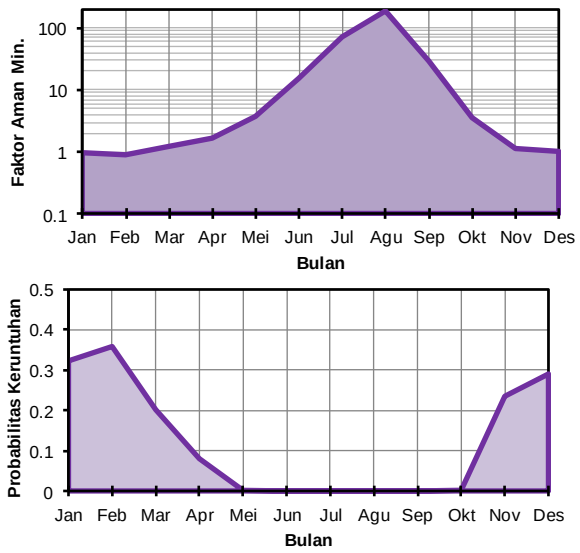

(a) RCP 2.6

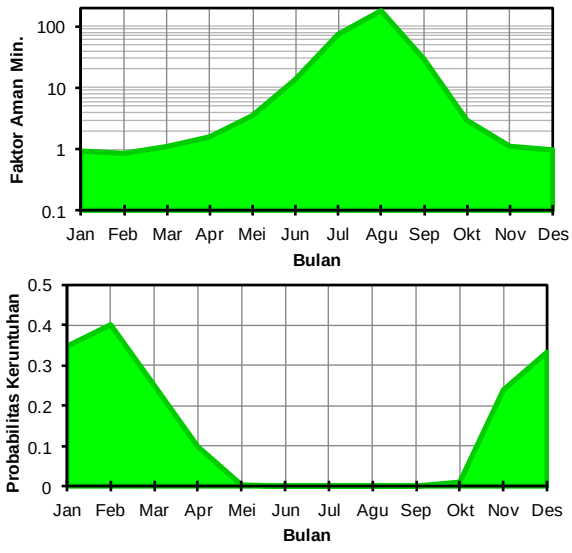

(b) RCP 4.5

Gambar 5.18 Estimasi Stabilitas Lereng Pada Tahun 2020 – 2040 di Kulonprogo

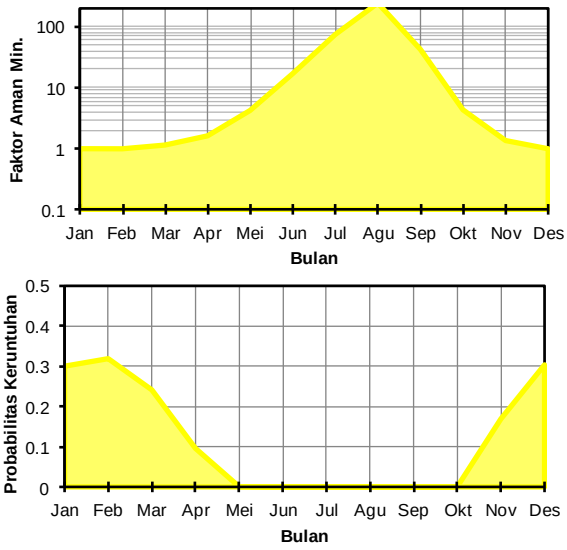

(c) RCP 6.

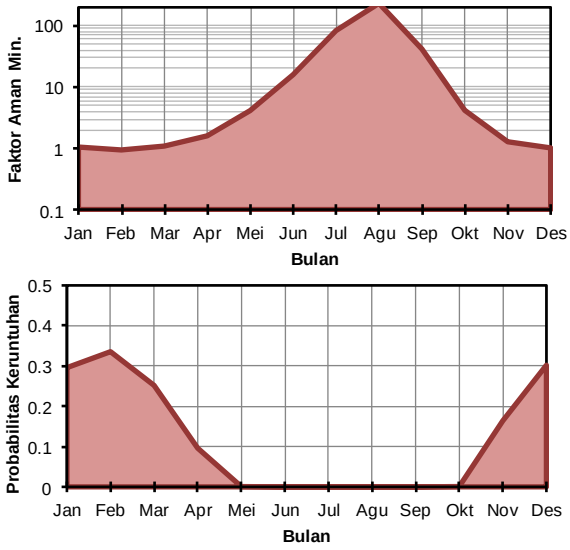

(d) RCP 8.5

Gambar 5.18 Lanjutan

BAB VI
RENCANA TAHAPAN BERIKUTNYA

Penelitian yang akan dilakukan pada saat ini dan pengembangannya disajikan dalam bentuk diagram pada Gambar 3.1. Kegiatan yang akan dilakukan adalah mengkaji skenario iklim yang meliputi intensitas hujan dan geo-hidrologi terhadap potensi pergerakan tanah pada lereng di Daerah Istimewa Yogyakarta, yaitu :

a. Simulasi stabilitas lereng akibat skenario iklim saat ini dan masa yang akan datang,
b. Pemodelan kontribusi akar tanaman terhadap analisis stabilitas lereng,
c. Menentukan angka faktor aman lereng eksisting yang dimodelkan berdasarkan pada *fact-finding* kasus-kasus kelongsoran pada lereng alami (*natural slope*) dan lereng buatan (*cut-slope*).

Penelitian akan dikembangkan untuk mencapai tujuan utama untuk penyusunan model Sistem Manajemen Pergerakan Lereng Terintegrasi (*Integrated Landslide Management System*). Kegiatan yang akan dikembangkan meliputi :

a. Studi eksperimental 3D lereng pada skala laboratorium untuk mengetahui pengaruh perubahan hujan, infiltrasi dan vegetasi,
b. Uji skala lapangan (*full scale*) dan instrumentasi pada lereng natural dan lereng buatan untuk memantau pergerakan lereng akibat perubahan hujan, infiltrasi, dan vegetasi dan validasi model numerik,
c. Pembuatan perangkat lunak manajemen pergerakan lereng berbasis *website* dan sistem informasi geografis (SIG) yang mengintegrasikan *real-monitoring* hujan, temperatur, dan pangkalan data geoteknik lereng.

BAB VII
KESIMPULAN DAN SARAN

A. Kesimpulan

1. Stabilitas Lereng Pada Musim Basah Tahun 2000 – 2012 di Kulonprogo

a. Hasil simulasi menunjukkan bahwa probabilitas keruntuhan lereng berkisar dari 0,126 hingga 0,302. Nilai probabilitas keruntuhan terendah dan tertinggi dicapai masing-masing pada musim hujan periode Desember 2009 – Maret 2010 dan Desember 2005 – Maret 2006.

b. Mengacu pada kriteria U.S. Army Corps of Engineers (1997), maka tingkat unjuk kerja lereng di Kulonprogo dikategorikan dalam tingkat "hazardous".

2. Proyeksi Iklim dan Stabilitas Lereng

a. Model iklim CESM1-CAM5 memberikan pola distribusi rekaman hujan 1980 -2000 lebih dekat daengan pola rekaman hujan 1998 – 2012.

b. Perbedaan curah hujan dari skenario perubahan iklim pada model CMIP3 (scenario A2 dan B1) dan CMIP5 (skenario RCP2.6, RCP4.5, RCP6, dan RCP8.5) tidak berbeda banyak. Curah hujan bulanan rata-rata tertinggi dicapai pada scenario RCP4.5 yaitu sebesar 330,35 mm yang terjadi pada bulan Januari. Sedangkan curah hujan bulanan rata-rata terendah terjadi pada bulan Juli pada skenario RCP6 yaitu sebesar 38,5 mm.

c. Faktor aman minimum pada bulan-bulan Januari, Februari, November, dan Desember berkisar 0,84 – 1,33 untuk semua skenario perubahan iklim. Probabilitas keruntuhan pada bulan-bulan tersebut berkisar 0,29–0,40. Sedangkan pada bulan-bulan kering Mei–Oktober, faktor aman minimum lereng FS > 1,5, dengan probabilitas keruntuhan mendekati nol. Mengacu pada kriteria U.S. Army Corps of Engineers (1997), maka tingkat unjuk kerja lereng di Kulonprogo dikategorikan dalam tingkat "hazardous" pada bulan-bulan basah, sedangkan pada bulan-bulan kering berada dalam tingkat "good" hingga "high", maka tingkat unjuk kerja lereng dikategorikan dalam tingkat "hazardous".

3. Probabilitas Keruntuhan Lereng Doi Inthanon, Thailand

a. Probabilitas keruntuhan lereng pada pola hujan 5 menitan berkisar dari 0,05 hingga 0,37. Sementara pada pola hujan jam-jaman dan harian, probabilitas keruntuhan lereng masing-masing adalah 0,04 – 0,36 dan 0,05 – 0,38. Hasil ini menunjukkan bahwa probabilitas keruntuhan maksimum untuk masing-masing parameter masukan dalam simulasi adalah berkisar 0,36 – 0,38.
b. Simulasi yang dilakukan pada kajian ini menggunakan konsep sampel variabel acak (*random sampling*). Pengaruh derajat ketidaktentuan parameter telah dikaji dengan memvariasikan tiga niai koefisien variansi yaitu 0,02; 0,01, dan 0,005. Nilai cov yang besar mengindikasikan derajat ketidaktentuan variabel yang tinggi, sehingga menghasilkan lebar distribusi faktor aman yang besar pula. Densitas probabilitas terhadap waktu terdistribusi lebih lebar untuk ilai cov yang besar (cov = 0,02), dan sebaliknya untuk nilai cov yang kecil (cov = 0,005), maka densitas distribusi probabilitas lebih rapat.

4. Pengaruh kedalaman muka air tanah terhadap stabilitas lereng akibat infiltrasi hujan.

a. Secara umum infiltrasi air hujan akan menyebabkan permukaan tanah menjadi jenuh air. Kondisi ini akan meningkatkan kedalaman zona pembasahan (*wetting zone*) dan pengurangan suction.
b. Semakin dekat kedalaman muka air tanah ke permukaan lereng, faktor aman awal yang diperoleh semakin rendah.
c. Posisi muka air tanah yang lebih dekat dengan permukaan lereng menyebabkan penurunan suction yang lebih cepat akibat hujan. Kedalaman muka air tanah berkisar 3-4 m atau suction sebesar 68 kPa merupakan batas nilai initial suction yang disarankan di permukaan lereng untuk lokasi studi di Kalibawang.

B. Saran

Penelitian akan dikembangkan untuk mencapai tujuan utama untuk penyusunan model Sistem Manajemen Pergerakan Lereng Terintegrasi (*Integrated Landslide Management System*). Kegiatan yang akan dikembangkan meliputi :

d. Studi eksperimental 3D lereng pada skala laboratorium untuk mengetahui pengaruh perubahan hujan, infiltrasi dan vegetasi,
e. Uji skala lapangan (*full scale*) dan instrumentasi pada lereng natural dan lereng buatan untuk memantau pergerakan lereng akibat perubahan hujan, infiltrasi, dan vegetasi dan validasi model numerik,

f. Pembuatan perangkat lunak manajemen pergerakan lereng berbasis *website* dan sistem informasi geografis (SIG) yang mengintegrasikan *real-monitoring* hujan, temperatur, dan pangkalan data geoteknik lereng.

DAFTAR PUSTAKA

ALDRIAN, E., SEIN, D., JACOB, D., GATES, L. D. & PODZUN, R. 2005. Modelling Indonesian rainfall with a coupled regional model. *Climate Dynamics*, Vol. 25**:** 1–17.

ALEOTTI, P. 2004. A warning system for rainfall-induced shallow failures. *Engineering Geology*, Vol. 73**:** 247–265.

ALI, F. H. & OSMAN, N. 2008. Shear strength of a soil containing vegetation roots. *Soils and Foundations*, Vol. 48**:** 587–596.

ASTM 2005. ASTM D 6431-99, Standard Guide for Using the Direct Current Resistivity Method for Subsurface Investigation Pennsylvania: ASTM International.

BROOKS, R. H., & COREY, A.T., 1966, Properties of porous media affecting fluid flow, *Journal of Irrigation and Drainage Division, ASCE Proceeding*, Vol. 72(IR2): 61-88.

CHEN, L., & YOUNG, M.H., 2006, Green-Ampt infiltration model for sloping surface, *Water Resources Research*, Vol. 42: 1-9

CHIRICO, G. B., BORGA, M., TAROLLI, P., RIGON, R. & PRETI, F. 2013. Role of vegetation on slope stability under transient unsaturated conditions. *Procedia Environmental Sciences*, Vol. 19: 932 – 941.

CHO, S.E., & LEE, S.R., 2002, Evaluation of surficial stability for homogeneous slopes considering rainfall characteristics. *Journal of Geotechnical and Geoenvironmental Engineering*, Vol. 128(9): 756–763.

COE, J. A. & GODT, J. W. Review of approaches for assessing the impact of climate change on landslide hazards. *In:* EBERHARDT, E., FROESE, C., TURNER, A. K. & LEROUEIL, S., eds. Landslides and Engineered Slopes, Protecting Society Through Improved Understanding: Proceeding 11th International and 2nd North American Symposium on Landslides and Engineered Slopes, 3-8 June 2012 2012 Banff, Canada. Taylor & Francis, pp. 371-377.

CUOMO, S. & SALA, M. D. 2013. Rainfall-induced infiltration, runoff and failure in steep unsaturated shallow soil deposits. *Engineering Geology*, Vol. 162**:** 118-127.

DAMIANO, E. & MERCOGLIANO, P. 2013. Potential Effects of Climate Change on Slope Stability in Unsaturated Pyroclastic Soils. *In:* MARGOTTINI, C., CANUTI, P. & SASSA, K. (eds.) *Landslide Science and Practice*. Germany: Springer-Verlag Berlin Heidelberg.

DANJON, F., BARKER, D. H., DREXHAGE, M. & STOKES, A. 2008. Using Three-dimensional Plant Root Architecture in Models of Shallow-slope Stability. *Annals of Botany*, Vol. 101**:** 1281–1293.

DANNEELS, G., BOURDEAU, C., TORGOEV, I. & HAVENITH, H.-B. 2008. Geophysical investigation and dynamic modelling of unstable slopes: case-study of Kainama (Kyrgyzstan). *Geophysical Journal International*, Vol. 175**:** 17-34.

EL-RAMLY, H., MORGENSTERN, N. R. & CRUDEN, D. 2002. Probabilistic slope stability analysis for practice. *Canadian Geotechnical Journal*, Vol. 39: 665–683

EL-RAMLY, H., MORGENSTERN, N.R., & CRUDEN, D.M. 2005. Probabilistic assessment of stability of a cut slope in residual soil. *Géotechnique*, Vol. 55(1): 77–84

FAN, C.-C. & SU, C.-F. 2008. Role of roots in the shear strength of root-reinforced soils with high moisture content. *Ecological Engineering*, Vol. 33**:** 157–166.

FOURIE, A.B, OWE, D.R, & BLIGHT, G.E., 1999, The effect of infiltration on the stability of the slopes of a dry ash dump, *Geotechnique*, Vol. 49(1): 1–13.

FREDLUND, D.G., & RAHARDJO, H., 1993. *Soil Mechanics for Unsaturated Soils*. Wiley, NewYork.

FREDLUND, D.G., & XING, A., 1994 Equations for the soil-water characteristic curve, *Canadian Geotechnical Journal*, Vol. 31(4): 521-532

FREDLUND, D.G., 2006. Unsaturated soil mechanics in engineering practice. *Journal of Geotechnical and Geoenvironmental Engineering*, Vol. 132 (3): 286–321.

FREDLUND, D.G., MORGENSTERN, N.R., & WIDGER, R.A, 1978, The shear strength of unsaturated soils. *Canadian Geotechnical Journal*, Vol. 15(3): 313-321.
GEOSLOPE INTERNATIONAL, 2007a. SEEP/W User's Guide for Finite Element Analysis. Geoslope International Ltd., Calgary, Alberta, Canada.
GEOSLOPE INTERNATIONAL, 2007b. SLOPE/W User's Guide for Finite Element Analysis. Geoslope International Ltd., Calgary, Alberta, Canada.
GOFAR, N., & LEE, L.M. 2008. Extreme rainfall characteristics for surface slope stability in the Malaysian Peninsular, *Georisk: Assessment and Management of Risk for Engineered Systems and Geohazards*, Vol. 2(2), 65-78.
GUZZETTI, F., PERUCCACCI, S., ROSSI, M. & STARK, C. P. 2007. Rainfall thresholds for the initiation of landslides in central and southern Europe. *Meteorology and Atmospheric Physics*, Vol. 98**:** 239-267.
HARR, M. E. 1989. Probabilistic estimates for multivariate analyses. *Applied Mathematical Modeling*, Vol. 13(5): 313-318.
HARYANTI, S., SURYOLELONO, K. B. & JAYADI, R. 2010. Analysis on Rainfall Characteristics Effect to the Slope Movement. *Jurnal Ilmiah Semesta Teknika*, Vol. 13**:** 105-115.
HENDON, H.H. 2003 Indonesian Rainfall Variability: Impacts of ENSO and Local Air–Sea Interaction, *Journal of Climate*, Vol. 16: 1775-1790.
HOSSAIN, M. K. 2010. Effect of Rainfall on Matric Suction and Stability of a Residual Granite Soil Slope. *DUET Journal*, Vol. 1(1): 37-41.
IPCC, 2000. *Emissions Scenarios*, A Special Report of IPCC Working Group III.
IPCC, 2013. *Climate Change 2013: The Physical Science Basis. Contribution of Working Group I to the Fifth Assessment Report of the Intergovernmental*, Cambridge, Cambridge University Press.
IPCC, 2014. *Climate Change 2014: Mitigation of Climate Change. Contribution of Working Group III to the Fifth Assessment Report of the Intergovernmental*, Cambridge, Cambridge University Press.
JONGMANS, D., BIÈVRE, G., RENALIER, F., SCHWARTZ, S., BEAUREZ, N. & ORENGO, Y. 2009. Geophysical investigation of a large landslide in glaciolacustrine clays in the Trièves area (French Alps). *Engineering Geology*, Vol. 109**:** 45–56.
JOTISANKASA, A., MAHANNOPKUL, K., AND SAWANGSURIYA. A, 2015. Slope Stability and Pore-Water Pressure Regime in Response to Rainfall: a Case Study of Granitic Fill Slope in Northern Thailand. *Geotechnical Engineering Journal of the SEAGS & AGSSEA*, Vol. 46(1): 45-65.
KHALILNEJAD, A., ALI, F. H. & OSMAN, N. 2012. Contribution of the Root to Slope Stability. *Geotechnical & Geological Engineering*, Vol. 30**:** 277–288.
KOSUGI, K., 1996a, Lognormal distribution model for unsaturated soil hydraulic properties, *Water Resources Research*, Vol. 32(9): 2697-2703
LEE, H.S. 2015 General Rainfall Patterns in Indonesia and the Potential Impacts of Local Season Rainfall Intensity. *Water*, Vol. 7: 1751-1768
LEE, L. M., GOFAR, N., & RAHARDJO, H. (2009). A simple model for preliminary evaluation of rainfall-induced slope instability. *Engineering Geology*, Vol. 108: 272–285.
LEE, L-M., GOFAR, N. & RAHARDJO, H. 2009. A simple model for preliminary evaluation of rainfall-induced slope instability. *Engineering Geology*, Vol. 108**,** 272-285.
LEUNG, A. K. & NG, C. W. W. 2013. Analyses of groundwater flow and plant evapotranspiration in a vegetated soil slope. *Canadian Geotechnical Journal*, Vol. 50**,** 1204-1218.
LIAO, Z., HONG, Y., WANG, J., FUKUOKA, H., SASSA, K., KARNAWATI, D. & FATHANI, F. 2010. Prototyping an experimental early warning system for rainfall-induced landslides in Indonesia using satellite remote sensing and geospatial datasets. *Landslides*, Vol. 7**,** 317–324.
LIND, N. C., 1983. Modeling uncertainty in discrete dynamical systems. *Applied Mathematical Modelling*, Vol. 7 (3):146-152.
LUMB, P. 1969. Safety factors and the probability distribution of soil strength. *Canadian Geotechnical Journal*, Vol. 7 (3): 225-242.
MA ,Y., FENG, S., ZHAN, H, LIU, X., SU, D., KANG, S., & SONG, X. 2010. Water Infiltration in Layered Soils with Air Entrapment: Modified Green-Ampt Model and Experimental Validation. *Journal of Hydrologic Engineering*, Vol. 16(8): 628-638.

MALKAWI, A. I. H., HASSAN, W. F., & ABDULLA, F.A. 2000. Uncertainty and reliability analysis applied to slope stability. *Structural Safety*, Vol. 22(2) : 161-187

MISHRA, S.K., TYAGI, J.V., & SINGH, V.P., 2003. Comparison of Infiltration Models, *Hydrological Processes*, Vol. 17(13): 2629–2652

MONTGOMERY, D.R., & DIETRICH, W.E., 1994. A Physically Based Model for the Topographic Control on Shallow Landslide, *Water Resources Research*, Vol. 30: 83–92.

MUALEM, Y., 1976, A new model for predicting the hydraulic conductivity of unsaturated porous media, *Water Resources Research*, Vol. 12(3): 513-522.

MUNTOHAR, A. S. 2008. Toward Regional Rainfall Threshold For Landslide Occurrence In Yogyakarta and Central of Java. *Jurnal Teknik Sipil*, 3**,** 40-47.

MUNTOHAR, A. S., IKHSAN, J. & SOEBOWO, E. 2013 *Mechanism of rainfall triggring landslides in Kulonprogo, Indonesia*. *In:* MEEHAN, C. L., PRADEL, D., PANDO, M. A. & LABUZ, J. F., eds. Geo-Congress, March 3-7, 2013, San Diego, California. Geo Institutes American Society of Civil Engineer, pp.452-461.

MUNTOHAR, A.S. & IKHSAN, J. 2013. *Development A Simple Model for Preliminary Evaluation on Extreme Rainfall Induces Shallow Slope Failure*. The 13rd International Conference on QIR (Quality in Research), 3-4 June 2013, Yogyakarta, Indonesia, pp.1284-1411.

MUNTOHAR, A.S. & LIAO, H.-J. 2009. Analysis of rainfall-induced infinite slope failure during typhoon using a hydrological–geotechnical model. *Environmental Geology*, Vol. 56**:** 1145-1159.

MUNTOHAR, A.S. & LIAO, H.-J. 2010. Rainfall infiltration: infinite slope model for landslides triggering by rainstorm. *Natural Hazards*, Vol. 54**:** 967-984.

MUNTOHAR, A.S. & SAPUTRO, R.I. 2014. *Pengaruh Kedalaman Muka Air Awal Terhadap Analisis Stabilitas Lereng Tak Jenuh*. Seminar Nasional X Teknik Sipil, 2 Februari 2014 Surabaya. Jurusan Teknik Sipil, FTSP, ITS, pp.985-990.

MUNTOHAR, A.S., & IKHSAN, J., 2012. *Studi Numerik dan Eksperimental Infiltrasi Hujan Pada Lereng*. Laporan Akhir Penelitian Fundamental, Universitas Muhammadiyah Yogyakarta – Direktorat Penelitian dan Pengabdian kepada Masyarakat, Ditjen Dikti.

MUNTOHAR, A.S., 2010. *Application of Probabilistic Analysis for Prediction for Initiation of Landslide*. The 1st International Workshop on Multimodal Sediment Disasters Triggered by Heavy Rainfall and Earthquake and the Countermeasures, Yogyakarta, Indonesia, 8-9 March 2010, pp.33-44.

MUNTOHAR, A.S., IKHSAN, J., & LIAO, H.J, 2013, Influence of Rainfall Patterns on the Instability of Slopes. *Civil Engineering Dimension*, Vol. 15(2): 120-128.

OLDEMAN, L.R. 1975, *An Agroclimatic Map of Java*, Contributions of the Central Research Institute of Agriculture, No. 17, Bogor

RAHARDJO, H., & RAHIMI, A., 2015, Controlling factors of rainfall-induced slope failures in residual soils, in P.P. Rahardjo & A. Tohari, *Proceeding of Slope 2015*, September 27-30th 2015, Bali, pp. 4.1 –4.21

RAHARDJO, H., NIO, A.S., LEONG, E.C. & SONG, N.Y. 2010. Effects of Groundwater Table Position and Soil Properties on Stability of Slope during Rainfall. *Journal of Geotechnical and Geoenvironmental Engineering*, Vol. 136**:** 555–1564.

RAHARDJO, H., ONG, T. H., REZAUR, R.B., & LEONG, E. C. 2007. Factors Controlling Instability of Homogeneous Soil Slopes under Rainfall. *Journal of Geotechnical and Geoenvironmental Engineering*, Vol. 133(12): 1532-1543.

RAHIMI, A., RAHARDJO, H., & LEONG, E.C., 2010, Effect of hydraulic properties of soil on rainfall-induced slope failure, *Engineering Geology*, Vol. 114: 135–143

RAHIMI, A., RAHARDJO, H., & LEONG, E.C., 2015, Effect of range of soil–water characteristic curve measurements on estimation of permeability function, *Engineering Geology*, Vol. 185: 96–104.

RAY, R. L., JACOBS, J.M., & ALBA, P.D., 2010. Impacts of Unsaturated Zone Soil Moisture and Groundwater Table on Slope Instability. *Journal of Geotechnical and Geoenvironmental Engineering*, Vol. 136(10): 1448-1458.

ROUAINIA, M., DAVIES, O., O'BRIEN, T. & GLENDINNING, S. 2009. Numerical modelling of climate effects on slope stability. *Proceedings of the Institution of Civil Engineers: Engineering Sustainability*, Vol. 162**:** 81-89.

SANTOSO, A.M., PHOON, K.-K., & QUEK, S.-T. 2011. Effects of soil spatial variability on rainfall-induced landslides. *Computers and Structures*, Vol. 89: 893–900.

SARAH, D. & SOEBOWO, E. 2011. Studi karakteristik curah hujan pemicu gerakan tanah di daerah Cibeber, Cianjur Selatan Jawa Barat. *Buletin Geologi Tata Lingkungan*, Vol. 21: 1 – 12.

SCHMIDT, J. & DIKAU, R. 2004. Modeling historical climate variability and slope stability. *Geomorphology*, Vol. 60**:** 433–447.

ŠIMŮNEK, J., VAN GENUCHTEN, M. Th., & ŠEJNA, M., 2005, *The HYDRUS-1D software package for simulating the one-dimensional movement of water, heat, and multiple solutes in variablysaturated media. Version 3.0, HYDRUS Software Series 1*, Department of Environmental Sciences, University of California Riverside, Riverside, CA, 270 p.

SUBIYANTI, H., RIFA'I, A. & JAYADI, R. 2011. Analisis Kelongsoran Lereng Akibat Pengaruh Tekanan Air Pori di Saluran Induk Kalibawang Kulonprogo. *Jurnal Ilmiah Semesta Teknika*, Vol. 14**:** 15-25.

TOHARI, A. 2013. Variations of pore-water pressure responses in a volcanic soil slope to rainfall infiltration. *Jurnal RISET Geologi dan Pertambangan*, Vol. 23: 97-111.

TOHARI, A., SUGIANTI, K. & HATTORI, K. 2013. Monitoring and Modelling of Rainfall-Induced Landslide in Volcanic Soil Slope. *In:* MARGOTTINI, C., CANUTI, P. & SASSA, K. (eds.) *Landslide Science and Practice, Vol. 2: Early Warning, Instrumentation and Monitoring.* Germany: Springer-Verlag Berlin Heidelberg

TSAI, T.-L. 2011. Influences of soil water characteristic curve on rainfall-induced shallow landslides. *Environmental Earth Sciences*, Vol. 64**:** 449-459.

TSAI, T.L., & WANG, J.K. 2011. Examination of influences of rainfall patterns on shallow landslides due to dissipation of matric suction, *Environmental Earth Sciences*, Vol. 63(1): 65-75.

TSAPARAS, I., RAHARDJO, H., TOLL, D. G. & LEONG, E.-C. 2002. Controlling parameters for rainfall-induced Landslides. *Computers and Geotechnics*, Vol. 29**:** 1-27.

U.S. ARMY CORPS OF ENGINEERS. 1997. Engineering and design: introduction to probability and reliability methods for use in geotechnical engineering. Department of the Army, Washington, D.C. Engineer Technical Letter 1110-2-547

VAN GENUCHTEN, M.T., 1980, A closed-form equation for predicting the hydraulic conductivity of unsaturated soils, *Soil Science Society of American. Journal*, Vol. 44: 892-898.

VAN GENUCHTEN, M.T, & Nielsen, D.R. 1985, On Describing and Predicting the Hydraulic Properties of Unsaturated Soils. *Annual Geophysics*, Vol. 3(5): 615-628.

VANAPALLI, S.K., FREDLUND D.G., PUFAHL, D.E. & CLIFTON, A.W., 1996. Model for the Prediction of Shear Strength with respect to Soil Suction. *Canadian Geotechnical Journal*, 33, 379-392.

VANAPALLI, S.K., FREDLUND, D.G., PUFAHL, D.E., & CLIFTON, A.W., 1996, Model for the prediction of shear strength with respect to soil suction. *Canadian Geotechnical Journal*, Vol. 33: 379–392.

VIMONT, D. J., BATTISTI, D. S. & NAYLOR, R. L. 2010. Downscaling Indonesian precipitation using large-scale meteorological fields. *International Journal of Climatology*, Vol. 30**,** 1706-1722.

VOGEL, T., & CÍSLEROVÁ, M., 1988, On the reliability of unsaturated hydraulic conductivity calculated from the moisture retention curve, *Transport in Porous Media*, Vol. 3: 1-15.

WORLD METEOROLOGICAL ORGANIZATION, 2014. WMO statement on the status of the global climate in 2013. WMO-No. 1130, Geneva, Switzerland

WU, T. H. 2013. Root reinforcement of soil: review of analytical models, test results, and applications to design. *Canadian Geotechnical Journal*, Vol. 50**:** 259-274.

XIE, M-W., ESAKI, T., & CAI, M-F., 2004. A time-space based approach for mapping rainfall-induced shallow landslide hazard, *Environmental Geology*, 46(7): 840-850.

ZHAI, Q., & RAHARDJO, H., 2013, Quantification of uncertainties in soil–water characteristic curve associated with fitting parameters, *Engineering Geology*, Vol.163: 144–152

ZHANG, J., TANG, W., & ZHANG, L. 2010. Efficient Probabilistic Back-Analysis of Slope Stability Model Parameters. *Journal of Geotechnical and Geoenvironmental Engineering*, 136(1): 99–109.

Lampiran A

Surat Dukungan Kerjasama dengan Kasetsart University

Dr.Eng. Agus Setyo Muntohar
Dr. Jazaul Ikhsan

Department of Civil Engineering
Kasetsart University

50 Ngam Wong Wan Road, Chatuchak, Bangkok, Thailand 10900
Telephone: (66-2)-797-0999 Ext. 1301-4
Tel./Fax: (66-2)-579-7565

July 8th, 2015

To
Agus Setyo Muntohar, Ph.D.
Department of Civil Engineering
Faculty of Engineering
Universitas Muhammadiyah Yogyakarta,

LETTER OF AGREEMENT FOR RESEARCH COLLABORATION

Hereby the Geotechnical Engineering Division of the Department of Civil Engineering, Faculty of Engineering, Kasetsart University would like to state our agreement to participate and contribute actively in the international collaboration research project that is proposed to us by the Geotechnical Engineering Research Group of the Department of Civil Engineering, Faculty of Engineering, Universitas Muhammadiyah Yogyakarta. The research collaborative agreement shall proceed for 3 years from 2015 to 2018. The research group of Kasetsart University will give full support to this collaboration in order to actively contribute in the research project entitled "MODELING OF RAINFALL INDUCES RESIDUAL SLOPE FAILURES DURING RAIN SESSION IN SOUTHEAST ASIA: A CASE STUDY IN INDONESIA AND THAILAND". Within its budget, the research group of Kasetsart University shall be responsible for the expenses of materials and equipments used for field study and laboratory research to be conducted in Thailand and Indonesia, domestic travel expenses and support in domestic field activities, and also willing to be the host of scientific seminars related to this research collaboration.

Yours sincerely,

Apiniti Jotisankasa, PhD DIC
Head of Geotechnical Engineering Division
Department of Civil Engineering
Faculty of Engineering, Kasetsart University Bangkok

Lampiran B

Naskah Publikasi:

1. SLOPE 2015
2. 7th RSID
3. PIT/KOGEI HATTI 2015
4. Jurnal Teknologi

Dr.Eng. Agus Setyo Muntohar
Dr. Jazaul Ikhsan

ABSTRACT REVIEW AND EVALUATION

Please answer the following questions :

TITLE OF PAPER : Stability Analysis of a Shallow Slope Failure during Wet Session in Kulonprogo, Indonesia

AUTHORS : Agus Setyo Muntohar, Eko Soebowo

Based on your opinion, the abstract is relevant to the conference theme

(1) Disagree (2) Fairly Agree (3) Agree (4) Strongly Agree

1. The abstract is well organized and meet the expectation for inclusion in the proceeding

   (1) Disagree (2) Fairly Agree (3) Agree (4) Strongly Agree

2. The abstract is original and give clear insight to the practicing engineers

   (1) Disagree (2) Fairly Agree (3) Agree (4) Strongly Agree

3. The abstract has no commercial promotion

   (1) Yes (2) No

4. The abstract may be extended for full paper

   (1) Yes (2) Yes after some revision (3) No

COMMENT :

- The paper presents stability analysis of slope failure due to infiltration of water during rainy season. Green-Ampt infiltration equations are used.
- It is interesting to define the pore water pressure distribution behind the slope.
- The authors are suggested to elaborate whether the analysis is based on saturated or unsaturated condition.

PAPER REVIEW AND EVALUATION

Please answer the following questions :

TITLE OF PAPER : STABILITY ANALYSIS OF A SHALLOW SLOPE FAILURE DURING RAINY SEASON IN KULONPROGO, INDONESIA

AUTHORS : Agus Styo Muntohar, Eko Soebowo

1. **The paper is well organized and meet the expectation for inclusion in the proceeding**

   (1) Disagree (2) Fairly Agree (3) Agree (4) Strongly Agree

2. **The paper is original and give clear insight to the practicing engineers**

   (1) Disagree (2) Fairly Agree (3) Agree (4) Strongly Agree

3. **The paper has no commercial promotion**

   (1) Yes (2) No (3) Indifferent

4. **The paper may be considered for oral presentation**

   (1) Yes (2) Yes after some revision (3) No

COMMENT :

1. English Structures : OK
2. Figures and Tables : OK
3. Content of Paper : OK
4. Conclusions : OK
5. References : OK

STABILITY ANALYSIS OF A SHALLOW SLOPE FAILURE DURING WET SEASON IN KULONPROGO, INDONESIA

Agus Setyo Muntohar[1], and Eko Soebowo[2]

ABSTRACT: In Indonesia, landslides commonly occurred during the rainy season in December to March. In this period, the rainfall intensities were very high and precipitated continuously. A case history of shallow landslide type in Kulonprogo, Indonesia is presented in this paper. The slope experienced to shallow failure on 21 November 2001, and the after that slope is prone to movement during the wet season in December to February every year. The aim of the paper is to evaluate the slope stability, in term of the probability of failure, during the wet season from 2004 to 2012. A probabilistic model of stability analysis incorporating infiltration was computed in this study. Direct Monte Carlo Simulation (*MCS*) method was performed to obtain the failure probability. The results show that the failure probability of the slope ranges from 0.126 to 0.302. The lowest and highest probability of failure was obtained for the rainfall period of December 2009 – March 2010 and December 2005 – March 2006 respectively. The performance level of the studied slope can be classified as "hazardous". In general, the study concludes that the proposed model can be applied to the preliminary analysis of slope stability during the wet season.

Keywords: slope stability, shallow landslide, rainfall, wet season, probability of failure

INTRODUCTION

In Indonesia, as a tropical country, the major climate is dry and wet season. This season was marked by the precipitation occurred in whole the years. Figure 1a show the average monthly rainfall in Indonesia. Indonesia receives significant rainfall year-round but experiences a wet season that peaks in January and a dry season that peaks in August (Hendon, 2003; Lee, 2015). Landslides commonly occurred during the wet season in December to February. In this period, the rainfall intensities were very high and precipitated continuously. In Yogyakarta, the mean monthly rainfall is shown in Figure1b.

A case history of shallow landslide type in Kulonprogo, Indonesia is presented in this paper. Muntohar and Ikhsan (2012) and Muntohar et al. (2013a) did a back analysis to investigate the strength properties and initial pore water pressure of the slope at the failure. The seepage triggering mechanism has shown that pore water pressure distribution of rainfall affected the slope failure. The rigorous analysis of the seepage and pores water pressure may result in a good prediction of slope failure. However, the distribution pattern can be simplified to obtain a simple but acceptable analysis for the stability of the slope. The objective of the paper is to evaluate the slope stability during the wet season. The stability analysis incorporating simplified pore water

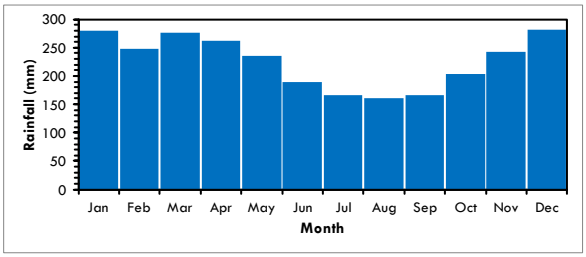

(a)

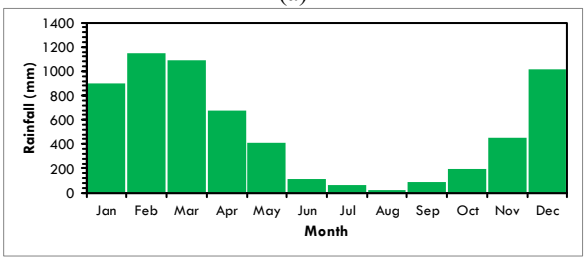

(b)

Figure 1. (a) Average monthly rainfall in Indonesia from 1900 – 2009 (World Meteorological Organization, 2014), (b) Average monthly rainfall in Yogyakarta from 2002-2011 (Muntohar & Ikhsan, 2012)

[1]Associate Professor, Department of Civil Engineering, Universitas Muhammadiyah Yogyakarta, Jl. Lingkar Selatan Taman Tirto, D.I. Yogyakarta, INDONESIA. Email: muntohar@umy.ac.id
[2]Geotechnology Research Center, Indonesian Institute of Sciences, JL. Sangkuriang, Kompleks LIPI, Bandung, INDONESIA

distribution was investigated. The evaluated slope was an andesitic residual soil where is located in Kulonprogo, Yogyakarta. The slope experienced to shallow failure on 21 November 2001, and the after that slope is prone to movement during the wet season in December to February every year. This paper is aimed to investigate the failure probability of the slope in Kedungrong during the rain season after the first failure in 2001.

Previous researchers have carried out the analysis of shallow slope instability under steady and unsteady infiltration (Montgomery and Dietrich, 1994; Xie et al., 2004; Muntohar and Liao, 2011; Tsai and Wang, 2011, Muntohar et al., 2013b). Chen and Young (2006) applied the Green-Ampt model on sloping ground under steady-state rainfall infiltration. The Green-Ampt equation is the analytical solution available for the computation of wetting front location that only two parameters required for characterizing the soil properties (Mishra et al., 2003; Ma et al., 2010). Muntohar and Ikhsan (2013) developed slope stability analysis incorporation with Green – Ampt infiltration. The studies showed that the factor of safety obtained from the proposed model was 5% lower than the results obtained from the finite element model.

SIMULATION AND ANALYSIS

Slope Geometry and Soil Properties

Data input for the slope stability modeling of the studied area has been taken from topographic and geotechnical investigations. The slope angle (α) varied from 10^o to 37^o, in which the mean value and standard deviation of the slope was 22^o and 9^o respectively. The depth of bedrock (H_b) was observed that range from 5 m to 11 m, which the mean and standard deviation was 10 m and 2.6 m respectively.

Soil geotechnical parameters were collected from a series of in-situ and laboratory tests, including grain size analysis, measurement of Atterberg limits, and drained direct shear tests (Soebowo et al. 2003). The geotechnical properties of the soil is presented in Table 1. The values in Table 1 are the mean (μ_x) of the parameter. The variability of the parameter is presented by the coefficient of variance (cov) or μ_x/σ_x = 0.01. Muntohar et al. (2013b) did back analysis to determine the pore water pressure distribution. The pressure at slope surface varied from -50 kPa to -1 kP, while the water pressure at failure surface range from -50 kPa to 7 kPa.

Table 1. Properties of the soil

Parameter	Mean value
Natural moisture content (w_N)	33.2 %
Bulk unit weight (γ_b)	17.7 kN/m^3
Unit weight above water table (γ_d)	13.4 kN/m^3
Degree of saturation (S_r)	90.1%
Saturated volumetric water content (θ_s)	0.48
Saturated permeability coefficient, (k_{sat})	1.19x10^{-4} m/s
Peak cohesion (c')	16 kPa
Residual cohesion, (c'$_r$)	12 kPa
Peak internal friction angle (ϕ')	24^o
Residual internal friction angle (ϕ'_r)	18^o

Infiltration and Slope Stability Analysis

Instability of unsaturated soil slopes after rainfall is common in many countries, and these failures are generally shallow and are usually parallel to the slope surface. The stability of these slopes can be analyzed by a simple infinite slope analysis. The model slope stability analysis in combination with infiltration analysis was preformed from the model developed by Muntohar and Ikhsan (2013). The model incorporated one-dimensional infiltration analysis and infinite slope stability analysis. The infiltration analysis was developed from Green – Ampt infiltration model. Time-varying and unsteady rainfall intensity was considered in the model. The basic Green – Ampt infiltration for sloping ground is written in Equation 1 and 2.

$$F(t)-\frac{\Delta\theta\psi_f}{\cos\alpha}\ln\left(1+\frac{F(t)\cos\alpha}{\Delta\theta\psi_f}\right)=k_s\cos\alpha\cdot t \qquad (1)$$

$$f(t)=k_s\left(\cos\alpha+\frac{\Delta\theta\psi_f}{F(t)}\right) \qquad (2)$$

Equation (1) and (2) are the GA equations for cumulative infiltration and infiltration rate respectively for sloping ground. For non-uniform rainfall with respect to time *t*, those equations can be solved by iteration method. The infiltration analysis determines the depth of wetting front (z_w*) and condition of the pore water pressure (u_w). Theses two variables are used for calculation the factor of safety.

The slope stability can be expressed by calculating the factor of safety as written in Equation (3).

$$FS(t)=\frac{c'+\left[\gamma_t\cdot z_f(t)\cos^2\alpha-u_w(t)\right]\tan\phi'}{\gamma_t\cdot z_f(t)\cdot\sin\alpha\cdot\cos\alpha} \qquad (3)$$

The water pressure (u_w) is calculated in two conditions. The pressure $u_w = \psi_f.\gamma_w$, if the ground surface is unsaturated, but if the surface is saturated the pore water pressure $u_w = z_w*.\gamma_w$ (Muntohar and Ikhsan, 2013). The depth of failure-plane z_f is determined from depth of wetting front z_w*. which is limited by the depth of impermeable layers or bedrock. In this case, the maximum z_w* is the depth of bedrock H_b.

Rainfall Record

The slope was evaluated during the rainy season in December to March. The rainfall records from 2004 to 2012 were used. The rainfall data were collected from the nearest automatic rain-gauge at rainfall station in Kalibawang catchment area. Figure 2 presents the rainfall hyetograph of the rainy season in December – March from 2004 to 2012.

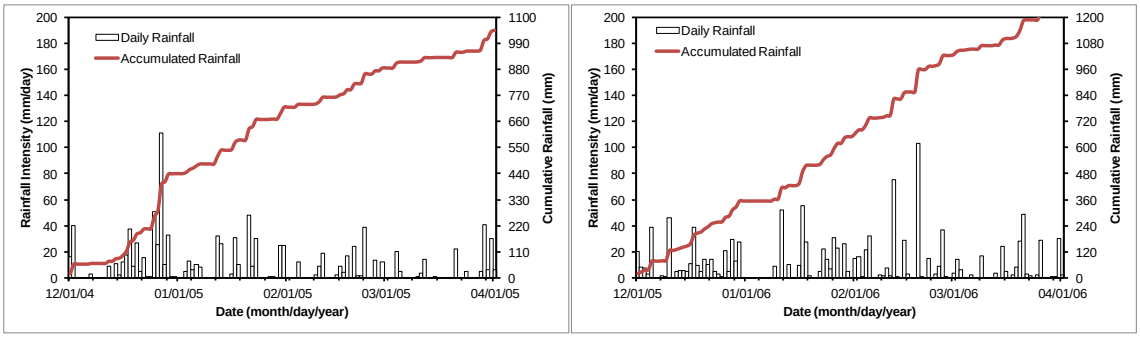

(a) December 2004 – March 2005

(b) December 2005 – March 2006

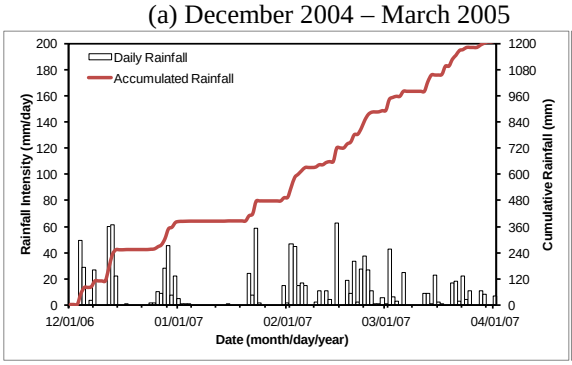

(c) December 2006 – March 2007

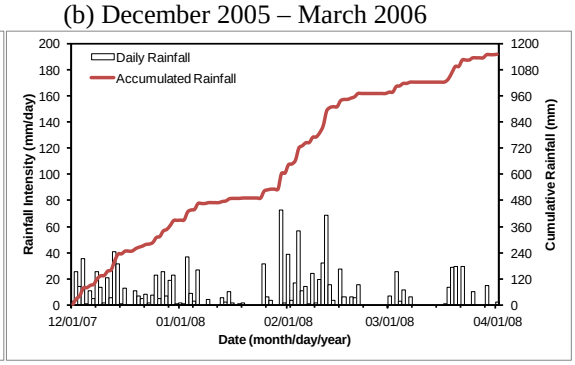

(d) December 2007 – March 2008

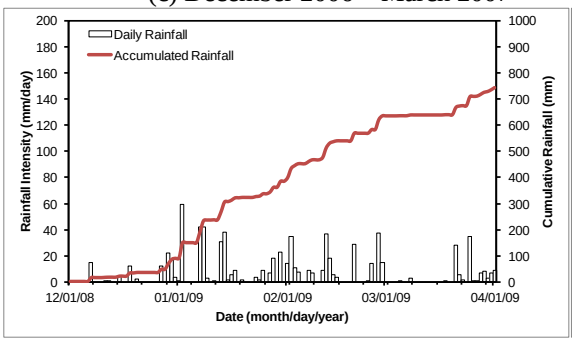

(e) December 2008 – March 2009

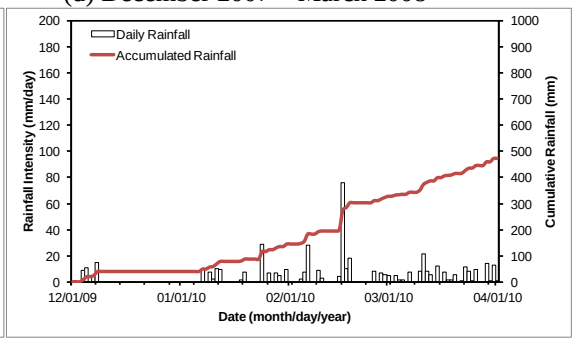

(f) December 2009 – March 2010

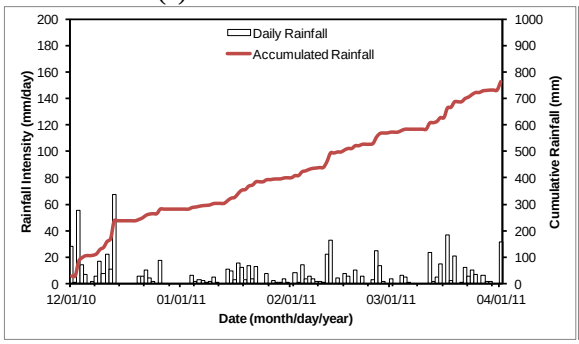

(g) December 2010 – March 2011

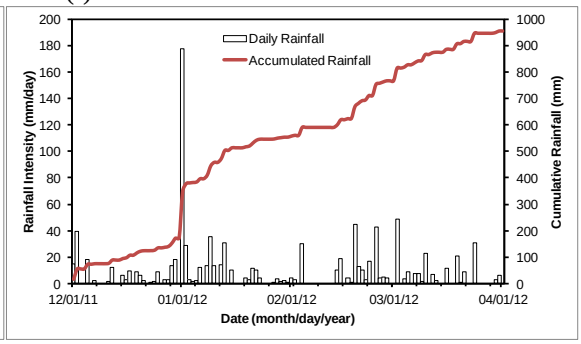

(h) December 2011 – March 2012

Figure 2. The rainfall hyetograph from December 2004 to March 2012

Reliability and failure probability

Reliability is the probability of an object (item or system) performing its required function adequately for a specified period under stated conditions (Harr, 1989). As it applies in the present context, the reliability of a slope is the probability that the slope will remain stable under specified design conditions. In slope reliability analysis, the performance function $g(X)$ of slope stability can be stated by a factor of safety equation in Equation (3). The variables $X = \{x_{1\ldots n}\}$ are n input uncertain variables which impact the slope reliability. The variables are $X_i = \{\alpha_i, c_i', \phi'_i, \gamma_{t,i}, H_{b,i}, k_{s,i}, \psi_{f,i}, \Delta\theta_i\}$. The function $FS(X,t)$ reflects the performance or state of the slope as time dependent function. The slope will be safe when $FS(X,t) > 0$; unsafe or failure when $FS(X,t) < 1$; limit state when $FS(X,t) = 1$, which is also called the limit state function of slopes.

In this study, direct Monte Carlo Simulation (*MCS*) method was performed to obtain the failure probability. Values of each uncertain variable were randomly sampled as an identically-independent distribution (i.i.d) from the probability distribution function (*PDF*) for each N simulation cycles. The number of simulation was 10000. The sample distribution was approached by a lognormal PDF (Muntohar and Ikhsan, 2012). Each set of samples and the resulting outcome from that sample was recorded.

In reliability theory, the reliability index β of the slope stability can be represented by Equation 6 if the probability density function of safety factor is normally distributed.

$$\beta = \frac{\mu_{FS(X,t)} - 1}{\sigma_{FS(X,t)}} \quad (6)$$

where $\mu_{FS(X,t)}$ and $\sigma_{FS(X,t)}$ are mean and standard deviation of the safety factor. Then, the probability of failure can be calculated from the reliability index by Equation (7), which is defined as the probability that the minimum factor of safety (FS) is less than unity i.e., $P_f = P(FS < 1)$.

$$P_f = 1 - \Phi(\beta) \quad (7)$$

where, $\Phi(\beta)$ is the standard normal cumulative distribution function for the given β.

RESULTS

Variation of the Probability of Failure

Figure 3 present the maximum probability of failure during the rainfall period in December – March for 2004 – 2012. The results show that the failure probability of the slope ranges from 0.126 to 0.302. The lowest and highest probability of failure was obtained for the rainfall period of December 2009 – March 2010 and December 2005 – March 2006 respectively. Table 2 lists β and P_f for representative geotechnical components and systems and their expected performance levels (U.S. Army Corps of Engineers, 1997). Hence, the performance level of the studied slope can be classified as "hazardous". In practice, geotechnical designs require a β value of at least 2 or $P_f < 0.023$) for an expected performance level better than ''poor''. In general, a higher probability of failure indicates the occurrence of failing is high, whereas a lower probability of failure indicates the slope close to a not-failure state. In fact based on the field observation, the slope is remaining stable. However, tilting trees to the downstream on the slope was observed that indicated a light ground movement took place.

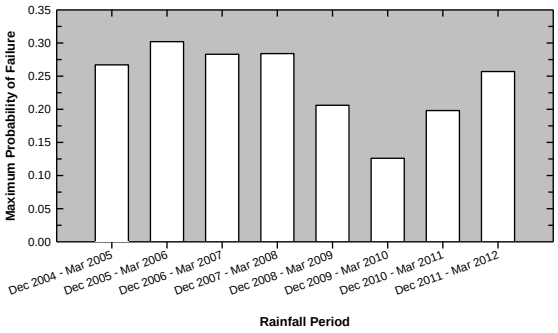

Figure 3. Variation of the probability of failure

Table 2 Relationship between reliability index and the probability of failure (U.S. Army Corps of Engineers, 1997).

Reliability index, β	Probability of failure, $P_f = \Phi(-\beta)$	Performance level
1.0	0.16	Hazardous
1.5	0.07	Unsatisfactory
2.0	0.023	Poor
2.5	0.006	Below average
3.0	0.001	Above average
4.0	0.00003	Good
5.0	0.0000003	High

Estimation of failure occurrence

The probability of failure has been calculated during the rain season from December to March for 2004 to 2012. The probability distribution with time is shown in Figure 4. The figures show the density of the samples that have $FS(X,t) < 1$. In the direct MCS, the density count the amount of value $FS(X,t) < 1$ out of the total samples (N = 10000). The density is commonly known as frequency in statistical theory.

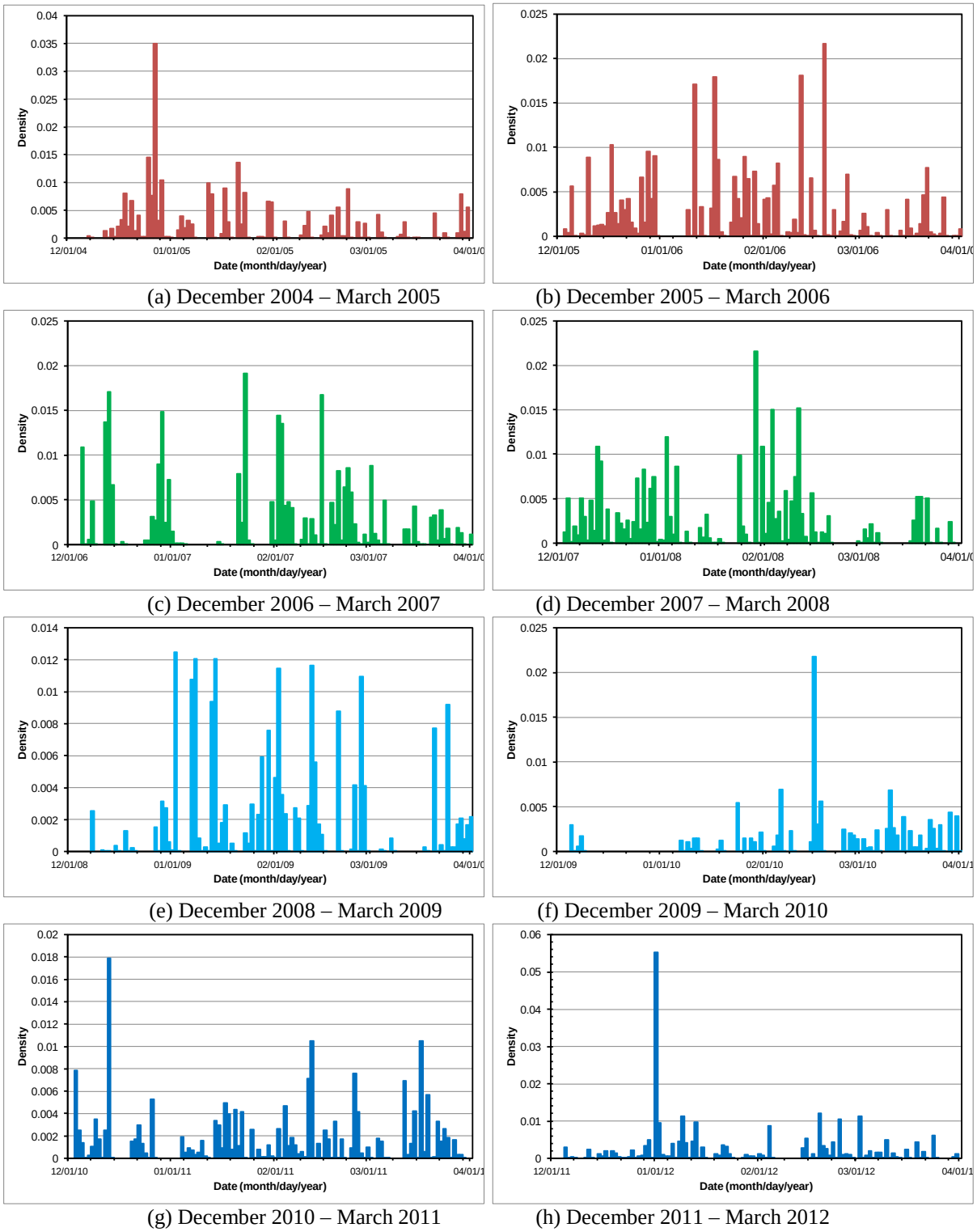

(a) December 2004 – March 2005 (b) December 2005 – March 2006

(c) December 2006 – March 2007 (d) December 2007 – March 2008

(e) December 2008 – March 2009 (f) December 2009 – March 2010

(g) December 2010 – March 2011 (h) December 2011 – March 2012

Figure 4 Distribution of the Probability of Failure

A higher-density, it indicates that the occurrence of the time interval is more frequent to occur. Hence, the density can be applied to estimate the occurrence of slope failure.

The relationship in Figure 4 shows that the probability density is widely distributed with the elapsed time. It is clearly shown that probability density differed every year. In general, the occurrence is concentrated within end of December to February, but less in March. Muntohar (2010) suggested that the failure occurrence is presented in the monthly or daily time interval to obtain a good estimation.

DISCUSSION

The focus of this paper is to quantify the uncertainty of the factor of safety due to uncertainty

in soil properties and fluctuation of rainfall. In slope - probabilistic analysis, the establishment of the probability distribution of every random variable is a fitting process based on the limited data from measurements or tests. Therefore, there are three major sub-categories introduced: site characterization uncertainty, model uncertainty, and parameter uncertainty (Lumb, 1969; Lind, 1983; Malkawi et al., 2000). In the calculation of reliability index (Equation 6), a large variance of the factor of safety might result in an overestimate the probability of failure since the FS < 1 was located at the tail of the distribution. It is important to note, however, that probabilistic analyzes can be erroneous and misleading. El-Ramly et al. (2002) mentioned that ignoring the spatial variability of soil properties and assuming perfect autocorrelations as in the simplified analysis can significantly overestimate the performance level of the slope or probability of unsatisfactory performance.

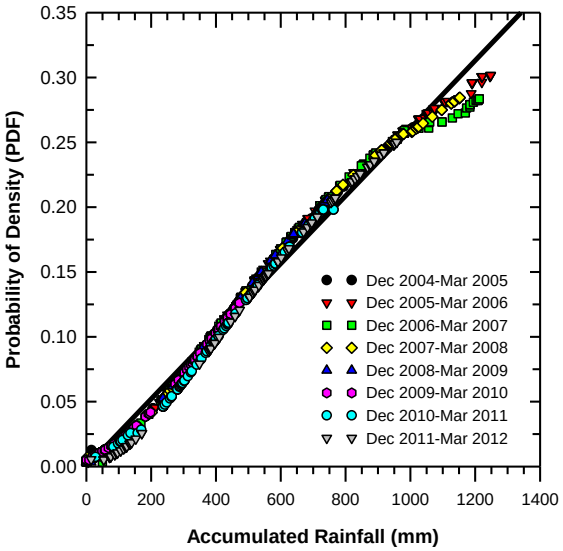

(a)

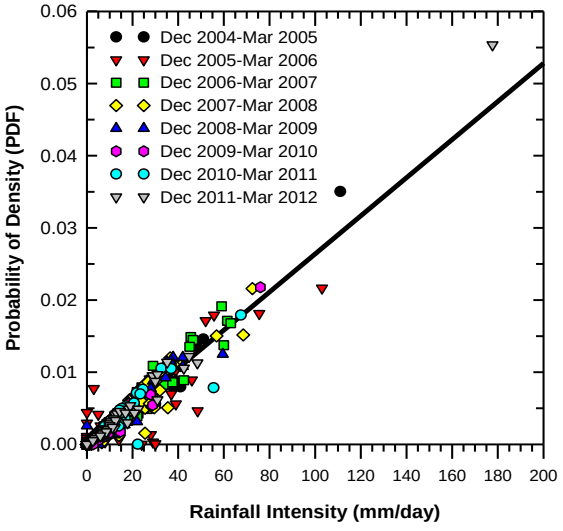

(b)

Figure 5. (a) Correlation between accumulated rainfall and probability of slope failure (b) Correlation between rainfall intensity and probability density of slope failure.

It has been illustrated in Figure 4 that the probability of slope failure varied and depended on accumulated rainfall as shown in Figure 5a. A linear correlation was shown between the probability of failure and the accumulated rainfall. A lower amount of rainfall, a lower probability of failure was reached. It is true since the computed factor of safety (Equation 3) was the function of accumulated infiltration (Equation 1) that depends on the input accumulated rainfall. While, the probability density of slope failure looks like to depend on the rainfall intensity. Figure 5b show the correlation between rainfall intensity and probability density of slope failure. The figure clearly shows a linear correlation between rainfall intensity and probability density of slope failure.

Malkawi et al. (2000) suggested that the proposed model can be compared to the other slope stability or probability method to gain a more reliable model. The variability of input parameter was contributed by spatial variability of the soils. Buttt, less contribution was generated by the statistical sources of uncertainty such as sparse data or the use of empirical correlations and factors (El-Ramly et al., 2005). The factor of safety changed considerably because of the contribution the greatest uncertainty in the probability distribution of the parameter. This condition is valid if the updated parameters are not correlated in the prior distribution (Zhang et al., 2010).

CONCLUSIONS

This paper outlines the evaluation of the performance level of the slope during a wet season in 2004 to 2012. A probabilistic analysis of slope stability has been performed using direct Monte Carlo simulation method. The results showed that the failure probability of the slope varied from 0.126 to 0.302 that depend on the accumulated rainfall. The lowest and highest probability of failure was obtained for the rainfall period of December 2009 – March 2010 and December 2005 – March 2006 respectively. This result concluded that the performance level of the studied slope can be classified as “hazardous”. Correlation of the probability density and time indicated that the time of failure can be estimated from the rainfall intensity distribution for a time interval. The conclusions of this study was limited for the proposed model. I is suggested that the proposed model can be compared to the other slope

stability or probability method to gain a more reliable model.

ACKNOWLEDGEMENTS

The work in this paper was substantially supported by grants from the Ministry of Research, Technology and Higher Education for the research grant in 2015 under the research scheme "*Penelitian Hibah Kompetensi*" (DIPA No. 023.04.1.673453/2015.

REFERENCES

Chen, L., and Young, M.H., (2006), Green-Ampt infiltration model for sloping surface, Water Resources Research, 42: 1-9

El-Ramly, H., Morgenstern, N. R. and Cruden, D. (2002). Probabilistic slope stability analysis for practice. Canadian Geotechnical Journal, 39: 665–683

El-Ramly, H., Morgenstern, N.R., and Cruden, D.M., (2005) Probabilistic assessment of stability of a cut slope in residual soil. Géotechnique, 55(1): 77–84

Harr, M. E. (1989). Probabilistic estimates for multivariate analyses. Applied Mathematical Modeling, 13 (5): 313-318.

Hendon, H.H. (2003) Indonesian Rainfall Variability: Impacts of ENSO and Local Air–Sea Interaction, Journal of Climate, 16: 1775-1790.

Lee, H.S. (2015) General Rainfall Patterns in Indonesia and the Potential Impacts of Local Season Rainfall Intensity. Water, 7: 1751-1768

Lind, N. C., (1983) Modeling uncertainty in discrete dynamical systems. Applied Mathematical Modelling, 7 (3):146-152.

Lumb, P. (1969) Safety factors and the probability distribution of soil strength. Canadian Geotechnical Journal, 7 (3): 225-242.

Ma Y, Feng S, Zhan H, Liu X, Su D, Kang S, and Song X., (2010) Water Infiltration in Layered Soils with Air Entrapment: Modified Green-Ampt Model and Experimental Validation. Journal of Hydrologic Engineering, 16(8): 628-638.

Malkawi, A. I. H., Hassan, W. F., and Abdulla, F. A. (2000) Uncertainty and reliability analysis applied to slope stability. Structural Safety, 22(2) : 161-187

Mishra, S.K., Tyagi, J.V., and Singh, V.P., (2003) Comparison of Infiltration Models, Hydrological Processes, 17(13): 2629–2652

Montgomery, D.R., and Dietrich, W.E., (1994) A Physically Based Model for the Topographic Control on Shallow Landslide, Water Resources Research, 30: 83–92.

Muntohar A.S., and Ikhsan J., (2012). Numerical and Experimental Studies of Rainfall Infiltration Induced Slope Stability, Final Report of Fundamental Research Grant, Universitas Muhammadiyah Yogyakarta – Directorate General Higher Education Ministry of Education and Culture.

Muntohar, A.S, and Liao, H-J., (2011). Rainfall infiltration: infinite slope model for landslides triggering by rainstorm, Natural Hazards, 54(3): 967–984

Muntohar, A.S, Ikhsan, J., and Soebowo, E. (2013) Mechanism of rainfall triggering landslides in Kulonprogo, Indonesia. Geo-Congress 2013: 452-461

Muntohar, A.S., (2010) Application of Probabilistic Analysis for Prediction for Initiation of Landslide. Proceeding the 1st International Workshop on Multimodal Sediment Disasters Triggered by Heavy Rainfall and Earthquake and the Countermeasures, Yogyakarta, Indonesia, 8-9 March 2010, pp.33-44.

Muntohar, A.S., and Ikhsan, J., (2013). Development A Simple Model for Preliminary Evaluation on Extreme Rainfall Induces Shallow Slope Failure. Quality in Research (QiR 2013): 1291-1296.

Muntohar, A.S., Ikhsan, J., and Liao, H.J, (2013b), Influence of Rainfall Patterns on the Instability of Slopes. Civil Engineering Dimension, 15(2):120-128.

Soebowo,E., Anwar, H.Z., Siswandi, U.S., and Rukmana, I., (2003). Mitigation model for landslide disaster in tropical region: A case study in Kedungrong, Kulonprogo. Research Report of Resources and Geo-disaster Mitigation, Geotechnology Research Center, Indonesian Institute of Sciences, 55p (in Indonesia)

Tsai T.L., Wang J.K., (2011) Examination of influences of rainfall patterns on shallow landslides due to dissipation of matric suction, Environmental Earth Sciences, 63(1): 65-75.

U.S. Army Corps of Engineers. (1997). Engineering and design: introduction to probability and reliability methods for use in geotechnical engineering. Department of the Army, Washington, D.C. Engineer Technical Letter 1110-2-547

World Meteorological Organization, (2014) WMO statement on the status of the global climate in 2013. WMO-No. 1130, Geneva, Switzerland

Xie M.W., Esaki T., and Cai M.F., (2004) A time-space based approach for mapping rainfall-induced shallow landslide hazard, Environmental Geology, 46(7): 840-850.

Zhang, J., Tang, W., and Zhang, L. (2010) Efficient Probabilistic Back-Analysis of Slope Stability Model Parameters. Journal of Geotechnical and Geoenvironmental Engineering, 136(1): 99–109.

SYMBOLS AND NOTATIONS

The following symbols are used in this paper
c' = cohesion,
F(t) = cumulative infiltration at time t,
f(t) = infiltration rate at time t.
FS = factor of safety,
H_b = depth of impermeable layers or bedrock,
k_s = saturated hydraulic conductivity,
P_f = probability of failure.
u_w = pore water pressure,
z_f = depth of sliding-plane,
z_w*= depth of wetting front,
$\Delta\theta$ = deficit soil moisture,
α = slope angle,
β = reliability index,
ϕ' = internal friction angle,
γ_t = saturated unit weight of soil,
γ_w = unit weight of water,
ψ_f = suction head at wetting front,
$\Phi(\beta)$ = the standard normal cumulative distribution function for the given β,
$X = \{x_{1...n}\}$ = n input uncertain variables.

Department of Civil Engineering
Kasetsart University
50 Ngam Wong Wan Road, Chatuchak, Bangkok, Thailand 10900
Telephone: (66-2)-797-0999 Ext. 1342
Tel./Fax: (66-2)-579-7565

July 1, 2015

Dear Assoc. Prof. Dr. Agus Setyo Muntohar

On behalf of the organizing committee, I would like to invite you to participate in the 7th Regional Symposium on Infrastructure Development (RSID 7) to be held in Bangkok on November 5-7, 2015. As you are a special guest for this event, the registration fee will be waived. Please let me know by email or by returning the invitation acceptance form (rsid@ku.ac.th), if you are able to participate in this event. I do very much hope that you will be able to join us.

I look forward to hearing from you at your earliest convenience.

Sincerely,

Wanchai Yodsudjai, D.Eng.
Associate Professor
Chair, RSID 7 Organizing Committee
Department of Civil Engineering, Faculty of Engineering
Kasetsart University

Name. Assoc.Prof.Dr.. Agus Setyo Muntohar ....E-mail: muntohar@umy.ac.id ..

☐ I agree to participate in the 7th Regional Symposium on Infrastructure Development.

☐ I could not participate in the 7th Regional Symposium on Infrastructure Development.

Please submit this acceptance form at your earliest convenience to rsid@ku.ac.th or (66)2-579-7565.

Predicting of Shallow Slope Failure Using Probabilistic Model: a Case Study of Granitic Fill Slope in Northern Thailand

A.S. Muntohar
Department of Civil Engineering, Universitas Muhammadiyah Yogyakarta, D.I. Yogyakarta, Indonesia. Email: muntohar@umy.ac.id
A. Jotisankasa
Department of Civil Engineering, Kasetsart University, Bangkok, Thailand. E-mail: fengatj@ku.ac.th
H.J. Liao
Department of Construction Engineering, National Taiwan University of Science and Technology, Taipei, Taiwan. E-mail: hjliao@mail.ntust.edu.tw
RM.N. Barus
Department of Civil Engineering, Universitas Muhammadiyah Yogyakarta, D.I. Yogyakarta, Indonesia.

Abstract

Slope failure occurred during rainfall in September 2009 near the peak of Doi-Inthanon national Park, Northern Thailand. Progressive studies have been conducted to monitor the pore water pressure variation during the monitored rainfall in September 2011. Lack of data for back analysis generated uncertainties in slope failure analysis. This paper presents probability analysis of the slope failures. The analysis considers the uncertainties of the influencing factor such as rainfall intensity, hydraulic and strength parameter of the soil. The probability analysis was calculated using Monte Carlo Simulation method (MCS). The slope failure was modeled using the infinite slope. Infiltration analysis was analyzed using Green – Ampt model. Three models of the rainfall hyetographs, including hourly rainfall, 15 minutes rainfall, and 5 minutes rainfall, were used to analysis the probability of failure. The simulation results show that the probability of failure (P_f) ranges about 0.36-0.38 for the corresponding rainfall. The highest probability of failure was obtained when daily rainfall was simulated. The probability of failure was strongly affected by the variability of the input parameter.

Keywords: rainfall, probability, shallow slope failure, factor of safety, residual soil

1. Introduction

This paper presents the extensive field monitoring results of pore-water pressure and rainfall of a granitic soil slope near the peak of Doi-Inthanon national park, Northern Thailand. Jotisankasa et al.[1] did back analysis of the soil slope that failed in 2011. The study was performed to determine the critical pore-water pressure at failure based on laboratory shear strength. The study also involved laboratory determination of the saturated-unsaturated shear strength and Soil-Water Characteristic Curves (SWCC). Although the early study has been successfully estimated the critical pore water pressure at the site, lack of data for back analysis generated uncertainties in slope failure analysis. Hence, continuous research needs to be conducted to determine the triggering rainfall. This paper presents a probability analysis of the slope failures. The analysis considers the uncertainties of the influencing factor such as rainfall intensity, hydraulic and shear strength parameter of the soil. The effect of rainfall intensities and the uncertainty of soil properties on the probability of failure of the slope is the primary objective of this research. In slope - probabilistic analysis, the establishment of the probability distribution of every random variable is a fitting process based on the limited data from measurements or tests. Therefore, there are three major sub-categories introduced: site characterization uncertainty, model uncertainty, and parameter uncertainty [2,3,4].

2. Method of Analysis

2.1. Rainfall Infiltration and Slope Stability Model

Instability of unsaturated soil slopes after rainfall is common in many countries, and these failures are generally shallow and are usually parallel to the slope surface. The stability of these slopes can be analyzed by a simple infinite slope analysis. The model slope stability analysis in combination with infiltration analysis was adopted from the model developed by Muntohar and Ikhsan [5]. The model incorporated one-dimensional infiltration analysis and infinite slope stability analysis. The infiltration analysis was developed from Green – Ampt infiltration model. Time-varying and unsteady rainfall intensity was considered in the model.

The slope stability can be expressed by calculating the factor of safety as written in Equation 1.

$$FS(t) = \frac{c' + \left[\gamma_t \cdot z_f(t)\cos^2\alpha - u_w(t)\right]\tan\phi'}{\gamma_t \cdot z_f(t)\cdot\sin\alpha\cdot\cos\alpha} \quad (1)$$

Where, u_w is the pore water pressure, γ_t is saturated unit weight of soil, c' and ϕ' are cohesion and internal friction angle respectively, z_f is depth of sliding-plane that is equal to depth of wetting front (z_w*). The depth of wetting front is limited by the depth of impermeable layers or bedrock. In this case, the maximum z_w* is the depth of bedrock (H_b). The pore water pressure is calculated in two condition: $u_w = \psi_f.\gamma_w$, if the ground surface is unsaturated, but if the surface is saturated the pore water pressure $u_w = z_w^*.\gamma_w$. [5].

2.2. Reliability and failure probability

Reliability is the probability of an object (item or system) performing its required function adequately for a specified period under stated conditions [6]. As it applies in the present context, the reliability of a slope is the probability that the slope will remain stable under specified design conditions. In slope reliability analysis, the performance function $g(X)$ of slope stability can be stated by a factor of safety equation in equation 1, and is always defined as in equation 2.

$$g(X,t) = \frac{R(X,t)}{L(X,t)} \quad (2)$$

where, $X = \{x_{1\ldots n}\}$ are n input uncertain variables which impact the slope reliability. The variables are $X_i = \{\alpha_i, c_i', \phi'_i, \gamma_{t,i}, H_{b,i}, k_{s,i}, \psi_{f,i}, \Delta\theta_i\}$. The function $g(X,t)$ reflects the performance or state of the slope as time dependent function. The slope will be safe when $g(X,t) > 0$; unsafe or failure when $g(X,t) < 1$; limit state when $g(X,t) = 1$, which is also called the limit state function of slopes.

In this study, Monte Carlo Simulation (MCS) method was performed to obtain the failure probability. Values of each uncertain variable are generated randomly as an identically-independent distribution (i.i.d) from the probability distribution function (*PDF*) for each N simulation cycles. A lognormal PDF was used in this study. Each set of samples and the resulting outcome from that sample was recorded. In reliability theory, the reliability index β of the slope

stability can be represented by Equation 3 if the probability density function of safety factor is normally distributed.

$$\beta = \frac{\mu_{FS(X,t)} - 1}{\sigma_{FS(X,t)}} \tag{3}$$

where $\mu_{FS(X,t)}$ is the mean of the safety factor and $\sigma_{FS(X,t)}$ is the standard deviation of the safety factor. If the probability density function of safety factor is log-normally distributed, the reliability index of slope can be given as Equation 4 [7].

$$\beta = \frac{\ln\left[\mu_{FS(X,t)} \Big/ \sqrt{1+\left(\sigma_{FS(X,t)}/\mu_{FS(X,t)}\right)^2}\right]}{\sqrt{\ln\left[1+\left(\sigma_{FS(X,t)}/\mu_{FS(X,t)}\right)^2\right]}} \tag{4}$$

For this reason, the distribution of the factor of safety will be evaluated. Then, the probability of failure can be calculated from the reliability index by Equation 5.

$$P_f = 1 - \Phi(\beta) \tag{5}$$

where, $\Phi(\beta)$ is the cumulative probability density function for the given β.

2.3. Slope and soil properties

Data input for the slope stability modeling of the studied area has been taken from topographic and geotechnical investigations by Jotisankasa et al. [1]. The data collected was determined as the mean value while the coefficient of variance (*cov*) was assumed to be varied by 0.01, 0.02, and 0.005. The geotechnical properties of the soil are presented in Table 1.

The rainfall was recorded from the nearest rainfall station on 1 - 14 September 2011. Originally, the rainfall record was transmitted as 5 minutes rainfall as shown in Figure 1a. The cumulative rainfall for two weeks was about 520 mm. The other rainfall hyetograph was analyzed for hourly rainfall, and daily rainfall as illustrated in Figure 1b and 1c respectively.

Table 1 Soil properties of the slope

Slope angle α	Hydraulic conductivity k_s (mm/h)	Moisture difference $\Delta\theta = \theta_s - \theta_i$	Wetting front suction head ψ_f (mm)	Cohesion c' (kPa)	Friction angle ϕ'	Soil unit weight γ_t (kN/m^3)	Bedrock Depth H_b (m)
33^o	2203.2	0.125	300	10.1	26.7^o	21.8	2
Note: The values are mean values (μ). The *cov* was varied by 0.01, 0.02, and 0.005. The Wetting front suction head was estimated from soil water retention curve.							

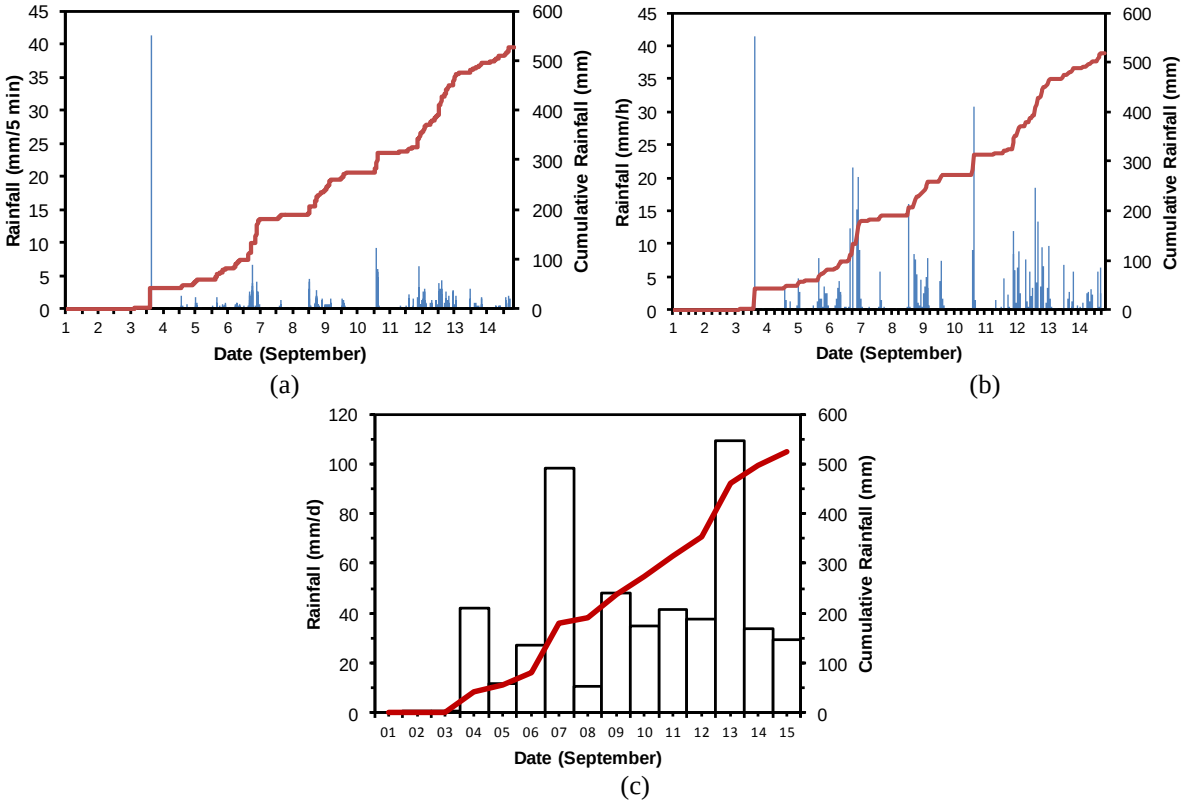

Figure 1 The rainfall hyetograph for the study (a) 5 minutes rainfall, (b) hourly rainfall, (c) daily rainfall

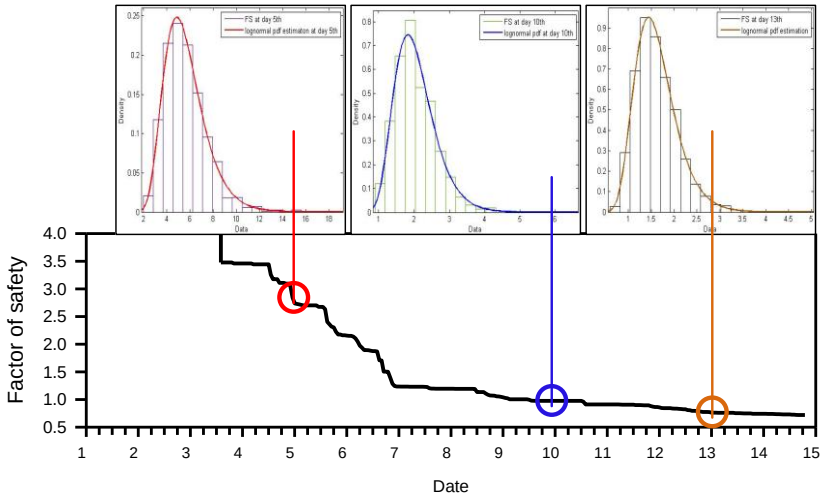

Figure 2 Typical the change of factor of safety and the probability distribution of time for the hourly rainfall

3. Results and Discussion

3.1. Probability density and Probability of Failure

The simulation will result in a variation of factor of safety with the elapsed time. Typical the change of factor of safety and the distribution with time is shown in Figure 2. The calculated factor of safety was not normally distributed but lognormal. Hence, the reliability index was determined using equation 4. As a consequence, the probability of failure was calculated based

on the lognormal probability density function. The variation of the probability density and failure probability with the elapsed time of the 5 minutes rainfall, hourly rainfall, and daily rainfall are shown in Figure 3, 4, and 5 respectively. The failure probability of the slope range from 0.05 to 0.37 due to the 5 minutes rainfall pattern, while the probability of slope failure was 0.04 – 0.36 and 0.05 – 0.038 for hourly and daily rainfall pattern respectively. The results show that the maximum failure probability for the given input parameter was about 0.36 – 0.38 due to the rainfall recorded at the site.

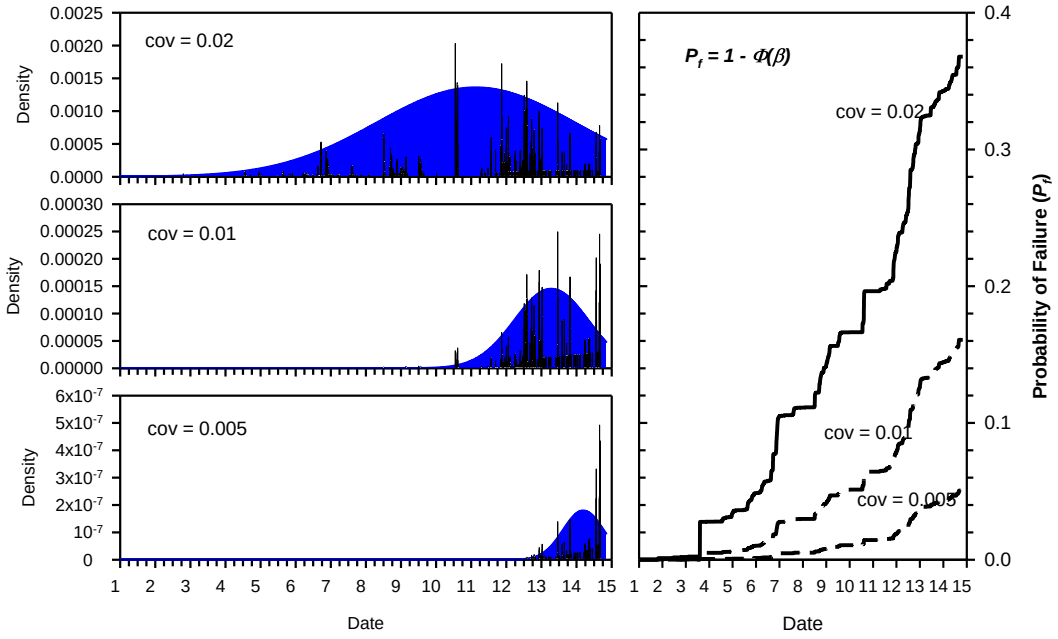

Figure 3 Distribution of failure occurrence and failure probability with the time of 5 minutes rainfall

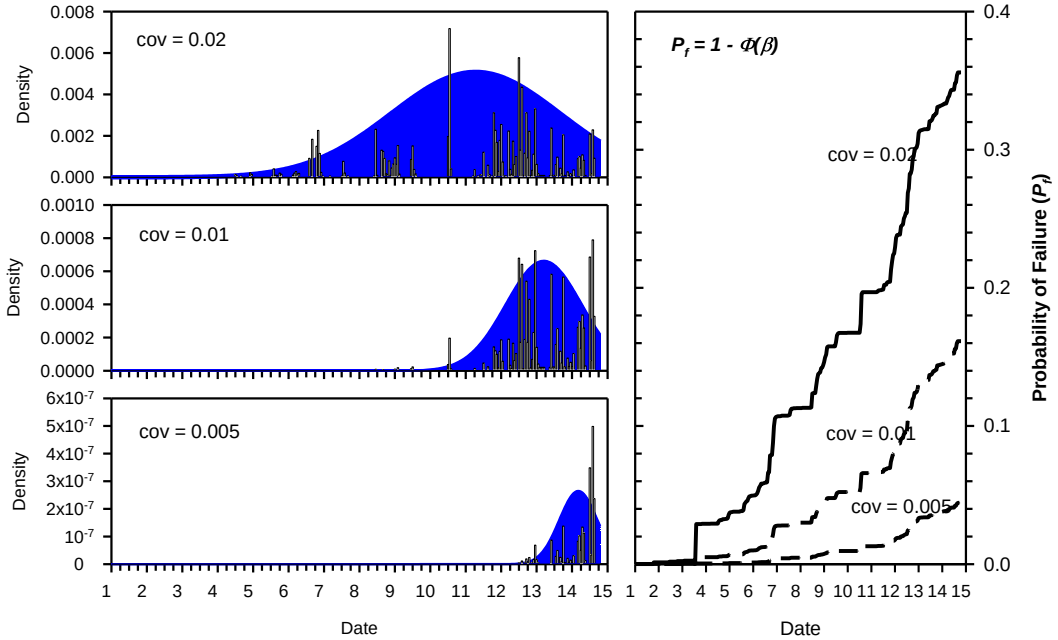

Figure 4 Distribution of failure occurrence and failure probability with the time of hourly rainfall

The relationship in Figure 3 to 5 show that the probability density is widely distributed with the elapsed time if the *cov* is large. In contrast, the probability density is closely distributed if the *cov* is small. In this study, the probability density of occurrence is estimated using the *normal probability density function*. Muntohar [8] proposed the estimated mean time to failure (MTTF) by using the statistical properties of its *pdf* i.e. mean (μ) and variance (σ^2) or standard deviation (σ). The μ value determines the center of the *pdf,* and the value of σ^2 determines the width. A small value of the variance implies that the time to failure is closer to the central value or less uncertain. Table 2 presents the MTTF for the simulated rainfall in this study. Based on this presentation, the slope failure can be estimated to be occurred between 9 to 13 September 2011 that depends on the rainfall patterns and variance of the input parameter. The failure probability for that time interval was about 0.38. For a slope failure in which the knowledge in pore water pressure is poor, the uncertainty in pore water pressure may dominate the analysis [9]. The probability density during the rainfall will present the "degree of belief" to estimate the time of slope failure.

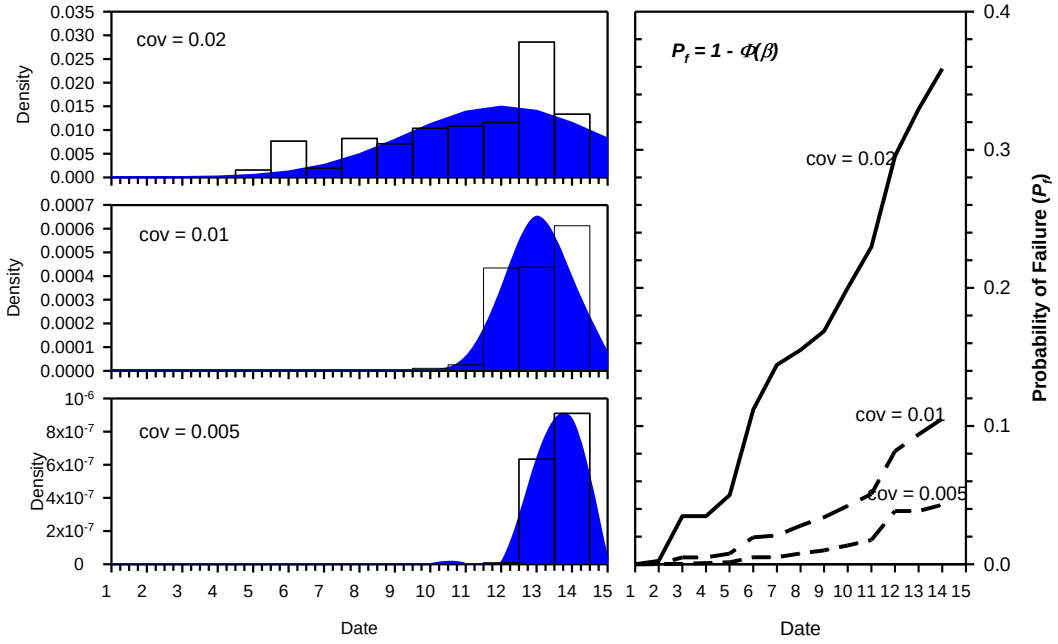

Figure 5 Distribution of failure occurrence and failure probability with the time of daily rainfall

Table 2 The statistical properties of *pdf* to determine the day of failure

Rainfall pattern	*cov* input parameter	Estimated time of failure (day)		Maximum Probability of failure (P_f)
		Mean, μ	Variance, σ^2	
5 minutes	0.02	9.725	7.305	0.37
	0.01	11.785	1.007	0.16
	0.005	12.659	0.300	0.05
Hourly	0.02	10.321	5.680	0.37
	0.01	12.241	1.148	0.16
	0.005	13.217	0.289	0.04
Daily	0.02	12.043	7.294	0.38
	0.01	13.051	0.871	0.11
	0.005	13.582	0.253	0.05

3.2 Impact of variability the input variables

The simulation in this study is based on random sampling of the input variables. The effect of variability of the input parameter is evaluated using three different coefficients of variance. A large coefficient of variation indicates that the uncertainty in a variable at failure is substantial in the variation of factor of safety. Hence, the calculated probability of performance function is also a variable. Figure 6 presents the variation of the failure probability with various *cov* of the input parameter. The relationship shows clearly that the failure probability tends to increase with the increases in *cov* value of the input parameter. The failure probability is affected by the variability of the input parameter. El-Ramly et al. [10] explained that the variability of input parameter was more contributed by spatial variability of the soils, rather than statistical sources of uncertainty such as sparse data or the use of empirical correlations and factors. While Zhang et al. [9] stated that the factor of safety changed considerably because of the contribution the greatest uncertainty in the probability distribution of the parameter. This condition is valid if the parameters to be updated are not correlated in the prior distribution.

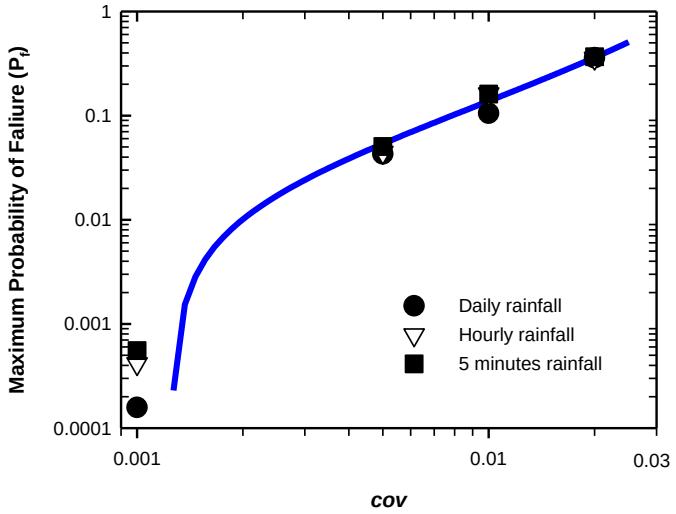

Figure 6 Relationship between failure probability and *cov*.

4. Conclusion

Based on this presentation, the slope failure can be estimated to be occurred between 9 to 13 September 2011 that depends on the rainfall patterns and variance of the input parameter. The results show that the maximum failure probability for the given input parameter was about 0.36 – 0.38 due to the rainfall recorded at the site. The failure probability tends to increase with the increases in *cov* value of the input parameter. The failure probability is affected by the variability of the input parameter. The probability density during the rainfall will present the "degree of belief" to estimate the time of slope failure. The use of a combination of probabilistic and deterministic slope analyses provided a more efficient framework for the investigation and design of remedial measures for the Doi Inthanon park slide in Northern Thailand. However, a probabilistic based back-analyses method need to be developed to obtain an acceptable input parameter at the site.

5. Acknowledgements

The first author thanks Ministry of Research, Technology and Higher Education for the research grant in 2015 under the scheme "Penelitian Hibah Kompetensi" based on the contract No. 1314/K5/KM/2015. Support from the Geotechnical Innovation Laboratory (GIL) of Kasetsart University is highly appreciated.

6. References

[1] Jotisankasa, A., Mahannopkul, K., and Sawangsuriya. A, "Slope Stability and Pore-Water Pressure Regime in Response to Rainfall: a Case Study of Granitic Fill Slope in Northern Thailand". *Geotechnical Engineering Journal of the SEAGS & AGSSEA*, Vol. 46 No. 1, 2015, pp. 45-65.

[2] Lumb, P. "Safety factors and the probability distribution of soil strength". Ca*nadian Geotechnical Journal*, Vol. 7 No. 3, 1969, pp. 225-242.

[3] Lind, N. C., "Modeling uncertainty in discrete dynamical systems". *Applied Mathematical Modelling*, Vol. 7 No. 3, 1983, pp. 146-152.

[4] Malkawi, A. I. H., Hassan, W. F., and Abdulla, F. A. "Uncertainty and reliability analysis applied to slope stability". *Structural Safety*, Vol. 22 No. 2, 2000, pp. 161-187.

[5] Muntohar, A.S., and Ikhsan, J., "Development A Simple Model for Preliminary Evaluation on Extreme Rainfall Induces Shallow Slope Failure". *Proceeding the 13th International Conference on Quality in Research*, 2013, pp. 1291-1296.

[6] Harr, M. E. "Probabilistic estimates for multivariate analyses". *Applied Mathematical Modeling*, Vol. 13 No. 5, 1989, pp. 313-318.

[7] Wong, F. S. "Slope reliability and response surface method". *Journal of Geotechnical Engineering* ASCE, Vol. 111 No. 1, 1985, pp. 32-53.

[8] Muntohar, A.S., "Application of Probabilistic Analysis for Prediction for Initiation of Landslide". *Proceeding the 1st International Workshop on Multimodal Sediment Disasters Triggered by Heavy Rainfall and Earthquake and the Countermeasures*, Yogyakarta, Indonesia, 8-9 March 2010, pp.33-44.

[9] Zhang, J., Tang, W., and Zhang, L. "Efficient Probabilistic Back-Analysis of Slope Stability Model Parameters." *Journal of Geotechnical and Geoenvironmental Engineering*, Vol. 136 No. 1, 2010, 99–109.

[10] El-Ramly, H., Morgenstern, N.R., and Cruden, D.M., "Probabilistic assessment of stability of a cut slope in residual soil". *Géotechnique*, Vol. 55, No. 1, 2005, 77–84

Influence of the Soil-Water Retention Curve Models on the Stability of Residuals Soils Slope

Agus Setyo Muntohar
Department of Civil Engineering, Universitas Muhammadiyah Yogyakarta, Indonesia

ABSTRACT: The study is focused on the investigation of effect the characterization of SWRC model and its effect on the slope stability on a simple infinite slope. The SWRC models were fitted to the laboratory test using mini tensiometer and filter paper. In particular, four unimodal SWRC models were evaluated for comparison in this study, i.e. van Genuchten model (VG), modified van Genuchten model (MVG), Brooks-Corey model (BC), and Kosugi log-normal model (KLN). The slope stability analysis was conducted in terms of Factor of Safety (FS) by applying the infinite slope model incorporating infiltration model. The infiltration model was analyzed by Richard's one-dimensional infiltration equation. The analysis resulted that The VG and KLN models produced lower estimation of safety factor than BC and MVG models. The distribution of pore water pressure varied with the SWRC models. Hence, different SWRC model contribute different FS values. The results indicate that the SWRC model shall be applied carefully since the model will have a different conclusion to the slope instability.

Keywords: rainfall, infiltration, soil water retention curve, slope stability, residual soil

1 INTRODUCTION

The mechanisms of rainwater infiltration causing slope instability had been analyzed and reviewed in many scientific works. Rainwater infiltration into the unsaturated soil increases the degree of saturation, hence affecting the shear strength properties and thus the probability of slope failure. It has been widely proved that the shear strength properties change with the soil water suction in unsaturated soils. Therefore, the accuracy to predict the relationship between soil water content and soil water suction, parameterized by the soil-water retention curve (SWRC), has significant effects on the slope stability analysis. The common method to obtain SWRC is by laboratory test by using mini tensiometer, pressure plate, and filter paper. However, sometimes, the data obtained need to be fitted to have a general equation of SWRC model. There are some SWRC models that commonly used for infiltration analysis such as van Genuchten (1980), Brooks and Corey (1964), Fredlund and Xing (1994), log-normal (Kosugi, 1996), etc.

The study is focused on the investigation of effect the characterization of SWRC model and its effect on the slope stability on a simple infinite slope. The SWRC models are fitted to the laboratory test using mini tensiometer and filter paper. In particular, four unimodal SWRC models were evaluated for comparison in this study, i.e. van Genuchten model (VG), modified van Genuchten model (MVG), Brooks-Corey model (BC), and Kosugi log-normal model (KLN). The slope stability analysis is conducted in terms of Factor of Safety (FS) by applying the infinite slope model incorporating infiltration model. The infiltration model is analyzed by Richard's one-dimensional infiltration equation.

2 LABORATORY TEST AND NUMERICAL MODELING

2.1 *Slope properties and rainfall record*

In this study, the studied slope was located at Kedungrong village, in Kalibawang, Kulonprogo. The average slope angle was 22^o, while the steepest slope angle was about 40^o.

The slope was covered by red residual soil from weathered breccias. The soil thickness (*H*) and unit weight (γ_t) were 8 m and 22 kN/m^3 respectively. The basic properties of the soil are presented in Table 1, while the particle size distribution is shown in Figure 2. Based on the properties, the soil was classified into *SM*.

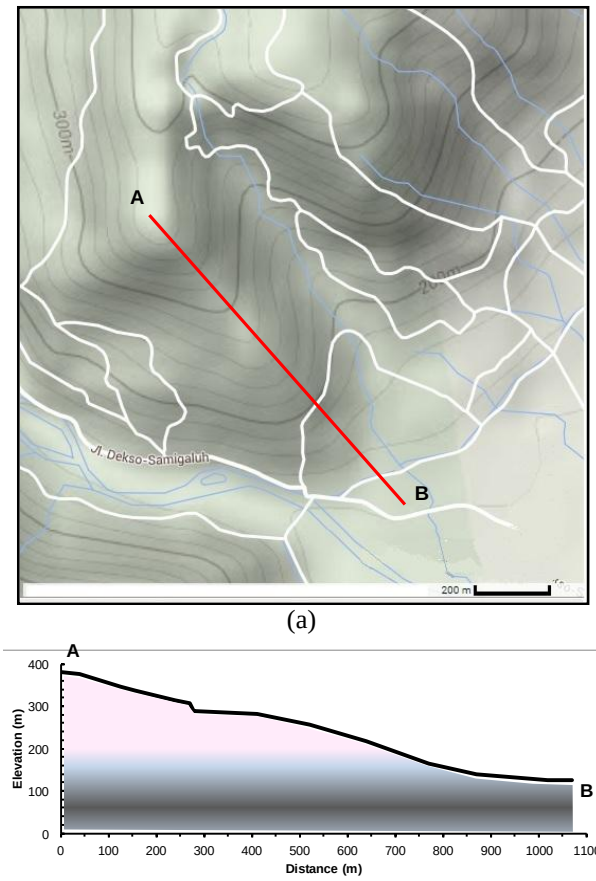

(a)

(b)

Figure 1. (a) Topography of the study area, (b) Slope cross section.

Table 1 Properties of the soil layer

Parameter	Unit
Specific gravity, G_s	2.73
Unit weight, γ_t	22 kN/m^3
Particles size:	
Coarse grained: Gravel/sand	86%
Fine-grained: Silt/clay	14%
Liquid limit, LL	50.05%
Plasticity index, PI	19.4%

The rainfall boundary is shown in Figure 7. The precipitation was recorded from the automatic rain gauge station in Kalibawang catchment area. The saturated hydraulic conductivity (k_{sat}) of the soil was 1.0264 x 10^{-1} m/day.

2.2 *Determination soil-water retention*

In this study, soil-water retention curve (SWRC) was determined using miniature KU tensiometer (for ψ < 100 kPa) and filter paper (for ψ > 100 kPa). The filter paper method used Whatman filter paper No. 42 and its calibration curve referred to ASTM D 5298. Figure 4 and 5 presents the schematic cross section of the tensiometer and filter paper apparatus.

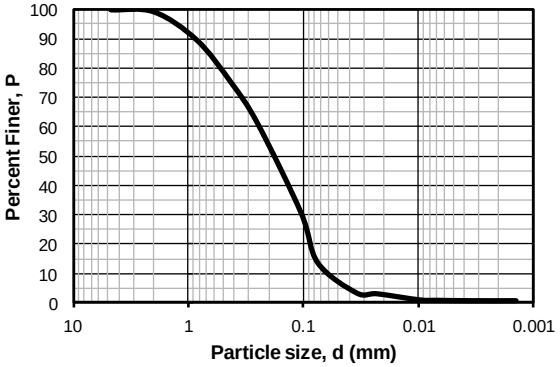

Figure 2 Particle size distribution of the residual soil sample

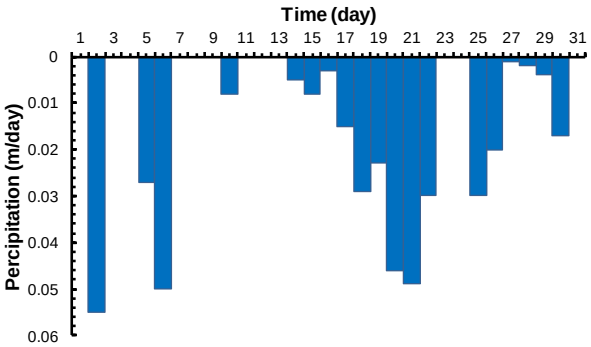

Figure 3. The daily rainfall hyetograph for the analysis

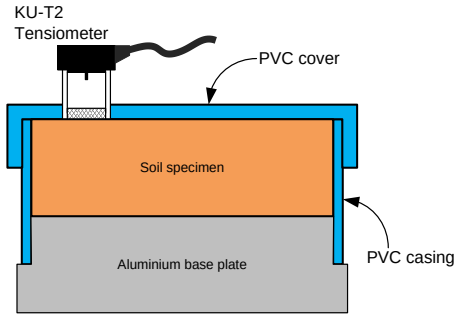

(a)

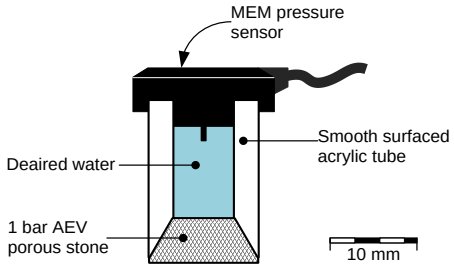

(b)

Figure 4 (a) Cross section of the SWCC test using KU tensiometer, (b) Detail of the KU tensiometer

The compacted soil about 63 mm in diameter and 20 mm thickness, were tested for Soil-Water Retention Curve (SWRC) using the

approach as explained by Jotisankasa et al. (2010b). The method involved gradually wetting soil sample, and during each stage suction of sample was monitored until equilibrium was reached. A minimum curing period of about 2-3 days between each increment was allowed for equilibration of the suction throughout the sample, which was carefully wrapped to prevent evaporation. Figure 6 shows the SWRC of the soils.

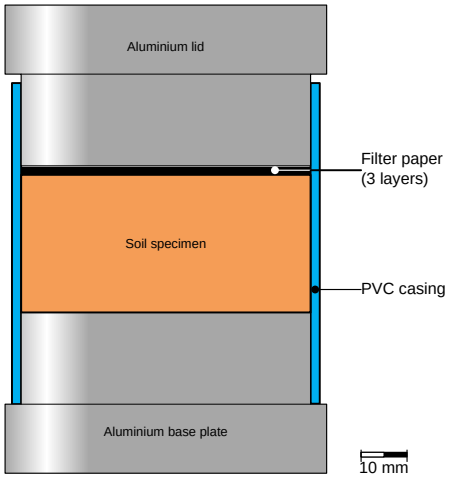

Figure 5 Schemaric cross-section of SWCC test using filter paper

2.3 *Shear strength test*

Shear strength characteristic of the soil was investigated in direct shear box. For this purpose, the samples were statically re-compacted in the laboratory to replicate closely the field condition by controlling the void ratios to be within ±5% the value of undisturbed soils. To determine the fully saturated shear strength of the soils, slow multistage-shearing direct shear tests were carried out at normal stresses of 31, 62, and 123 kPa and shearing rate of 0.05 mm/min. This rate was chosen such that no excess pore water pressure developed during shearing. The shear strength parameter was c' = 1.7 kPa, ϕ' = 19.6˚.

2.4 *One-dimensional infiltration model*

The one-dimensional infiltration model was solved using HYDRUS-1D code. The model was based on the one-dimensional Richards equation to simulate water movement in variably saturated media, and the equation was solved by numerical method (Šimůnek et al., 2005). The basic water movement equation was described as:

$$\frac{\partial\theta(\psi,t)}{\partial t}=\frac{\partial}{\partial z}\left[K(\psi)\left(\frac{\partial\psi}{\partial z}+1\right)\right] \quad (1)$$

where ψ is the soil water pressure head, θ is the volumetric water content, t is time, z is the vertical coordinate with the origin at the soil surface (positive upward), and $K(\psi)$ is the unsaturated hydraulic.

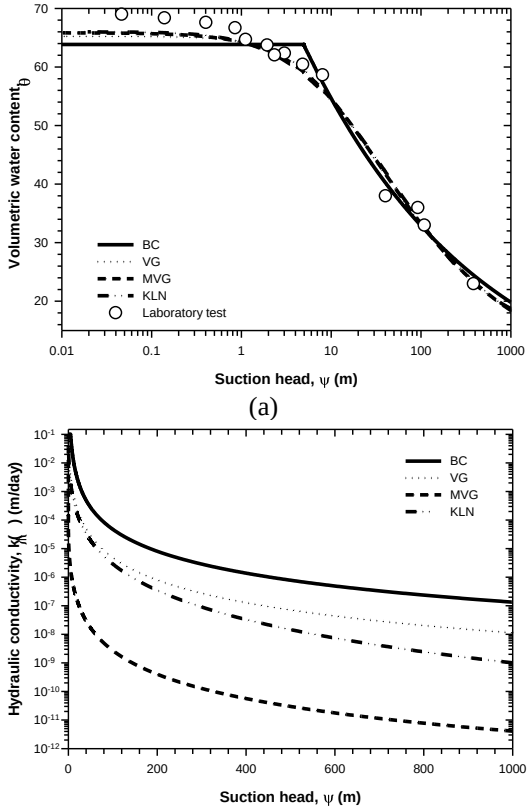

Soil hydraulic parameter

Models		θ_r	θ_s	α	n	l
BC	:	-	63.848	0.203	0.220	2.0
VG	:	-	65.248	0.127	1.262	0.5
MVG	:	6.211	65.851	0.080	1.005	0.5
KLN	:	14.933	65.997	47.49	2.112	0.5

Figure 6. (a) The soil-water retention curve, (b) Hydraulic conductivity function of the soil.

The unsaturated soil hydraulic properties, $\theta(\psi)$ and $K(\psi)$), in Equation (1) are in general highly nonlinear functions of the pressure head. The hydraulic properties can be presented using analytical models as written by Brooks and Corey (1964), van Genuchten (1980), Vogel and Císlerová (1988), and Kosugi (1996).

Brooks and Corey Model (BC)

The soil water retention, $\theta(\psi)$, and hydraulic conductivity, $K(\psi)$, functions

according to Brooks and Corey [(964) are given by Equation 2a and 2b.

$$\theta(\psi) = \theta_r + (\theta_s - \theta_r)|\alpha\psi|^{-n} \quad (2a)$$

$$K(\psi) = K_s \left[\frac{\theta(\psi) - \theta_r}{\theta_s - \theta_r} \right]^{\frac{2}{n}+l+2} \quad (2b)$$

in which θ_r and θ_s denote the residual and saturated water contents, respectively; K_s is the saturated hydraulic conductivity, α is the inverse of the air-entry value (or bubbling pressure), n is a pore-size distribution index, and l is a pore-connectivity parameter assumed to be 2.0 in the original study of Brooks and Corey (1964). The parameters α, n and l are empirical coefficients affecting the shape of the hydraulic functions.

van Genuchten – Mualem model (VGM)

The soil-hydraulic functions of van Genuchten (1980) used the statistical pore-size distribution model of Mualem [1976]. The expressions of van Genuchten [1980] are given by

$$\theta(\psi) = \theta_r + (\theta_s - \theta_r)\left[1 + |\alpha\psi|^n\right]^{-m} \quad (3a)$$

$$K(\psi) = K_s S_e^l \left[1 - \left(1 - S_e^{1/m}\right)^m\right]^2 \quad (3b)$$

where

$$S_e = \left[\frac{\theta(\psi) - \theta_r}{\theta_s - \theta_r} \right] \quad (3c)$$

and, $m = 1 - 1/n$ (3d)

The above equations contain five independent parameters: θ_r, θ_s, α, n, and K_s. Mualem (1976) estimated the pore connectivity parameter l in the hydraulic conductivity function was about 0.5 as an average for many soils.

Modified van Genuchten model (MVG)

Vogel and Císlerová (1988) modified the equations of van Genuchten (1980) to add flexibility in the description of the hydraulic properties near saturation. The soil water retention, $\theta(\psi)$, and hydraulic conductivity, $K(\psi)$ are given by equation (4a) and (4b) respectively.

$$\theta(\psi) = \theta_a + (\theta_m - \theta_a)\left[1 + |\alpha\psi|^n\right]^{-m} \quad (4a)$$

$$K(\psi) = K_k + \frac{(\psi - \psi_k)(K_s - K_k)}{(\psi_s - \psi_k)} \quad (4b)$$

The hydraulic characteristics contain 9 unknown parameters: θ_r , θ_s, θ_a, θ_m, α, n, K_s, K_k, and θ_k . When $\theta_a = \theta_r$, $\theta_m = \theta_k = \theta_s$ and $K_k = K_s$, the soil hydraulic functions of Vogel and Císlerová (1988) reduce to the original expressions of van Genuchten (1980). The parameters are determined as shown in Figure 7.

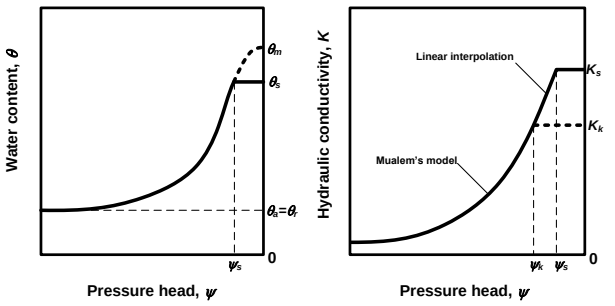

(a) (b)

Figure 7 (a) Schematics of the soil water retention and (b)hydraulic conductivity functions.

Kosugi lognormal model

Kosugi (1996) suggested the lognormal distribution model for the soil hydraulic properties. Application of Mualem's pore-size distribution model (Mualem, 1976) leads to the following hydraulic conductivity function.

$$\theta(\psi) = \theta_r + (\theta_s - \theta_r)\frac{1}{2} erfc\left[\frac{\ln(\psi/\alpha)}{\sqrt{2n}} \right] \quad (5a)$$

$$K(\psi) = K_s S_e^l \left\{ \frac{1}{2} erfc\left[\frac{\ln(\psi/\alpha)}{\sqrt{2n}} + \frac{n}{\sqrt{2}} \right] \right\}^2 \quad (5b)$$

2.5 *Slope stability analysis*

The methods used in traditional infinite slope analysis must be modified to take into account the variation of the pore water pressure profile that results from the infiltration process. Based on the extended Mohr–Coulomb failure criterion (Fredlund et al., 1978), the safety factor of an unsaturated soil slope with a slip surface parallel to ground surface as shown in Figure 8, can be expressed as written in Equation (6). Consider the model for the shear strength with respect to soil suction by

$$FS = \frac{c' + (\sigma_n - u_a)\tan\phi' + (u_a - u_w)\tan\phi^b}{\gamma_t \cdot z_f \cdot \sin\beta \cdot \cos\beta} \quad (6)$$

$$FS = \frac{c'}{\gamma_t \cdot z_f \cdot \sin\beta \cdot \cos\beta} + \frac{\tan\phi'}{\tan\beta}\left[1 + \frac{\psi \cdot \Theta}{\gamma_t \cdot z_f \cdot \cos^2\beta \cdot}\right] \quad (7)$$

where, $\Theta = \frac{\theta - \theta_r}{\theta_s - \theta_r}$ (8)

Vanapalli et al. (1996), the equation can be written as in Equation (7), where *FS* is the safety factor of slope stability, z_f is the distance from the ground to the slip surface, *c'* is the effective cohesion, ϕ' is the effective friction angle, β is the slope angle, γ_t is the total unit weight of the soil, u_a is the pore air pressure, u_w is the pore-water pressure, (u_a - u_w) is the matric suction, σ_n is the total normal stress, (σ_n - u_a) is the net normal stress on the slip surface; ϕ^b is the angle defining the increase in shear strength for an increase in matric suction.

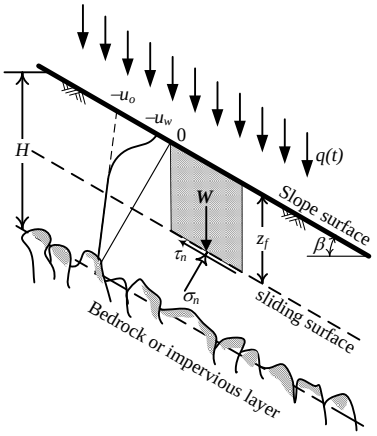

Figure 8. Schematic plot of an infinite slope and boundary conditions of unsaturated soil infiltration.

3 RESULTS

The effect of four models soil-water retention (that is BC, VG, MCG, and KLN) were compared to evaluate their performance in this study. Changing of pore water pressure and safety factor were analyzed during a month period of precipitation event.

Pore water pressure profile

Figure 9 show the changing of pore water pressure with depth for various time of rainfall. The initial suction at surface and bottom layers is 490 kPa and 410 kPa respectively. The suction decreased with the elapsed time of rainfall. The suction propagates to a deeper wetting front. Comparing pore water pressure profile in Figure 9a and 9c with Figure 9b and 9d, it can be observed that the rates of downward movement of the wetting front are comparable. The BC and MVG models have similar suction distribution profile, while the VG and KLN models show a similar suction profile. The results indicate that different SWRC model affect the pore water pressure profile. In general, the suction varies with the elapsed time of rainfall which corresponds to the rainfall intensity.

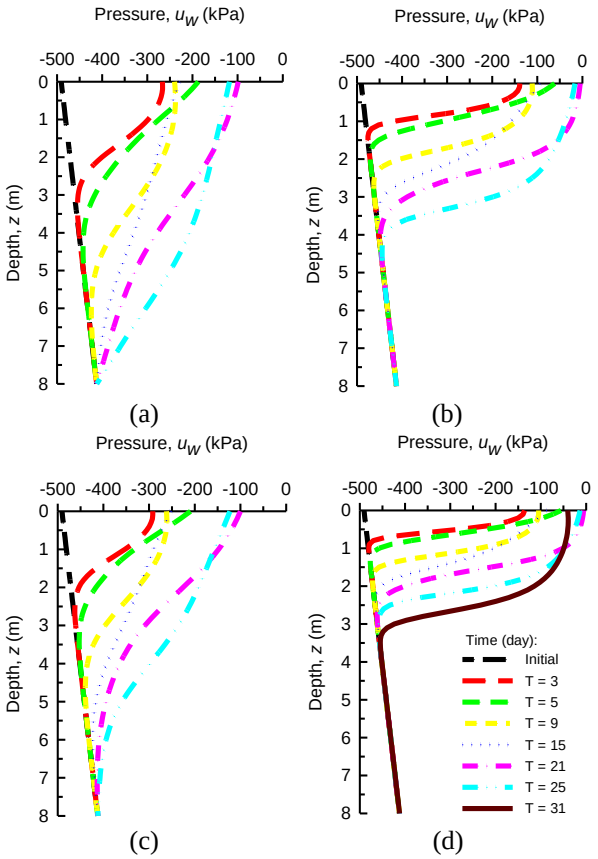

Figure 9 Pore water pressure profile, (a) BC, (b) VG, (c) MVG, (d) KLN models.

Variation in Slope stability

Figure 9b and 9d show that the deepest wetting front depth reached 5 m and 3 m for VG and KLN models respectively, while the wetting front depth goes to a deeper for the other models. Use equation 7, Figure 10 illustrates the variation of safety factor (FS) profile with the depth for various time of precipitation. At the beginning of the rainfall events, the initial safety factors at all depths of the potentially unstable soil layer are significantly higher than 100 (Fig. 10) at near ground surface, as a consequence of high suction values. The safety factor decreased with the depth. The lowest safety factor was 2.05, 1.59, 2.10, and 1.89 for BC, VG, MVG, and KLN models respectively. At the end of rainfall event, the potential sliding depth Z_f can be estimated as 5 m, 2.5 m, 7 m, and 1.7 m for BC, VG, MVG, and KLN models respectively.

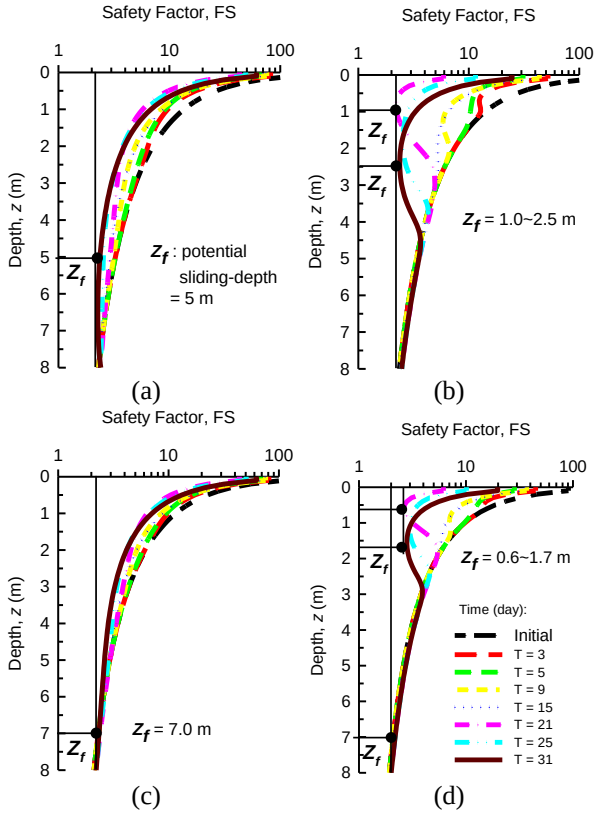

Figure 9 Saftey factor variation with depth for various elapsed time of rainfall, (a) BC, (b) VG, (c) MVG, (d) KLN models.

Figure 10 shows the variation of safety factor with the elapsed time of rainfall event for depth of failure (z_f) up to 3 m. In general, the FS of slope decrease with increasing of time of rainfall for all models. The FS value fluctuates which follow the rainfall pattern. At shallow depth failure, z_f = 1 m, modeling SWRC using VG and KLN yield a lower safety factor that the other SWRC models. A rapid change in FS was observed at shallower failure depth (Figure 10a), while the change was lesser at a deeper failure depth. (Figure 10c). Again, the modeling with VG gained a rapid decreasing of the FS at a deeper failure depth. The rapid decreasing of the FS was gained after intense rainfall at day of 6th and 21st. The lowest FS value is obtained after day of 21st after six days intense rainfall as shown in Figure 10. The results indicated that the ancedent rainfall affect the FS pattern. The characteristics was also stated in Rahardjo and Rahimi (2015).

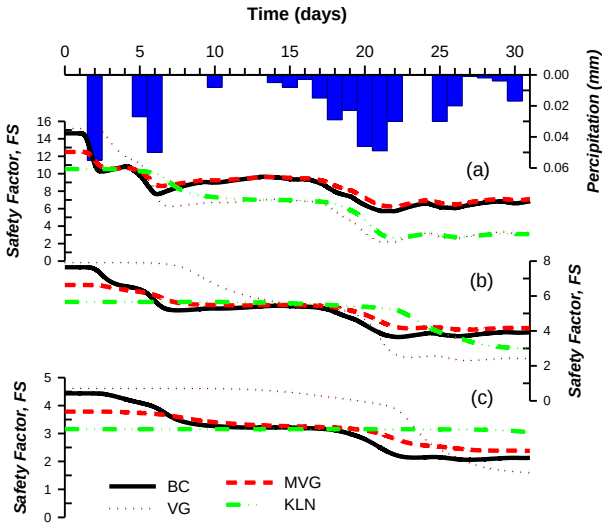

Figure 10 Variation of safety factor of the slope with the elapsed time of rainfall (a) z_f = 1 m, (b) z_f = 2m, (c) z_f = 3 m.

4 DISCUSSION

Soil–water characteristic curve (SWCC) is a graphical relationship that shows the relationship between the amount of water in a soi, i.e. gravimetric water content w, volumetric water content θ_w or degree of saturation S (Fredlund and Rahardjo, 1993) and matric suction ψ. As introduced by Fredlund (2006), the entire suction range of the SWCC can be divided into three zones such as boundary effect zone, transition zone and residual zone and they are separated by air-entry value and residual suction. Zhai and Rahadjo (2013) mentioned that high variability in water content occurs in the transition zone, suggesting that more data points need to be measured within the transition zone in order to obtain a more accurate SWCC.

The wetting front depths are found sharply in VG and KLN models while the others do not show a clear wetting front depth. BC model a power function with respect to the suction which the inflection point was unclear defined. Regarding the accuracy of predicting the moisture content near at saturated condition, van Genuchten and Nielsen (1985) concluded that VG model performed better than BC model because the θ-ψ curve has an inflection point (ψ_o). Kosugi (1996b) was shown that the VG model was analogous to the KLN model under the restriction bubling pressure ψ_c = 0, the BC model was similar to the KLN model when air entry pressure close to suction at inflection point ($\psi_c \rightarrow \psi_o$).

Comparing the four models, Kosugi (1996a) mentioned that the models which are not derived based on soil pore radius distribution, nor do they emphasize the physical significance of their empirical parameters are not necessarily suitable models for evaluating the effect of the soil pore radius distribution on the water movement in the soil.

The lowest pore water pressure bound at the end of rainfall event for all SWRC models. Lee et al. (2009) mentioned the lowest bound of suction as suction envelope. The suction envelope indicated the minimum suction existed in the soil slope under various durations of extreme rainfalls. Using the lowest boundary of the pore water pressure, the redistribution of pore water pressure is shown in Figure 11a. Fourie et al. (1999) have identified the key role of suction in maintaining the stability of steep slopes. Use the suction envelope in Figure 11a, the minimum factor of safety for four SWRC models is shown in Figure 11b. The figure is alluding to conclude that the stability of slope is affected by the SWRC models applied for analysis.

The variation of FS (Figure 10) shows that different SWRC model contribute different FS values. Initial suction at slope surface was about 490 kPa. Then, the suction at surface decreases to about 4 kPa during the rainfall (Figure 12). The matric suction can be eliminated only when the ground surface moisture flux is equal to or greater than the saturated coefficient of permeability. It is the possible reason that the hydraulic conductivity function affect the pore water pressure profile. As the result, the safety factor is controlled by the hydraulic conductivity function (Rahimi et al., 2010; Rahardjo et al., 2007). It was found that the range of SWCC measurements greatly affect the estimated permeability functions. Rahimi et al. (2015) found that the effect of the range of SWCC measurements is more significant than the selected best-fit SWCC equation used. The results indicate that the SWRC model shall be applied carefully, since the model will have a different conclusion to the slope instability.

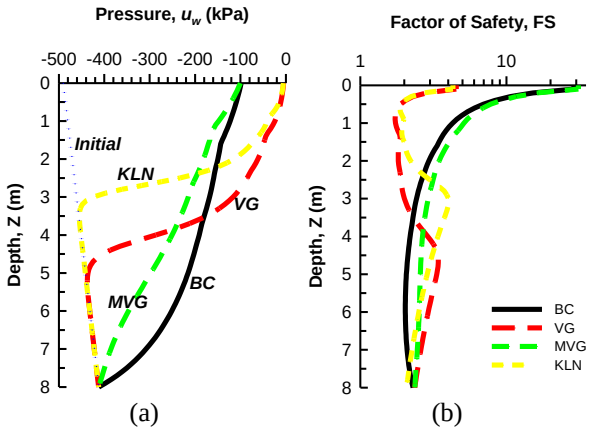

Figure 11 (a) Pore water pressure envelope, (b) Boundary of factor of safety for various SWRC models.

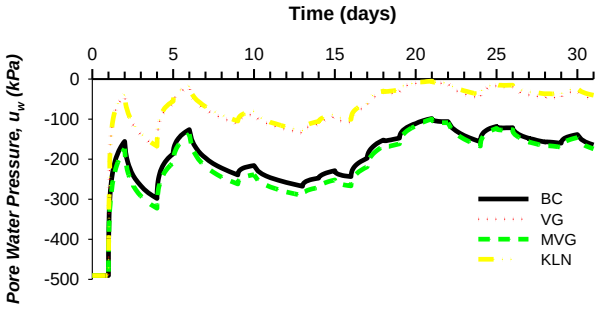

Figure 12 Variation of pore water pressure at the surface for various SWRC model

5 CONCLUSIONS

The result of this study concluded that a good expression for the SWCC is essential to combine with constitutive modeling. Comparisons between measured and modeled SWCCs proved that the models resulted different suction profiles. As consequence, the safety factor of slope was affected by the applied SWRC model. This study concluded that the VG and KLN models produced lower estimation of safety factor than BC and MVG models. Finally, the study indicated that the SWRC model shall be applied carefully, since the model will have a different conclusion to the slope instability. However, further studies should focus on the effect of hysteresis and uncertainity of the SWRC models.

ACKNOWLEDGEMENTS

The author thanks for the financial support from Ministry of Research, Technology, and Higher Education, the Republic of Indonesia under research scheme "Penelitian Hibah Kompetensi" in 2015. Support from Apiniti Jotisankasa, Ph.D., Kasetsart University, Thailand is acknowledged.

REFERENCES

Brooks, R. H., and A. T. Corey, 1966, Properties of porous media affecting fluid flow, Journal of Irrigation and Drainage Division, ASCE Proceeding. Vol. 72(IR2), 61-88.

Cho, S.E., and Lee, S.R., 2002, Evaluation of surficial stability for homogeneous slopes considering rainfall characteristics. Journal of Geotechnical and Geoenvironmental Engineering, Vol. 128(9), 756–63.

Fourie, A.B, Owe, D.R, and Blight, G.E., 1999, The effect of infiltration on the stability of the slopes of a dry ash dump, Geotechnique, Vol. 49(1), 1–13.

Fredlund, D.G., Morgenstern, N.R., and Widger, R.A, 1978, The shear strength of unsaturated soils. Canadian Geotechnical Journal, Vol. 15(3), 313-321.

Fredlund, D.G., Rahardjo, H., 1993. Soil Mechanics for Unsaturated Soils. Wiley, NewYork.

Fredlund, D.G., and Xing, A., 1994 Equations for the soil-water characteristic curve, Canadian Geotechnical Journal, Vol. 31(4), 521-532

Fredlund, D.G., 2006. Unsaturated soil mechanics in engineering practice. Journal of Geotechnical and Geoenvironmental Engineering 132 (3), 286–321.

Kosugi, K., 1996a, Lognormal distribution model for unsaturated soil hydraulic properties, Water Resources Research, Vol. 32(9): 2697-2703

Lee, L. M., Gofar, N., & Rahardjo, H. (2009). A simple model for preliminary evaluation of rainfall-induced slope instability. Engineering Geology, Vol. 108, 272–285.

Mualem, Y., A new model for predicting the hydraulic conductivity of unsaturated porous media, Water Resources Research, Vol. 12(3), 513-522, 1976.

Rahimi, A., Rahardjo, H., and Leong, E.C., 2010, Effect of hydraulic properties of soil on rainfall-induced slope failure, Engineering Geology, Vol. 114, 135–143

Rahardjo, H., Ong, T.H., Rezaur, R.B., Leong, E.C., 2007. Factors controlling instability of homogeneous soil slopes under rainfall. Journal of Geotechnical and Geoenvironmental Engineering, Vol. 133 (12), 1532–1543.

Rahardjo, H., and Rahimi, A., 2015, Controlling factors of rainfall-induced slope failures in residual soils, in P.P. Rahardjo & A. Tohari, Proceeding of Slope 2015, September 27-30th 2015, Bali, 4.1 –4.21

Rahimi, A., Rahardjo, H., and Leong, E.C., 2015, Effect of range of soil–water characteristic curve measurements on estimation of permeability function, Engineering Geology,Vol. 185, 96–104.

Šimůnek, J., M. Th. van Genuchten, and M. Šejna, 2005, The HYDRUS-1D software package for simulating the one-dimensional movement of water, heat, and multiple solutes in variablysaturated media. Version 3.0, HYDRUS Software Series 1, Department of Environmental Sciences, University of California Riverside, Riverside, CA, 270 p.

van Genuchten, M. Th., 1980, A closed-form equation for predicting the hydraulic conductivity of unsaturated soils, Soil Science Society of American. Journal, Vol. 44: 892-898.

van Genuchten, M.T, and Nielsen, D.R. 1985, On Describing and Predicting the Hydraulic Properties of Unsaturated Soils. Annual Geophysics, Vol. 3(5), 615-628.

Vanapalli, S.K., Fredlund, D.G., Pufahl, D.E., and Clifton, A.W., 1996, Model for the prediction of shear strength with respect to soil suction. Canadian Geotechnical Journal, Vol. 33, 379–392.

Vogel, T., and M. Císlerová, 1988, On the reliability of unsaturated hydraulic conductivity calculated from the moisture retention curve, Transport in Porous Media, Vol. 3: 1-15.

Jurnal Teknologi

Full Paper

FACTORS AFFECTING RAIN INFILTRATION ON A SLOPE USING GREEN-AMPT MODEL

Agus Setyo Muntohar *, Hung-Jiun Liao

Department of Civil Engineering, Universitas Muhammadiyah Yogyakarta, Indonesia
Department of Construction Engineering, National Taiwan University of Science and Technology, Taipei, Taiwan

Article history
Received
28 Ausgut 2015
Received in revised form
Under Review
Accepted
-

*Corresponding author
muntohar@umy.ac.id

Graphical abstract

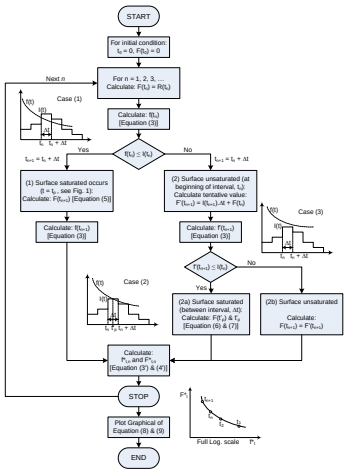

Abstract

Rainwater infiltration in the sloping surface is analyzed using the Green-Ampt model in this study. The Green-Ampt model was originally developed for water infiltration on a horizontal surface. Hence, the effect of slope steepness on rainwater infiltration during typhoon needs to be taken into account as well as the effect of soil type and soil-water suction. The results show that the increase in saturated hydraulic conductivity and moisture-suction will increase the infiltration rate. However, increase the slope steepness will decrease the infiltration rate. For slope covered with high permeability material, significant variation in moisture-suction will change the infiltration rate considerably comparing with the slope covered with lower permeability material. Finally, this study proposes a graphical aid to represent the basic Green-Ampt equation for the sloping surface.

Keywords: rain infiltration, Green-Ampt model, sloping surface, typhoons, hydraulic conductivity, moisture-suction

Abstrak

Dalam kajian ini penyusupan air hujan di permukaan miring dianalisis menggunakan model Green-Ampt. Model Green-Ampt pada asalnya dibangunkan untuk penyusupan air pada permukaan mendatar, kesan kecuraman cerun di penyusupan air hujan semasa taufan perlu diambil kira dan juga kesan dari jenis tanah dan sedutan tanah-air. Keputusan menunjukkan bahawa peningkatan dalam tepu kekonduksian hidraulik dan kelembapan-sedutan akan meningkatkan kadar penyusupan. Walau bagaimanapun, meningkatkan kecuraman cerun akan mengurangkan kadar penyusupan. Untuk cerun dilindungi dengan bahan kebolehtelapan yang tinggi, perubahan ketara dalam kelembapan-sedutan akan mengubah kadar penyusupan jauh membandingkan dengan cerun yang dilindungi dengan bahan kebolehtelapan yang lebih rendah. Akhir sekali, kajian ini mencadangkan bantuan grafik untuk mewakili persamaan Green-Ampt asas untuk permukaan miring.

Kata kunci: penyusupan hujan, model Green-Ampt, permukaan miring, taufan, kekonduksian hidraulik, kelembapan-sedutan

1.0 INTRODUCTION

Landslide is a worldwide disaster that has paid attention many researchers to investigate the triggering and causing factors, including the mechanism. Landslides in various types, e.g. shallow and deep, occasionally happen during the typhoon season and heavy rainfall periods. Rainfall is widely known as the major triggering factor of landslides. It is related to the landslides by the ways of rain

infiltration into the ground and the consequent rising of transient pore water pressure during rainfall. Research indicated that slope failure was initiated by saturation on the slope surface. Then, the saturation will advance to wetting front depth during an intense rainfall [1,2]. Hence, initiation time for saturation can be determined by a preliminary analysis of slope failure. However, estimating the rain infiltration is by no means a straightforward problem in the natural slopes. Many efforts have been tried to quantify the rain infiltration behavior. Among the models used for rain infiltration analysis, Green-Ampt infiltration model is by far the most commonly used. The Green-Ampt model is relatively a simple model. However, it can generate results that are in good agreement with other more rigorous infiltration models such as Richard's equation and Philip's model.

The Green-Ampt model is a simplified representation of infiltration process that assumes that the ground surface is horizontal. In other words, the original Green-Ampt model does not applicable to the sloping surface. However, up to now, it is still used by many researchers to quantify, properly or improperly, the rain infiltration factors and input them to the slope stability analysis analysis [1,3,4]. To better quantify the rain infiltration on a sloping surface, this paper propose a modified Green-Ampt model to account for the influence of sloping ground surface. A parametric study has been carried out by using the modified Green-Ampt model to evaluate the effect of sloping surface on rain infiltration. The contents of this paper will focus on the impact of slope steepness and the moisture-suction characteristics of soil in the infiltration process under heavy rainfall condition.

2.0 Green-Ampt Infiltration Model

The Green-Ampt model has been extensively used to estimate the infiltration process during both steady and unsteady rainfall events [5,6]. The basic Green-Ampt infiltration equations for the horizontal surface are written in Equation 1 and 2.

$$f(t)=k_{sat}\left[1+\frac{(\psi_f\cdot\Delta\theta)}{F(t)}\right] \quad (1)$$

$$F(t)-(\psi_f\cdot\Delta\theta)\ln\left[1+\frac{F(t)}{(\psi_f\cdot\Delta\theta)}\right]=k_{sat}\cdot t \quad (2)$$

The equations 1 and 2 do not account for the influence of slope steepness. To take into account the effect of sloping ground surface, Chen and Young [7] (2006) modified the Green-Ampt equations as in Equation 3 and 4.

$$f(t)=k_{sat}\left[\cos\beta+\frac{(\psi_f\cdot\Delta\theta)}{F(t)}\right] \quad (3)$$

$$F(t)-\frac{(\psi_f\cdot\Delta\theta)}{\cos\beta}\ln\left[1+\frac{F(t)\cos\beta}{(\psi_f\cdot\Delta\theta)}\right]=k_y\cdot t \quad (4)$$

where $f(t)$ = infiltration rate at time t, $F(t)$ = cumulative infiltration at time t, ψ_f = suction head at wetting front, $\Delta\theta$ = volumetric water content deficit (= $\theta_s - \theta$), β = slope angle, and $k_y = k_{sat.}\cos\beta$, and k_{sat} = saturated hydraulic conductivity. For horizontal surface where $\beta = 0$ and $\cos\beta = 1$, Equations (3) and (4) become the same as equations (1) and (2). Equation (3) shows that the increasing slope angle reduces the infiltration rate. This equation is in agreement with the field infiltration test done by Lu et al. [8] and Fox et al. [9]. Use equation (1) and (3), the reduction of infiltration rate can be expressed as

$$\begin{aligned} f(t)_{\beta=0}-f(t)_{0<\beta<90} &= k_{sat}\left[1+\frac{(\psi_f\cdot\Delta\theta)}{F(t)}\right] \\ &\quad -k_{sat}\left[\cos\beta+\frac{(\psi_f\cdot\Delta\theta)}{F(t)}\right] \\ &= k_{sat}(1-\cos\beta) \end{aligned} \quad (5)$$

During a rainfall event, three types of rain infiltration can occur as shown in Figure 1: (1) Case 1: Rainfall intensity is greater than infiltration rate, then saturation on the ground surface occurs at this time interval; (2) Case 2: Rainfall intensity is lesser than the infiltration rate at the beginning of the time interval. Then, the intensity will be larger than the later infiltration rate. So the ground surface changes from unsaturated to saturated at this stage; and (3) Case 3: There is no surface saturation in this time interval. For case 3, all the rainfall infiltrates into the soil since the rainfall intensity is smaller than infiltration rate.

The surface saturation occurs only if the potential infiltration rate becomes less than the rainfall intensity. Hence, the infiltrated rainfall can be calculated using Equation 6.

$$\begin{aligned} &F(t+\Delta t)-F(t) \\ &-\frac{(\psi_f\cdot\Delta\theta)}{\cos\beta}\cdot\ln\left[\frac{(F(t+\Delta t)\cos\beta+\psi_f\cdot\Delta\theta)}{(F(t)\cos\beta+\psi_f\cdot\Delta\theta)}\right]=k_y\cdot\Delta t \end{aligned} \quad (6)$$

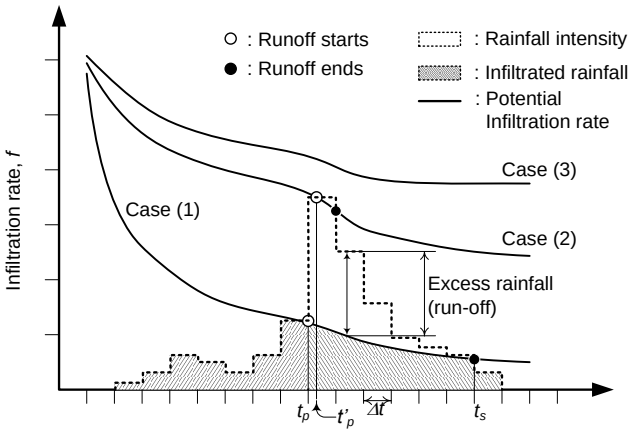

Figure 1 Typical of infiltration and excess rainfall under unsteady rainfall

After surface saturation, any additional rainfall will become the surface run-off. If case 2 occurs, the time needed to reach saturation is defined as in Equation 7.

$$t'_p = \frac{F\left|t'_p\right| - F(t)}{I(t)} \tag{7}$$

Thus, the infiltrated rainfall can be calculated using the following equation:

$$F\left(t'_p\right) = \frac{k_{sat}\cdot\left(\psi_f \cdot \Delta\theta\right)}{I(t) - k_{sat}\cos\beta} \tag{8}$$

Equations (3) and (4) need iteration techniques to carry out the calculation for unsteady rainfall. So, they are re-written with different implicit forms as presented in Equation 9 and 10.

$$\frac{f(t)}{k_{sat}} = \left(\cos\beta + \frac{1}{F_t^*}\right) = f_t^* \tag{9}$$

From equation (4):

$$\frac{F(t)}{\left(\psi_f \cdot \Delta\theta\right)} = \cos^{-1}\beta \cdot \ln\left[1 + \frac{F(t)}{\left(\psi_f \cdot \Delta\theta\right)}\cos\beta\right] + \frac{k_y \cdot t}{\left(\psi_f \cdot \Delta\theta\right)} = F_t^* \tag{10}$$

where f_t^* and F_t^* are the normalized infiltration rate and cumulative infiltration for the unsteady rainfall respectively. Both of f_t^* and F_t^* are dimensionless.

3.0 Data and Analysis

3.1 Rainfall Record

In this study, the precipitations were recorded from three rain gauges installed along the T-18 mountain road in central Taiwan at mileages of 27K+200, 56K+200, and 64K+800 (Figure 2). Three typhoons that attacked Taiwan in July 2006 were chosen as the rainfall events for infiltration analysis. Those were Ewiniar (July 7 to 9, 2006), Bilis (July 13 to 16, 2006), and Kaemi (July 23 to 26, 2006). The hourly rainfall and accumulated rainfall for each typhoon recorded at mileage 27K+200 are shown in Figure 3. Among these three Typhoons, Typhoon Bilis brought in an intense rainfall with the accumulated rainfall approaching 800 mm, and the maximum rainfall intensity reached 51.5 mm/h. In comparison, the recorded accumulated rainfalls for the other two typhoons were around 400 mm and 200 mm for typhoons Ewiniar and Kaemi respectively.

3.2 Green-Ampt Parameters

The parameters used in the Green-Ampt model include the moisture content conditions ($\Delta\theta$), suction head (ψ_f), and saturated hydraulic conductivity (k_{sat}). The saturated hydraulic conductivity and suction are known as the inherent parameters for soil. Those parameters can be obtained from the laboratory or field tests. Table 1 summarizes the range of Green-Ampt parameters for various soil textures (USDA classification). It can be found that disparities in the suction head parameter (ψ_f), as tabulated in column 4, are large for the soils chosen in this study. When the input to the Green-Ampt model, the moisture deficit, and suction head are combined as one parameter ($\psi_f \Delta\theta$) as shown in Table 2.

3.3 Simulation Procedure

Slope angle was varied from 0 to 70° to study the effect of slope steepness on the infiltration process. The rain infiltration is calculated using equations (3) to (10). The computation algorithm was modified from

Figure 2 Location of a rain gauge at T18 road

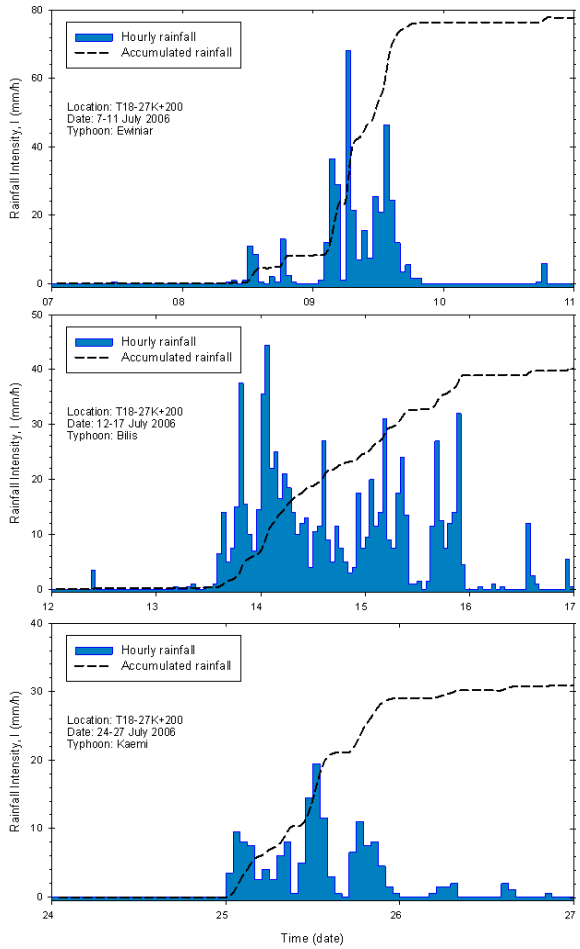

Figure 3 Rainfall hyetograph in July 2006: three typhoons attacked Taiwan i.e. Ewiniar, Bilis and Kaemi at mileage 27K+200 along T18 road

the procedures proposed by Chow et al. [11]. The simulation included evaluating whether or not the surface run-off will occur in a rainfall event based on the relative values of infiltration rate *f(t)* and rainfall intensity *I(t)* at time *t*. For the case 1 shown in Figure 1, *f(t)* is equal to or smaller than *I(t)*, indicating that the ground surface saturated. Rainfall with this intensity will not only infiltrate into the ground but also generate surface run-off. For case 2, *f(t)* is larger than *I(t)*. It indicates that the soil surface will remain unsaturated under this rain condition (Case 3). However, for case 2, the ground surface will become saturated sometime between t_n and $t_n+\Delta t$ interval although it is not yet saturated at time t_n.

4.0 RESULTS AND DISCUSSION

4.1 Infiltration response process

Figure 4 shows the typical infiltration rate for soils with k_{sat} = 36 mm/h, $\psi_f \Delta\theta$ = 30 mm, and for slopes with angle β = 0° to 70°. The infiltration rates for soils with k_{sat} = 18, 36, and 72 mm/h are compared in Figure 4a. The first feature of the typical infiltration figure (like Figure 4) shows that the infiltration rate declines with elapsed time. Once the surface gets saturated, surface runoff starts and infiltration capacity decreases over time until the minimum infiltration capacity is reached. In the Green-Ampt model, the infiltration capacity is assumed to be equal to soil hydraulic conductivity at the saturated condition. For example, the soil with hydraulic conductivity at saturated condition (k_{sat}) equal to 18 mm/h, then the infiltration rate of the soil will drop to 18 mm/h at the end (Figure 4a). If the rainfall intensity is lesser than the infiltration capacity ($I(t) < k_{sat}$), then all the rainfall infiltrates into the soil, and no run-off occurs. During typhoon Ewiniar period (July 8 to 10, 2006), rainfall infiltrated completely into the subsurface soil if k_{sat} is equal to 72 mm/h.

The second feature of the infiltration figure is to identify the moment when the rainfall intensity is greater than the saturated hydraulic conductivity, $I(t) > k_{sat}$. The rainfall intensity fell above the curve of infiltration rate will result in surface run-off. As shown in Figure 4a, the white points on the infiltration curve stand for the time when the run-off starts; the black points stand for the time when the run-off stops. So the shaded area from point 2 to 3 below the curve of infiltration rate represents the amount of rainwater will infiltrate into the ground.

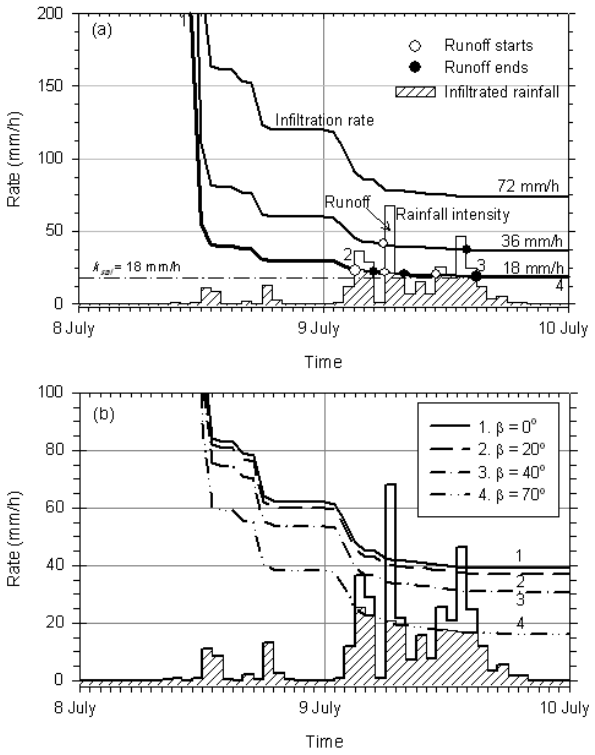

Figure 4 (a) Typical infiltration rate for unsteady rainfall for β = 20° with various k_{sat}; (b) Effect of slope angle for k_{sat} = 36 mm/h

The third feature of the infiltration figure is to determine the time when the surface begins to become saturated or the time to start run-off (tp).

Table 1 Green Ampt infiltration parameters for typical soils [10] (Rawls et al., 1983)

Soil Type	Range of η	Range of θ_e	Range of ψ_f (mm)	k (mm/h)	ψ_f (mm)	k_{sat} (= 2k) (mm/h)
Sand	0.374~0.5	0.354~0.48	9.7~253.6	117.8	49.5	235.6
Loamy Sand	0.363~0.506	0.329~0.473	13.5~279.4	29.9	61.3	59.8
Sandy Loam	0.351~0.555	0.283~0.541	26.7~454.7	10.9	110.1	21.8
Loam	0.375~0.551	0.334~0.534	13.3~593.8	3.4	88.9	6.8
Silt Loam	0.42~0.582	0.394~0.578	29.2~953.9	6.5	466.8	13
Sandy Clay Loam	0.332~0.464	0.235~0.425	44.2~1080	1.5	218.5	3
Clay Loam	0.409~0.519	0.279~0.501	47.9~911	1	208.8	2
Silty Clay Loam	0.418~0.524	0.347~0.517	56.7~1315	1	273	2
Sandy Clay	0.37~0.49	0.207~0.435	40.8~1402	0.6	239	1.2
Silty Clay	0.425~0.533	0.334~0.512	61.3~1394	0.5	292.2	1
Clay	0.427~0.523	0.269~0.501	63.9~1565	0.3	316.3	0.6

Table 2 The Green-Ampt parameters and soil shear strength properties used in this study

Soil type	ksat (mm/h)	$\psi\Delta\theta$ * (mm)	Degree of permeability
1	360 (1 x 10-4)	30, 120, 240, 360	Higher to lower
2	36 (1 x 10-5)	30, 120, 240, 360	
3	3.6 (1 x 10-6)	30, 120, 240, 360	
4	0.36 (1 x 10-7)	30, 120, 240, 360	

Values in the brackets are in m/s. * $\Delta\theta = 0.3$

Time to saturation can be continued till the end of rainfall if the rainfall intensity remains smaller than the hydraulic conductivity at saturation (k_{sat}). Soil with k_{sat} = 18 mm/h reaches saturation earlier than the soil with ksat = 36 mm/h. This feature explicates that a soil with lower permeability will get saturated earlier than a soil with higher permeability at the same initial moisture-suction condition.

Infiltration rate decreases with increase in slope as shown in Figure 4b. This behavior is in agreement with the field infiltration experiments carried out by Lu et al. [8]. Lower infiltration rate on the steeper slope is caused by higher flow velocities and shorter detention time of rainwater on the steeper surface [9]. Theoretically, a longer detention time increases the surface water storage and results in higher infiltration rate.

Figure 5 presents a graphical aid to represent the infiltration rate and cumulative infiltration as depicted by equation (9) and (10). Correlation between these equations shows a unique relationship. The infiltration decreases with increasing slope angle of the surface. However, beyond point ***P*** (inset graph in Figure 5), the rain infiltration does not change greatly with the slope angle. Because all the rainwater infiltrates into subsurface layer if the rain infiltration rate goes beyond point ***P***. Comparing the infiltration rate of horizontal surface (β = 0o) and sloping surface ($\beta > 0^o$), hence, using equation (5) for slope with $\beta = 70^o$, the infiltration rate reduced 66 percents compared to that of the horizontal surface ($\beta = 0^o$).

4.2 Effect of saturated hydraulic conductivity

The saturated hydraulic conductivity k_{sat} of soil changes with soil types. For sandy soil, the k_{sat} is usually larger than 360 mm/h (10-4 m/s); for clayey or silty soil, the k_{sat} is lower than 0.36 mm/h (10-7 mm/s) [1]. Equation (3) shows that the infiltration rate is linearly correlated with the hydraulic conductivity. However, under the unsaturated condition, the hydraulic conductivity can vary considerably as a result of a change in the volume-water content of the soil. As described in the earlier section, moisture content at the ground surface increases gradually during rainwater infiltration until surface saturation is reached. At this moment, saturated hydraulic conductivity k_{sat} is reached. The Green-Ampt infiltration model is used to describe this phenomenon. To illustrate the effect of a change in saturated hydraulic conductivity on rainfall infiltration, Figure 6 shows the relationship between saturated hydraulic conductivity k_{sat} and infiltration rate corresponding to the maximum rainfall intensity for each typhoon.

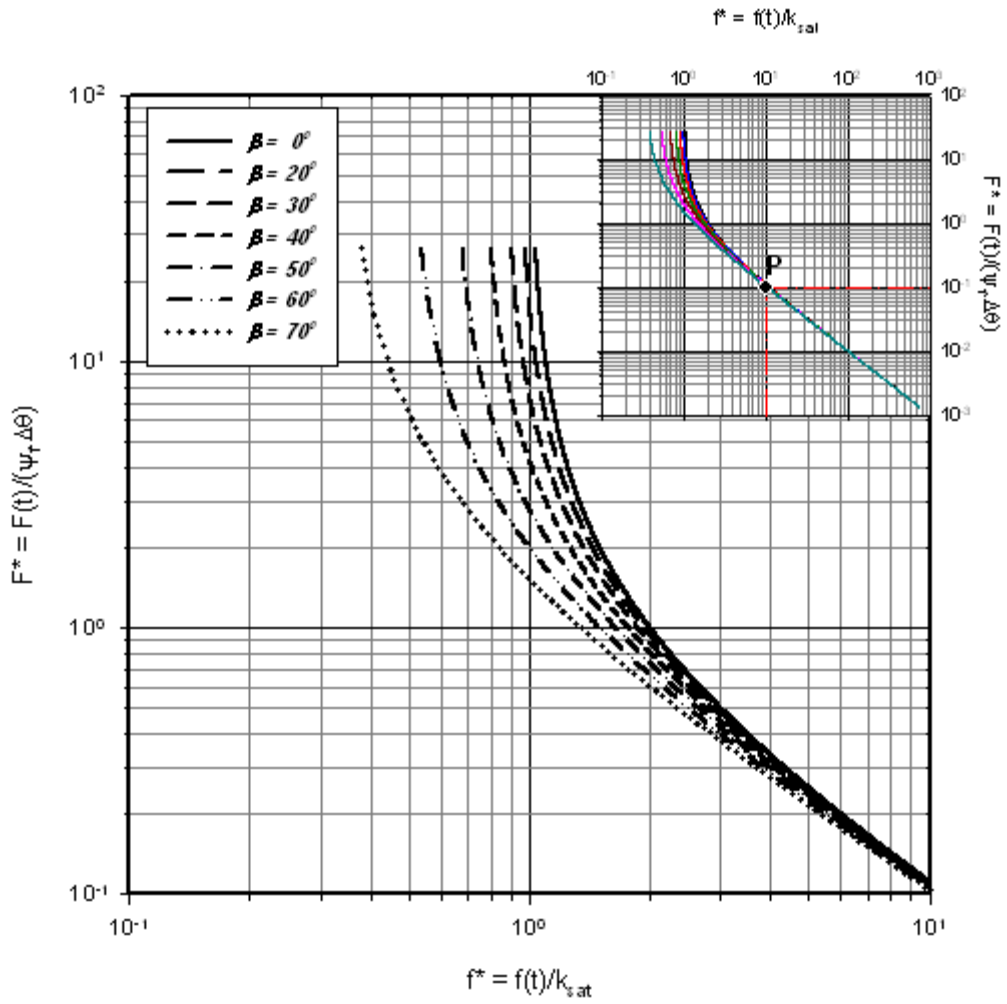

Figure 5 Representation chart of Green-Ampt equation on sloping surface

Figure 6a to 6c shows that the infiltration rate increases with increasing saturated hydraulic conductivity of the slope. The infiltration rate of the slope with higher permeability (k_{sat} = 360 mm/h) is always greater than the maximum rainfall intensity of each typhoon. It is because of the rainfall intensity is lesser than the infiltration capacity that is equal to the saturated hydraulic conductivity. So, if the rainfall lesser than the infiltration capacity will infiltrate into the subsurface with very higher rate. The infiltration rate will be slower if the infiltration capacity is reached. In contrast, the infiltration of soil with lower permeability, i.e. k_{sat} = 0.36 – 3.6 mm/h, is always lower than the maximum rainfall intensity of each typhoon. As described in previous section and Figure 2, surface saturation occurs if the infiltration rate is smaller than the rainfall intensity. So, the surface starts to become saturation if the rainfall rate is equal to the rainfall intensity. At this moment, there exists a threshold saturated hydraulic conductivity (k_{lim}) which corresponds to the beginning of surface saturation. Normalized the infiltration rate with the maximum rainfall intensity, Figure 7d plots the relationship between the normalized rainfall intensity $f(t)/I_{max}$ and saturated hydraulic conductivity for varying $\psi_f\Delta\theta$ (see Table 2) and slope angle β = 20°, 40°, 70°. Based on this relationship, the klim is determined at the intersection with $f(t)/I_{max}$ = 1. Thus, it results in a range of k_{lim} = 4 mm/h – 173 mm/h.

Figure 6a to 6c shows that the infiltration rate increases with increasing saturated hydraulic conductivity of the slope. The infiltration rate of the slope with higher permeability (k_{sat} = 360 mm/h) is always greater than the maximum rainfall intensity of each typhoon. It is because of the rainfall intensity is lesser than the infiltration capacity that is equal to the saturated hydraulic conductivity. So, if the rainfall lesser than the infiltration capacity will infiltrate into the subsurface with very higher rate. The infiltration rate will be slower if the infiltration capacity is reached. In contrast, the infiltration of soil with lower permeability, i.e. ksat = 0.36 – 3.6 mm/h, is always lower than the maximum rainfall intensity of each typhoon. As described in previous section and Figure 2, surface saturation occurs if the infiltration rate is smaller than the rainfall intensity. So, the surface starts

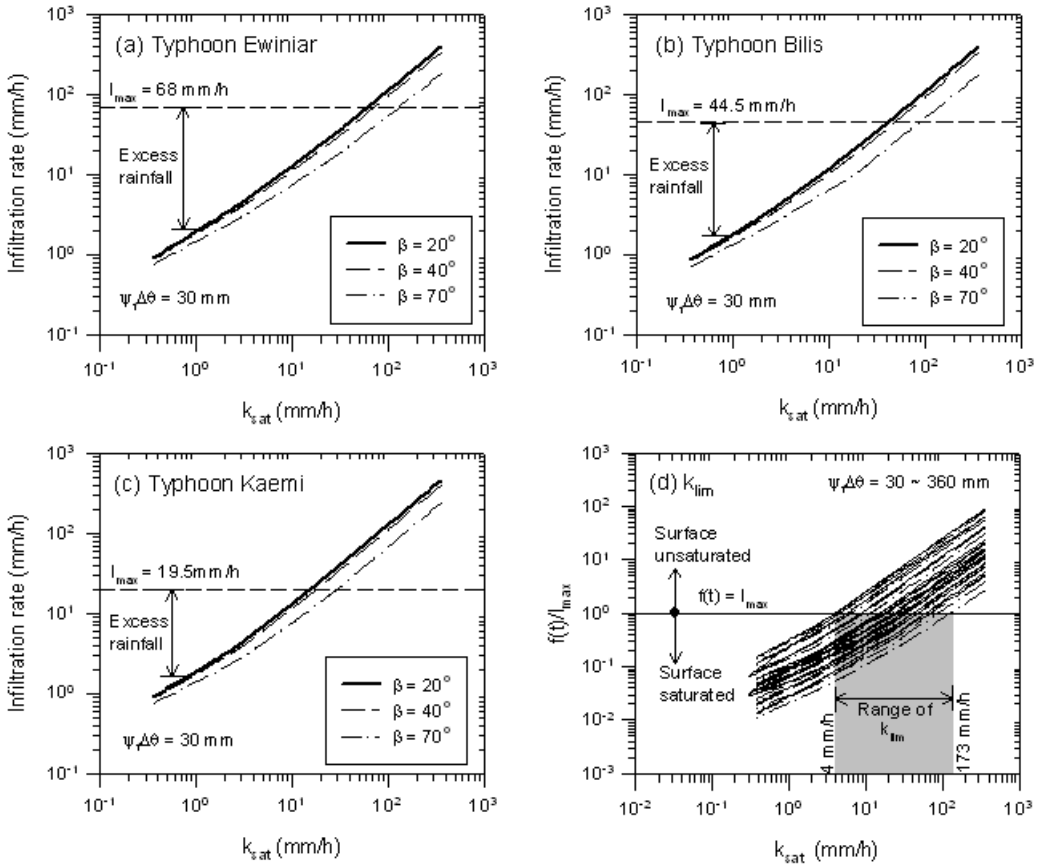

Figure 6 Change of infiltration rate with soil type for (a) Ewiniar, I_{max} = 68 mm/h, (b) Bilis, I_{max} = 44.5 mm/h, (c) Kaemi, I_{max} = 19.5 mm/h, (d) Determination of k_{lim}

to become saturation if the rainfall rate is equal to the rainfall intensity. At this moment, there exists a threshold saturated hydraulic conductivity (k_{lim}) which corresponds to the beginning of surface saturation. Normalized the infiltration rate with the maximum rainfall intensity, Figure 6d plots the relationship between the normalized rainfall intensity ($f(t)/I_{max}$) and saturated hydraulic conductivity for varying $\psi_f\Delta\theta$ (see Table 2) and slope angle β = 20°, 40°, 70°. Based on this relationship, the k_{lim} is determined at the intersection with $f(t)/I_{max}$ = 1. Thus, it results in a range of k_{lim} = 4 mm/h – 173 mm/h.

In practice, k_{lim} will be a valuable parameter as an indicator for slope stability. Because of in many slope failures cases, the slope is likely instable if the whole the slope depth is saturated. As shown in figure 6a to 6c and illustration given in Figure 1, excess rainfall occurs when the slope surface is in saturation state. This excess rainfall potentially becomes runoff which will result in surficial erosion and may cause shallow slip and/or limited debris flow. Pradel and Raad [1] noted that if k_{lim} reached 3.6 mm/h (1 x 10^{-6} m/s), rainfall induced slope instability might be resulted. Also, Lee et al. [12] also considered that k_{lim} between 0.28 – 2.82 mm/h (7.8 x 10^{-8} - 7.8 x 10^{-7} m/s) was likely to cause a shallow slip. For the slope studied here, the k_{lim} lay on the larger range that is between 4 – 173 mm/h.

4.3. Effect of moisture-suction head

The saturated hydraulic conductivity (ksat), suction head at wetting front (ψ_f) and deficit of volumetric water content ($\Delta\theta$) are three influencing parameters in the Green-Ampt equation to study the rainwater infiltration. The last two parameters can be aggregated in one parameter as a moisture-suction parameter ($\psi_f\Delta\theta$) since both parameters are closely related. Figure 7 shows the effect of moisture-suction on the infiltration rate for higher and lower permeability slope under three typhoons studied here.

In general, increasing moisture-suction increases linearly the infiltration rate as shown in Figure 7. This phenomenon can be explained by the unsaturated soil theory. In unsaturated soil, the matrix suction (u_a–u_w) is the pressure difference that is acting on the contractile skin of air–water interface in the pores. During transient infiltration process, pore air is draining out but pore water is flowing in simultaneously. Wang et al. [13] noted that the rate of pore water inflow is corresponding to the rate of pore air outflow during infiltration. In other words, higher suction will result in

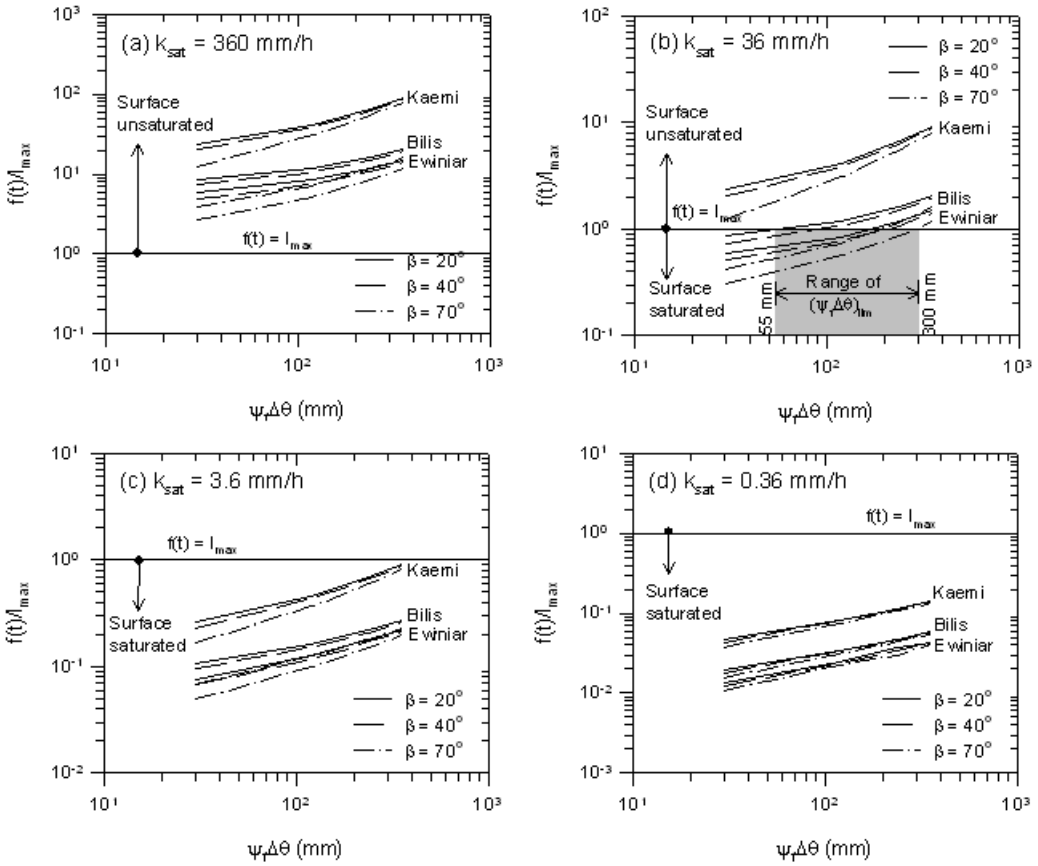

Figure 7 Change of infiltration rate with moisture-suction (a) k_{sat} = 360 mm/h, (b) k_{sat} = 36 mm/h, (c) k_{sat} = 3.6 mm/h, (d) k_{sat} = 0.36 mm/h

higher infiltration rate. The infiltration rate of the slope with lower hydraulic conductivity (k_{sat} = 0.36 mm/h and 3.6 mm/h) increased approximately 1.2 - 2 times by changing the moisture-suction from 30 mm to 360 mm (10 times increasing moisture-suction). For slope with a high hydraulic conductivity (i.e., k_{sat} = 36 mm/h and 360 mm/h), the infiltration rate increased about 5–6 times when the moisture-suction of soil increased from 30 mm to 360 mm. As presented in Table 1, the range of suction head (ψ_f) for the typical soil is very wide, for instances, the range of suction head of clay soils is 63.9–1565 mm (±25 times increasing suction head) and for sand soils is 9.7–253.6 mm (±26 times increasing suction head). In this study the suction head is varied in the range of 100–1200 mm (12 times increasing). According to the result of this study, the infiltration rate of the sand soils will vary significantly compared with clay soils. Parameter sensitivity analysis of Green-Ampt model done by Hsu et al. [14] also found that change in the suction head has increased considerably for loam and sand soils. However, it is contrary for clay soils. Therefore, determination of suction head in the Green-Ampt model should be well defined. Lu and Likos [15], Wang and Benson [16] proposed that the suction head at wetting front can be approached by air entry value (AEV) method. However, the suction head at the wetting front is close to zero at the moment of the saturated condition. For the some soils, Mein and Larson [17], Santos et al. [18] said that the suction value near saturation cannot be well defined. For this reason, the average suction head is proposed to represent suction at the wetting front.

As mentioned in previous section, the slope surface starts to saturate if the slope infiltration rate is the same as rainfall intensity. In Figure 7b, for k_{sat} = 36 mm/h under typhoon Ewiniar and Bilis, the slope was in unsaturated states at the beginning and tend to become saturation by decreasing the moisture-suction from 360 mm to 30 mm. At this case, the slope surface starts to saturate when the moisture-suction in the range between 55–300 mm. This phenomenon explains that changing moisture-suction not only changes the infiltration rate but also affects the degree of slope surface saturation. Therefore, the moisture-suction value should be well defined by relevant data or tests. However, it should be noted that the determination of the suction is a rather complex process, even if the data needed is available.

5.0 CONCLUSION

This paper has presented the result of rainfall infiltration analysis on sloping surface using Green-Ampt infiltration model. The study carried out the effect of slope angle, soil type and soil-water suction on the Green-Ampt infiltration model. Increasing slope steepness reduces the rainwater infiltration rate. Comparing the infiltration for sloping surface and horizontal surface, the reduction of infiltration rate is given by $k_{sat}(1 - \cos \beta)$ [equation (5)].

The infiltration rate increased linearly with increasing the saturated hydraulic conductivity. In this study, the slope surface starts to saturate when the saturated hydraulic conductivity is below the k_{lim} is defined as threshold saturated hydraulic conductivity which is corresponding to the infiltration rate equal with rainfall intensity. The k_{lim} range from 4 mm/h to 173 mm/h.

Increase in the moisture-suction head at wetting front will increase the infiltrability during rainfall. Change in moisture-suction increased considerably the infiltration rate of slope with high permeability such as sand soils comparing with slope with lower permeability such clay. Therefore, the difference in moisture-suction should be paid attention for a slope with higher hydraulic conductivity such as sand soils. By using equations (9) and (10), a graphical aid (Figure 5) has been developed to represent the basic Green-Ampt equation for sloping surface.

References

[1] Pradel D, Raad G (1993) Effect of permeability on surficial stability of homogeneous slopes, J Geotech Eng 119(2): 315-332.

[2] Rahardjo H, Lim TT, Chag MF, Fredlund DG (1995) Shear strength characteristics of a residual soil. Can Geotech J 32: 60-77.

[3] Xie M-W, Esaki T, Cai M-F (2004) A time-space based approach for mapping rainfall-induced shallow landslide hazard. Environ Geol46:840–850. doi 10.1007/s00254-004-1069-1

[4] Tofani V, Dapporto S, Vannocci P, and Casagli N. 2006. Infiltration, seepage and slope instability mechanisms during the 20–21 November 2000 rainstorm in Tuscany, central Italy. Natural Hazards Earth System Sciences 6: 1025–1033

[5] Clausnitzer, V., Hopmans, J.W., and Starr, J.L., 1998, Parameter Uncertainty Analysis of Common Infiltration Models, Soil Science Society American Journal 62: 1477–1487.

[6] Chu, T.C., 1978, Infiltration during an unsteady rain, Water Resources Research 14(3): 461-466.

[7] Chen, L., & Young, M.H., 2006, Green-Ampt infiltration model for sloping surface, Water Resources Research 42: 1-9.

[8] Lu HS, Hu SC, and Lin JP (1996) Infiltration model for soils on a sloping betel palm farm in the Lienhuachi are of Central Taiwan, Journal of Forest Science 11(4): 409-420

[9] Fox, D.M., Bryan, R.B., & Price, A.G., 1997, The influence of slope angle on final infiltration rate for interrill conditions, Geoderma, Vol. 80, 181-194.

[10] Rawls WJ, Ahuja LR, Brakensiek DL, and Shirmohammadi A. 1993. Infiltration and soil water movement, In: Maidment DR (ed.) Handbook of Hydrology, Mc. Graw-Hill, New York, Ch. 5.

[11] Chow, V.T., Maidment, D.R., & Mays, L.W., 1988, Applied hydrology, Mc. Graw-Hill New York, Ch. 4, 110-116.

[12] Lee KH, Jeong SS, and Kim TH. 2007. Effect of fines on the stability of unsaturated soil slopes, Journal of Korean Geotechnical Socety 23(3): 101-109.

[13] Wang Z, Feyen J, van Genuchten M.Th, Nielsen DR (1998) Air entrapment effect on infiltration rate and flow instability. Water Resour Res 34(2): 213-222.

[14] Hsu S.M., Ni C.F., and Hung P.F. 2002, Assessment of Three Infiltration Formulas based on Model Fitting on Richards Equation. Journal of Hydrologic Engineering 7(5): 373–379.

[15] Lu N, and Likos WJ (2004) Rate of capillary rise in soil. J Geotech Geoenviron Eng 130(6): 646-650.

[16] Wang X.D., and Benson C.H. 1995, Infiltration and saturated hydraulic conductivity of compacted clay, Journal of Geotechnical Engineering 121(10): 713-722.

[17] Mein RG, Larson CL (1973) Modeling infiltration during a steady rain. Water Resour Res 9(2): 384-394.

[18] Santos CAG, Suzuki K, Watanabe M, Srinivasan VS (1999) Determining the soil moisture-tension parameter in the Green-Ampt infiltration equation for runoff-erosion modeling. Proceeding of the 28th IAHR Congress, 22-27 August 1999, Graz, Austria.

Notation and Symbols in Used:

$F(t)$: cumulative infiltration at time t (mm)
$F'(t)$: tentative cumulative infiltration at time t (mm)
F^* : normalized cumulative infiltration
$f(t)$: infiltration rate at time t (mm/h)
$f'(t)$: tentative infiltration rate at time t (mm/h)
f^* : normalized infiltration rate
$I(t)$: rainfall intensity at time t (mm/h)
I_{max} : maximum rainfall intensity (mm/h)
k : coefficient of unsaturated hydraulic conductivity (mm/h)
k_{lim} : limit of ksat correspond to 10% infiltration rate
k_{sat} : coefficient of saturated hydraulic conductivity (mm/h)
k_y : coefficient of saturated hydraulic conductivity at sloping ground (mm/h)
$R(t)$: accumulative rainfall at time t (mm)
t : elapsed time (h)
t_p : ponding time (time to start surface saturation) (h)
t'_p : time needed to reach saturation between the time intervals (h)
t_s : time of the end of saturation (h)
Δt : time interval (h)
$\Delta\theta$: deficit of the volumetric moisture content
β : degree of slope angle
η : the soil porosity
θ : volumetric moisture content (mm3/mm-3)
θ_i : initial moisture content
θ_s : moisture content at saturated condition
ψ_f : soil-water suction head (mm)
$\psi_f \Delta\theta$: moisture-suction (mm)

Lampiran C

Penggunaan Anggaran

Dr.Eng. Agus Setyo Muntohar
Dr. Jazaul Ikhsan

Rekapitulasi Penggunaan Dana Penelitian

Judul	:	Studi Dampak Perubahan Iklim Terhadap Longsoran Lereng
Skema Hibah	:	Penelitian Kompetensi
Peneliti / Pelaksana		
Nama Ketua	:	AGUS SETYO MUNTOHAR Ph.D
Perguruan Tinggi		Universitas Muhammadiyah Yogyakarta
NIDN	:	0514087501
Nama Anggota (1)	:	JAZAUL IKHSAN S.T., M.T., Ph.D.
Tahun Pelaksanaan	:	Tahun ke 1 dari rencana 3 tahun
Dana Tahun Berjalan	:	Rp 145.000.000,00
Dana Mulai Diterima Tanggal	:	2015-06-08

Rincian Penggunaan

1. HONOR OUTPUT KEGIATAN

Item Honor	Volume	Satuan	Honor/Jam (Rp)	Total (Rp)
1. Honor Ketua Peneliti	3.00	bulan	3.000.000	9.000.000
2. Honor Anggota Peneliti	3.00	bulan	2.000.000	6.000.000
3. Pajak peneliti Pph 21	1.00	ls	750.000	750.000
			Sub Total (Rp)	15.750.000,00

2. BELANJA BAHAN

Item Bahan	Volume	Satuan	Harga Satuan (Rp)	Total (Rp)
1. Tabung pipa acrylic 11d2	2.00	batang	240.000	480.000
2. Tabung pipa acrylic 26d2	4.00	batang	360.000	1.440.000
3. Fotokopi formulir uji lab	720.00	lembar	200	144.000
4. Jilid laporan kemajuan penelitian	3.00	buku	11.500	34.500
5. Biaya materai	5.00	lembar	7.000	35.000
6. Fotokopi formulir uji lab	360.00	lembar	150	54.000
7. Fotokopi formulir uji lab	1585.00	lembar	200	317.000
8. Jilid biasa	5.00	buku	3.500	17.500
9. Fotokopi dan jilid buku referensi	10.00	buku	89.400	894.000
10. Fotokopi dan jilid buku referensi	5.00	buku	57.600	288.000
11. Jilid laporan kemajuan penelitian	1.00	buku	17.500	17.500
12. Biaya makan/minum	1.00	orang	90.000	90.000
13. Biaya makan/minum	5.00	orang	26.000	130.000

14. Biaya makan/minum	1.00	kotak	24.358	24.358
15. Biaya makan/minum	1.00	bungkus	11.500	11.500
16. Biaya makan/minum	10.00	orang	34.900	349.000
17. Biaya makan/minum	1.00	orang	10.000	10.000
18. Biaya makan/minum	4.00	orang	8.750	35.000
19. Biaya makan/minum	1.00	paket	67.100	67.100
20. Biaya makan/minum	6.00	orang	15.250	91.500
21. Biaya makan/minum	1.00	orang	6.000	6.000
22. Sewa studio/lab	1.00	jam	150.000	150.000
23. Biaya bahan penelitian viscocrete	1.00	kg	75.000	75.000
24. Biaya bahan penelitian MPX5100P	1.00	unit	316.500	316.500
25. Biaya alat penelitian bodem	1.00	unit	70.000	70.000
26. Biaya bahan penelitian OPS	1.00	unit	250.000	250.000
27. Semen Tiga Roda	2.00	zak	56.000	112.000
28. Kawat strimin	2.00	m	13.000	26.000
29. Biaya pembuatan alat V-funnel	1.00	unit	30.000	30.000
30. Biaya pembuatan alat L-box	1.00	unit	30.000	30.000
31. Biaya bahan penelitian pelat baja	10.50	kg	20.000	210.000
32. Biaya sewa laboratorium Geoteknik	6.00	bulan	1.000.000	6.000.000
33. Biaya penyelidikan geoteknik: SPT dan bor	8.00	titik	5.000.000	40.000.000
34. Tensiometer Laboratory KU-T2	3.00	unit	2.856.600	8.569.800
35. Readout	1.00	unit	4.600.000	4.600.000
36. Voltmeter	1.00	unit	2.500.000	2.500.000
			Sub Total (Rp)	67.475.258,00

3. BELANJA BARANG NON OPERASIONAL LAINNYA

Item Barang	Volume	Satuan	Harga Satuan (Rp)	Total (Rp)
1. Mata bor	3.00	batang	20.000	60.000
2. Biaya uji Lab Kimia UGM	1.00	ls	440.000	440.000
3. Kepala bor 13 mm	2.00	batang	35.000	70.000

4. Kunci bor	1.00	batang	15.000	15.000
5. Alat penyimpan benda uji suhu terkontrol	1.00	unit	1.720.000	1.720.000
6. Biaya transit penginapan Sta. Gambir	1.00	orang	65.000	65.000
7. Biaya konsumsi	1.00	orang	38.700	38.700
8. Pendaftaran Konferensi Internasional	1.00	orang	2.500.000	2.500.000
9. Biaya makan	1.00	orang	45.000	45.000
10. Biaya Wraping (THB150)	1.00	buah	63.000	63.000
11. Biaya makan	1.00	orang	567.000	567.000
12. Biaya pendaftaran PIT HATTI ke-19	1.00	orang	1.200.000	1.200.000
			Sub Total (Rp)	6.783.700,00
4. BELANJA PERJALANAN LAINNYA				
Item Perjalanan	Volume	Satuan	Biaya Satuan (Rp)	Total (Rp)
1. Perjalanan pengambilan data hujan YOG - JKT pp	1.00	pp	1.307.100	1.307.100
2. Biaya tiket KA Yog - Jkt	1.00	orang	380.000	380.000
3. Biaya tiket KA Jkt - Yog	1.00	orang	350.000	350.000
4. Biaya tiket pesawat Jog-Dps pp	1.00	orang	1.424.000	1.424.000
5. Biaya tiket pesawat Jog-Bkkpp	1.00	orang	6.585.400	6.585.400
6. Biaya bahan bakar mobil	15.95	liter	9.400	149.930
7. Biaya bahan bakar	15.96	liter	9.400	150.024
8. Biaya bahan bakar	2.43	liter	9.400	22.842
9. Biaya bahan bakar	2.49	liter	9.400	23.406
10. Biaya bahan bakar	20.27	liter	7.400	149.998
11. Biaya bahan bakar	10.00	liter	6.500	65.000
12. Biaya bahan bakar	15.95	liter	9.400	149.930
13. Biaya bahan bakar	16.21	liter	7.400	119.954
14. Biaya bahan bakar	16.04	liter	9.350	149.974
15. Biaya bahan bakar	15.70	liter	9.550	149.935
			Sub Total (Rp)	11.177.493,00
			Total Pengeluaran Dalam Satu Tahun (Rp)	101.186.451,00

Mengetahui,

(Hilman Latif, M.A., Ph.D)
NIP/NIK 19750912200004113033

Yogyakarta, , 7 - 12 - 2015
Ketua,

(AGUS SETYO MUNTOHAR Ph.D)
NIP/NIK 19750814199904123040